On the Constitutive Modeling of Coupled Thermomechanical Phase-change Problems

C. AGELET DE SARACIBAR[†], M. CERVERA[‡] & M. CHIUMENTI[♯]
ETS Ingenieros de Caminos, Canales y Puertos
International Center for Numerical Methods in Engineering
Edificio C1, Campus Norte, UPC, Jordi Girona Salgado 1-3, 08034 Barcelona, Spain

SUMMARY

This paper deals with a thermodynamically consistent numerical formulation for coupled thermoplastic problems including phase-change phenomena and frictional contact. The final goal is to get an accurate, efficient and robust numerical model, able for the numerical simulation of industrial solidification processes. Some of the current issues addressed in the paper are the following. A fractional step method arising from an operator split of the governing differential equations has been used to solve the nonlinear coupled system of equations, leading to a staggered product formula solution algorithm. Nonlinear stability issues are discussed and isentropic and isothermal operator splits are formulated. Within the isentropic split, a strong operator split design constraint is introduced, by requiring that the elastic and plastic entropy, as well as the phase-change induced elastic entropy due to the latent heat, remain fixed in the mechanical problem. The formulation of the model has been consistently derived within a thermodynamic framework. All the material properties have been considered to be temperature dependent. The constitutive behavior has been defined by a thermoviscous/elastoplastic free energy function, including a thermal multiphase change contribution. Plastic response has been modeled by a J2 temperature dependent model, including plastic hardening and thermal softening. The constitutive model proposed accounts for a continuous transition between the initial liquid state, the intermediate mushy state and the final solid state taking place in a solidification process. In particular, a pure viscous deviatoric model has been used at the initial fluid-like state. A thermomecanical contact model, including a frictional hardening and temperature dependent coupled potential, is derived within a fully consistent thermodinamical theory. The numerical model has been implemented into the computational Finite Element code COMET developed by the authors. Numerical simulations of solidification processes show the good performance of the computational model developed.

1. INTRODUCTION

Numerical solution of coupled problems using staggered algorithms, is an efficient procedure in which the original problem is partitioned into several smaller sub-problems which are solved sequentially. For thermomechanical problems the standard approach exploits a natural partitioning of the problem in a mechanical phase, with the temperature held constant, followed by a thermal phase at fixed configuration. As noted in SIMO & MIEHE [1991] this class of staggered algorithms falls within the class of product formula algorithms arising from an operator split of the governing evolution equations into an isothermal step followed by a heat-conduction step at fixed configuration. A recent analysis in ARMERO & SIMO [1992A,1992B,1993] shows that this isothermal split does not preserve the contractivity property of the coupled problem of (nonlinear) thermoelasticity, leading to staggered schemes that are at best only conditionally stable. ARMERO & SIMO [1992A,1992B,1993] proposed an alternative operator split, henceforth referred to as the isentropic split, whereby the problem is partitioned into an isentropic mechanical phase,

[†] Professor of Continuum Mechanics, [‡] Professor of Structural Mechanics, [♯] Graduate Research Assistant.

with total entropy held constant, followed by a thermal phase at fixed configuration. It was shown by ARMERO & SIMO [1992A,1992B,1993] that such operator split leads to an unconditionally stable staggered algorithm, which preserves the crucial properties of the coupled problem. The aim of the paper is to extend the formulation given by ARMERO & SIMO [1992A,1992B,1993] and SIMO [1994] to coupled thermoplastic problems with phase-change, to get an accurate, efficient and robust numerical model, able for the numerical simulation of solidification processes in the metal casting industry.

The remaining of the paper is as follows. Section 2 deals with the formulation of the local governing equations of the coupled thermoplastic problem, consistently derived within a thermodynamic framework. An additive split of the strain tensor and the entropy has been assumed. The constitutive behavior has been defined by a thermoviscous-elastoplastic free energy function, with temperature dependent material properties. Latent heat associated to the phase-change phenomena has been incorporated to the thermal contribution of the free energy function. Plastic response has been modeled by a J2 temperature dependent model, including nonlinear hardening due to plastic deformation and thermal linear softening. A thermofrictional contact model is derived within a fully consistent thermodinamical framework. Following LAURSEN [1998], contact temperature and entropy variables at the contact surface are introduced, and the energy balance equation at the contact surface is formulated. A particular thermofrictional contact model including frictional hardening and temperature coupling is outlined. Following an analogy with the bulk continua, an additive split of the tangential gap and the contact entropy, into elastic and inelastic parts, has been assumed. A pressure and contact temperature dependent thermal contact model has been used. Additionally, a gap dependent thermal model has been used to take into account surface heat transfer phenomena when the two bodies lose contact. Heat generation due to frictional dissipation is implicitly included. This Section ends with the variational formulation of the coupled problem.

In Section 3, fractional step methods arising from an operator split of the governing differential equations are considered. Isentropic and isothermal splits are introduced and nonlinear stability issues linked to the splits are adressed. A key point of the formulation of the isentropic split is the set up of the additional design constraints to define the mechanical problem. Here, a strong operator split design constraint is introduced, by requiring that the elastic and plastic entropy, as well as the phase-change induced elastic entropy due to the latent heat, remain fixed in the mechanical problem. These additional constraints motivate the definition of the sets of variables and nonlinear operators introduced in the present formulation. Within the time discrete setting, the additive operator splits lead to a product formula algorithm and to a staggered solution scheme of the coupled problem. Finally, the time discrete variational formulation of the coupled problem, using isentropic and isothermal splits, is introduced.

Section 4 deals with numerical simulations of solidification processes. Some concluding remarks are drawn in Section 5. Finally, a step-by-step formulation of the thermoplastic and thermofrictional return mapping algorithms within the mechanical and thermal problems arising from an isentropic split of their governing equations is given in Appendices I and II.

2. FORMULATION OF THE COUPLED THERMOPLASTIC PROBLEM

We describe below the system of quasi-linear partial differential equations governing the evolution of the coupled thermomechanical initial boundary value problem, including thermal multiphase change and thermofrictional contact.

2.1. Local Governing Equations

Let $2 \leq n_{dim} \leq 3$ be the space dimension and $\mathbb{I} := [0,T] \subset \mathbb{R}_+$ the time interval of interest. Let the open sets $\Omega \subset \mathbb{R}^{n_{dim}}$ with smooth boundary $\partial\Omega$ and closure $\bar{\Omega} := \Omega \cup \partial\Omega$, be the reference placement of a continuum body $\mathcal{B}$.

Denote by $\boldsymbol{\varphi} : \bar{\Omega} \times \mathbb{I} \to \mathbb{R}^{n_{dim}}$ the orientation preserving deformation map of the body $\mathcal{B}$, with material velocity $\boldsymbol{V} := \partial_t \boldsymbol{\varphi} = \dot{\boldsymbol{\varphi}}$, deformation gradient $\boldsymbol{F} := D\boldsymbol{\varphi}$ and absolute temperature $\Theta : \bar{\Omega} \times \mathbb{I} \to \mathbb{R}$. For each time $t \in \mathbb{I}$, the mapping $t \in \mathbb{I} \mapsto \boldsymbol{\varphi}_t := \boldsymbol{\varphi}(\cdot, t)$ represents a one-parameter family of configurations indexed by time t, which maps the reference placement of body $\mathcal{B}$ onto its current placement $\mathcal{S}_t : \boldsymbol{\varphi}_t(\mathcal{B}) \subset \mathbb{R}^{n_{dim}}$.

The local system of partial differential equations governing the coupled thermomechanical initial boundary value problem is defined by the momentum and energy balance equations, restricted by the inequalities arising from the second law of the thermodynamics. This system must be supplemented by suitable constitutive equations. Additionaly, one must supply suitable prescribed boundary and initial conditions, and consider the equilibrium equations at the contact interfaces.

(A) *Local form of momentum and energy balance equations.* The local form of the momentum and energy balance equations can be written in a first order system form as, see, e.g., TRUESDELL & NOLL [1965],

$$\left.\begin{aligned} \dot{\boldsymbol{\varphi}} &= \boldsymbol{V} \\ \rho_0 \dot{\boldsymbol{V}} &= \mathrm{DIV}[\boldsymbol{\sigma}] + \boldsymbol{B} \\ \Theta \dot{H} &= -\mathrm{DIV}[\boldsymbol{Q}] + R + \mathcal{D}_{int} \end{aligned}\right\} \quad \text{in} \quad \bar{\Omega} \times \mathbb{I} \tag{1}$$

where $\rho_0 : \bar{\Omega} \to \mathbb{R}_+$ is the reference density, $\boldsymbol{B}$ are the (prescribed) body forces per unit reference volume, $\mathrm{DIV}[\cdot]$ the reference divergence operator, $\boldsymbol{\sigma}$ the Cauchy stress tensor, H the entropy per unit reference volume, $\boldsymbol{Q}$ the (nominal) heat flux, R the (prescribed) heat source and $\mathcal{D}_{int}$ the internal dissipation per unit reference volume. Formally, the governing equations for a quasi-static case, may be obtained just by setting $\rho_0 = 0$ in (1).

(B) *Dissipation inequalities.* The specific entropy H and the Cauchy stress tensor $\boldsymbol{\sigma}$ are defined via constitutive relations, typically formulated in terms of the internal energy E, and subjected to the following restriction on the internal dissipation, see, e.g., TRUESDELL & NOLL [1965],

$$\mathcal{D}_{int} = \boldsymbol{\sigma} : \dot{\boldsymbol{\epsilon}} + \Theta \dot{H} - \dot{E} \geq 0 \qquad \text{in} \quad \bar{\Omega} \times \mathbb{I} \tag{2}$$

where $\boldsymbol{\epsilon} := \mathrm{SYMM}[\boldsymbol{F} - \boldsymbol{I}]$ is the infinitesimal strain tensor. Here $\mathrm{SYMM}[\cdot]$ denotes the symmetric operator and $\boldsymbol{I}$ is the second order identity tensor.

The heat flux $\boldsymbol{Q}$ is defined via constitutive equations, say Fourier's law, subjected to the restriction on the dissipation by conduction given by

$$\mathcal{D}_{con} = -\frac{1}{\Theta}\text{GRAD}[\Theta]\cdot\boldsymbol{Q} \geq 0 \qquad \text{in} \quad \bar{\Omega}\times\mathbb{I} \tag{3}$$

(C) *Thermoplastic/viscous constitutive equations.* Micromechanically based phenomenological models of infinitesimal strain plasticity adopt a local additive decomposition of the strain tensor into elastic and plastic parts. Hardening mechanisms in the material taking place at a microstructural level are characterized by an additional set of phenomenological internal variables collectively denoted here by ξ_α. A viscoelastic behaviour is characterized by an additional strain variable denoted as $\boldsymbol{\alpha}$. The aims behind the introduction of this viscous behaviour are to adopt a pure deviatoric viscous model at very high temperature, i.e. at the liquid state, and to introduce viscous effects at the mushy/solid state. In the coupled thermomechanical theory, an additive split of the local entropy into elastic and plastic parts is adopted, where the plastic entropy is viewed as an additional internal variable arising as a result of dislocation and lattice defect motion. This additive split of the local entropy was adopted by ARMERO & SIMO [1993]. The above considerations, motivate the following additive split of the infinitesimal strain tensor $\boldsymbol{\epsilon} := \boldsymbol{\epsilon}^e + \boldsymbol{\epsilon}^p$ and local entropy $H := H^e + H^p$ and the following set of microstructural plastic/viscous internal variables $\boldsymbol{G} := \{\boldsymbol{\epsilon}^p, H^p, \xi_\alpha, \boldsymbol{\alpha}\}$.

The internal energy function $\hat{E}$ depends on the elastic part of the strain tensor $\boldsymbol{\epsilon}^e$, the hardening internal variables ξ_α, the configurational entropy H^e and the viscous strain tensor $\boldsymbol{\alpha}$ taking the functional form $E = \hat{E}(\boldsymbol{\epsilon}^e, H^e, \xi_\alpha, \boldsymbol{\alpha})$. Introducing the functional form of the internal energy into the expression of the internal dissipation, taking the time derivative, applying the chain rule and using the additive split of the infinitesimal strain tensor and total entropy, a straightforward argument yields the following constitutive equations and reduced internal dissipation inequality

$$\left.\begin{aligned} \boldsymbol{\sigma} &:= \partial_{\boldsymbol{\epsilon}^e}\hat{E}(\boldsymbol{\epsilon}^e, H^e, \xi_\alpha, \boldsymbol{\alpha}),\\ \Theta &:= \partial_{H^e}\hat{E}(\boldsymbol{\epsilon}^e, H^e, \xi_\alpha, \boldsymbol{\alpha}),\\ \beta^\alpha &:= -\partial_{\xi_\alpha}\hat{E}(\boldsymbol{\epsilon}^e, H^e, \xi_\alpha, \boldsymbol{\alpha}),\\ \boldsymbol{\beta} &:= -\partial_{\boldsymbol{\alpha}}\hat{E}(\boldsymbol{\epsilon}^e, H^e, \xi_\alpha, \boldsymbol{\alpha}), \end{aligned}\right\} \tag{4}$$

$$\begin{aligned} &\mathcal{D}_{int} := \mathcal{D}_{mech} + \mathcal{D}_{ther} \geq 0, \quad \text{with}\\ &\mathcal{D}_{mech} := \boldsymbol{\sigma} : \dot{\boldsymbol{\epsilon}}^p + \beta^\alpha\,\dot{\xi}_\alpha + \boldsymbol{\beta} : \dot{\boldsymbol{\alpha}} \geq 0 \;\text{ and }\; \mathcal{D}_{ther} := \Theta\dot{H}^p. \end{aligned} \tag{5}$$

Using the Legendre transformation $\Psi = E - \Theta H^e$, the free energy function takes the functional form $\Psi = \hat{\Psi}(\boldsymbol{\epsilon}^e, \Theta, \xi_\alpha, \boldsymbol{\alpha})$. Taking the time derivative of the free energy function and applying the chain rule, a straightforward argument yields the following alternative

expressions for the constitutive equations

$$\left.\begin{aligned} \boldsymbol{\sigma} &:= \partial_{\boldsymbol{\epsilon}^e}\hat{\Psi}(\boldsymbol{\epsilon}^e, \Theta, \xi_\alpha, \boldsymbol{\alpha}), \\ H^e &:= -\partial_\Theta \hat{\Psi}(\boldsymbol{\epsilon}^e, \Theta, \xi_\alpha, \boldsymbol{\alpha}), \\ \beta^\alpha &:= -\partial_{\xi_\alpha}\hat{\Psi}(\boldsymbol{\epsilon}^e, \Theta, \xi_\alpha, \boldsymbol{\alpha}), \\ \boldsymbol{\beta} &:= -\partial_\alpha \hat{\Psi}(\boldsymbol{\epsilon}^e, \Theta, \xi_\alpha, \boldsymbol{\alpha}), \end{aligned}\right\} \tag{6}$$

Assuming a yield function of the form $\Phi := \hat{\Phi}(\boldsymbol{\sigma}, \beta^\alpha, \Theta)$, the evolution laws of the plastic internal variables, assuming associated flow, take the form

$$\left.\begin{aligned} \dot{\boldsymbol{\epsilon}}^p &:= \gamma\, \partial_{\boldsymbol{\sigma}}\hat{\Phi}(\boldsymbol{\sigma}, \beta^\alpha, \Theta), \\ \dot{\xi}_\alpha &:= \gamma\, \partial_{\beta^\alpha}\hat{\Phi}(\boldsymbol{\sigma}, \beta^\alpha, \Theta), \\ \dot{H}^p &:= \gamma\, \partial_\Theta \hat{\Phi}(\boldsymbol{\sigma}, \beta^\alpha, \Theta), \end{aligned}\right\} \tag{7}$$

and the following Kuhn-Tucker $\gamma \geq 0, \Phi \leq 0, \gamma\Phi = 0$ and consistency $\gamma\dot{\Phi} = 0$ conditions must be satisfied for a rate-independent plastic model.

The evolution law for the viscous strain $\boldsymbol{\alpha}$ takes the form

$$\dot{\boldsymbol{\alpha}} := \frac{1}{\eta_v}\boldsymbol{\beta} \tag{8}$$

where η_v is the effective elastic viscosity material property.

Additionally, the heat flux is related to the absolute temperature through the Fourier's law, which for the isotropic case takes the form $\boldsymbol{Q} = -K(\Theta)\ \mathrm{GRAD}[\Theta]$, where $K(\Theta)$ is the temperature dependent thermal conductivity.

REMARK 1. *Equivalent forms of the energy balance equation.* Using the additive split of the total entropy into elastic and plastic parts and the additive split of the internal dissipation into mechanical and thermal, the reduced energy equation can be expressed as

$$\Theta \dot{H}^e = -\mathrm{DIV}[\boldsymbol{Q}] + R + \mathcal{D}_{mech} \qquad \text{in} \quad \bar{\Omega} \times \mathbb{I}. \tag{9}$$

Alternatively, using the constitutive equation of the elastic entropy, taking its time derivative and applying the chain rule, the temperature-form of the reduced energy equation can be written as

$$c_0 \dot{\Theta} = -\mathrm{DIV}[\boldsymbol{Q}] + R + \mathcal{D}_{mech} - \mathcal{H}^{ep} \qquad \text{in} \quad \bar{\Omega} \times \mathbb{I}, \tag{10}$$

with

$$\begin{aligned} c_0 &:= -\Theta \partial^2_{\Theta\Theta}\hat{\Psi}(\boldsymbol{\epsilon}^e, \Theta, \xi_\alpha, \boldsymbol{\alpha}), \\ \mathcal{H}^{ep} &:= -\Theta[\partial^2_{\Theta\boldsymbol{\epsilon}^e}\hat{\Psi}(\boldsymbol{\epsilon}^e, \Theta, \xi_\alpha, \boldsymbol{\alpha}) : \dot{\boldsymbol{\epsilon}}^e + \partial^2_{\Theta\xi_\alpha}\hat{\Psi}(\boldsymbol{\epsilon}^e, \Theta, \xi_\alpha, \boldsymbol{\alpha}) \cdot \dot{\xi}_\alpha + \partial^2_{\Theta\alpha}\hat{\Psi}(\boldsymbol{\epsilon}^e, \Theta, \xi_\alpha, \boldsymbol{\alpha}) : \dot{\boldsymbol{\alpha}}], \end{aligned} \tag{11}$$

where c_0 is the reference heat capacity and $\mathcal{H}^{ep}$ the structural elastoplastic heating. Using the constitutive equations (6) the reference heat capacity and structural elastoplastic heating, take the compact form

$$\begin{aligned} c_0 &:= \Theta \partial_\Theta \hat{H}^e(\boldsymbol{\epsilon}^e, \Theta, \xi_\alpha, \boldsymbol{\alpha}), \\ \mathcal{H}^{ep} &:= -\Theta \partial_\Theta [\boldsymbol{\sigma} : \dot{\boldsymbol{\epsilon}} - \mathcal{D}_{mech}]. \ \square \end{aligned} \tag{12}$$

REMARK 2. *Thermal phase-change contributions.* The free energy function for a coupled thermomechanical model including phase change can be splitted into thermoelastic Ψ_{te}, thermoplastic Ψ_{tp}, thermal (except phase change) Ψ_t and thermal phase change Ψ_{tpc} contributions, taking the functional form, $\Psi = \hat{\Psi}_{te}(\boldsymbol{\epsilon}^e, \Theta, \boldsymbol{\alpha}) + \hat{\Psi}_{tp}(\Theta, \xi_\alpha) + \hat{\Psi}_t(\Theta) + \hat{\Psi}_{tpc}(\Theta)$.

Collecting into a thermoelastoplastic part $\hat{\Psi}_{tep}(\boldsymbol{\epsilon}^e, \Theta, \xi_\alpha, \boldsymbol{\alpha})$ all the terms appearing into the free energy function, except the thermal phase change contribution, and setting $H^e := H^e_{tep} + H^e_{tpc}$ with $H^e_{tep} := -\partial_\Theta \hat{\Psi}_{tep}(\boldsymbol{\epsilon}^e, \Theta, \xi_\alpha, \boldsymbol{\alpha})$ and $H^e_{tpc} := -\partial_\Theta \hat{\Psi}_{tpc}(\Theta)$, the reduced energy balance equation in entropy form, can be written as

$$\begin{aligned} \Theta \dot{H}^e_{tep} &= -\mathrm{DIV}[\boldsymbol{Q}] + R + \mathcal{D}_{mech} - \mathcal{H}^{pc} \quad \text{with} \\ \mathcal{H}^{pc} &:= \dot{L} = \Theta \dot{H}^e_{tpc} = -\Theta \partial^2_{\Theta\Theta} \hat{\Psi}_{tpc}(\Theta) \cdot \dot{\Theta}, \end{aligned} \tag{13}$$

where $\mathcal{H}^{pc} := \dot{L}$ is the phase-change heating given by the rate of latent heat L per unit reference volume.

Similarly, the reference heat capacity can be splitted into $c_0 = c_{0tep} + c_{0tpc}$ where $c_{0tep} = -\Theta \partial^2_{\Theta\Theta} \hat{\psi}_{tep}(\boldsymbol{\epsilon}^e, \Theta, \xi_\alpha, \boldsymbol{\alpha})$ and $c_{0tpc} = -\Theta \partial^2_{\Theta\Theta} \hat{\psi}_{tpc}(\Theta)$, and the temperature form of the energy balance equation takes the form

$$\begin{aligned} c_{0tep} \dot{\Theta} &= -\mathrm{DIV}[\boldsymbol{Q}] + R + \mathcal{D}_{mech} - \mathcal{H}^{ep} - \mathcal{H}^{pc} \quad \text{with} \\ \mathcal{H}^{pc} &:= \dot{L} = c_{0tpc} \dot{\Theta} = -\Theta \partial^2_{\Theta\Theta} \hat{\Psi}_{tpc}(\Theta) \cdot \dot{\Theta}. \ \square \end{aligned} \tag{14}$$

REMARK 3. *Mechanical modeling of the liquid phase.* The constitutive model presented above accounts for thermoviscous, themoelastic and thermoplastic behaviour. In particular, a pure thermoviscous constitutive model may be used at the initial liquid state and a thermoelastoplastic, with or without viscous effects, at the final solid state of a solidification process, while a continuous transition model between the initial liquid state, the intermediate mushy state and the final solid state may be defined in terms of the different phase fractions involved, i.e. the liquid fraction $f_l(\Theta) \in [0, 1]$ and the solid fraction $f_s(\Theta) \in [0, 1]$, such that $f_l(\Theta) = 1 - f_s(\Theta)$. A simple continuous model, able to characterize from a pure viscous (deviatoric) behaviour at the liquid state to a pure elastic behaviour at the solid state, can be obtained dividing by $f_s(\Theta)$ the shear deformation modulus and dividing by $f_l(\Theta)$ the elastic viscous material properties. $\square$

2.2. A J2-Thermoplastic constitutive model

Here the following J2-thermoplastic constitutive model described in BOX 1, BOX 2 and BOX 3 is considered. Uncoupled thermoelastic and hardening contributions to the free energy function given in BOX 1 are considered, as suggested by experimental results in ZBEDEL & LEHMANN [1987]. All thermomechanical material properties are considered to be temperature dependent. A particular interest has been placed in considering the case in which the specific heat is temperature dependent and the latent heat is non-zero. Note that in this case the functional related to the pure thermal contribution is obtained through an integral expression. Phase-change straining due to shrinkage is considered within the thermoelastic coupling contribution to the free energy function. Mechanical behaviour within the transition between the initial liquid-like state and the final solid state has been accounted for dividing by the solid volume fraction $f_s(\Theta)$ the given shear modulus $\bar{\mu}(\Theta)$ and dividing by the liquid volume fraction $f_l(\Theta)$ the given elatic viscosity $\bar{\eta}_v(\Theta)$.

BOX 3. J2-Thermoplastic constitutive model. Thermoplastic response.

■ **Thermoplastic response**

i. Von Mises yield function with flow stress $\sigma_Y(\Theta) := y_0(\Theta)$,

$$\hat{\phi}(\boldsymbol{\sigma}, q, \Theta) = \|\mathrm{dev}[\boldsymbol{\sigma}]\| - \sqrt{\frac{2}{3}}[\sigma_Y(\Theta) - q].$$

ii. Hardening variable q conjugate to ξ,

$$q := -\partial_\xi \hat{\psi} = -[h(\Theta)\xi - (y_0(\Theta) - y_\infty(\Theta))(1 - \exp(-\delta\xi))].$$

iii. Linear thermal softening,

$$\left.\begin{aligned} y_0(\Theta) &= y_0(\Theta_0)[1 - w_0(\Theta - \Theta_0)], \\ y_\infty(\Theta) &= y_\infty(\Theta_0)[1 - w_\infty(\Theta - \Theta_0)], \\ h(\Theta) &= h(\Theta_0)[1 - w_h(\Theta - \Theta_0)]. \end{aligned}\right\}$$

iv. Plastic evolution laws,

$$\left.\begin{aligned} \dot{\boldsymbol{\epsilon}}^p &:= \gamma\, \boldsymbol{n} \qquad \text{with} \qquad \boldsymbol{n} := \mathrm{dev}[\boldsymbol{\sigma}]/\|\mathrm{dev}[\boldsymbol{\sigma}]\|, \\ \dot{\xi}_\alpha &:= \gamma\, \sqrt{2/3}, \\ \dot{H}^p &:= -\gamma\, \sqrt{2/3}\, \sigma_Y'(\Theta). \end{aligned}\right\}$$

BOX 1. J2-Thermoplastic constitutive model. Free energy function.

■ **Free energy function**

$$\hat{\psi}(\boldsymbol{\epsilon}^e, \xi, \Theta, \boldsymbol{\alpha}) = \hat{W}(\boldsymbol{\epsilon}^e, \Theta, \boldsymbol{\alpha}) + \hat{M}(\boldsymbol{\epsilon}^e, \Theta, \boldsymbol{\alpha}) + \hat{T}(\Theta) + \hat{K}(\xi, \Theta)$$

i. Linear hyperelastic response ($\mu(\Theta) > 0$, $\kappa(\Theta) > 0$),

$$\hat{W}(\boldsymbol{\epsilon}^e, \Theta, \boldsymbol{\alpha}) = \hat{\bar{W}}(\mathrm{dev}[\boldsymbol{\epsilon}^e - \boldsymbol{\alpha}], \Theta) + \hat{U}(\mathrm{tr}[\boldsymbol{\epsilon}^e - \boldsymbol{\alpha}], \Theta)$$
$$\hat{\bar{W}}(\mathrm{dev}[\boldsymbol{\epsilon}^e - \boldsymbol{\alpha}], \Theta) = \mu(\Theta)\ \mathrm{dev}^2[\boldsymbol{\epsilon}^e - \boldsymbol{\alpha}],$$
$$\hat{U}(\mathrm{tr}[\boldsymbol{\epsilon}^e - \boldsymbol{\alpha}], \Theta) = \frac{1}{2}\kappa(\Theta)\ \mathrm{tr}^2[\boldsymbol{\epsilon}^e - \boldsymbol{\alpha}],$$

with $\mu(\Theta) = \bar{\mu}(\theta)/f_s(\Theta)$ where $f_s(\Theta) \in [0, 1]$.

ii. Thermoelastic coupling,

$$\hat{M}(\boldsymbol{\epsilon}^e, \Theta, \boldsymbol{\alpha}) = -\kappa(\Theta)[\hat{e}(\Theta) - \hat{e}(\Theta_0)]\ \mathrm{tr}[\boldsymbol{\epsilon}^e - \boldsymbol{\alpha}],$$

where

$$\hat{e}(\Theta) := 3\alpha(\Theta)(\Theta - \Theta_{ref}) + e^{ps}(\Theta),$$

iii. Thermal contribution ($c_s(\Theta) > 0$),

IF ($c_s(\Theta)$=constant AND $L(\Theta) = 0$) THEN

$$\hat{T}(\Theta) = \rho_0 c_s[(\Theta - \Theta_0) - \Theta \log(\Theta/\Theta_0)],$$

ELSE

$$\hat{T}(\Theta) = \int_{\Theta_0}^{\Theta} \hat{T}_\Theta(\bar{\Theta}) d\bar{\Theta}, \quad \hat{T}_\Theta(\Theta) = -\int_{\Theta_0}^{\Theta} [\rho_o c_s(\bar{\Theta}) + L'(\bar{\Theta})] \frac{d\bar{\Theta}}{\bar{\Theta}},$$

END IF

iv. Hardening potential,

$$\hat{K}(\xi, \Theta) = \frac{1}{2}h(\Theta)\xi^2 - [y_0(\Theta) - y_\infty(\Theta)]\hat{H}(\xi),$$

$$\text{where} \quad \hat{H}(\xi) := \begin{cases} \xi - [1 - \exp(-\delta\xi)]/\delta, & \text{if } \delta \neq 0; \\ 0, & \text{if } \delta = 0. \end{cases}$$

BOX 2. J2-Thermoplastic constitutive model. Thermoelastic/viscous response.

■ **Thermoelastic response**

i. Cauchy stresses,

$$\begin{aligned}\boldsymbol{\sigma} &= p\mathbf{1}_3 + \boldsymbol{s},\\ p &= \kappa(\Theta)\ \mathrm{tr}[\boldsymbol{\epsilon}^e - \boldsymbol{\alpha}] - \kappa(\Theta)[\hat{e}(\Theta) - \hat{e}(\Theta_0)],\\ \boldsymbol{s} &= 2\mu(\Theta)\ \mathrm{dev}[\boldsymbol{\epsilon}^e - \boldsymbol{\alpha}].\end{aligned}$$

ii. Elastic entropy,

IF ($c_s(\Theta)$=constant AND $L(\Theta) = 0$) THEN

$$\begin{aligned}H^e &= \rho_0 c_s \log(\Theta/\Theta_0) + \kappa(\Theta)[3\alpha(\Theta) + e^{ps}_{\Theta}(\Theta)]\ \mathrm{tr}[\boldsymbol{\epsilon}^e - \boldsymbol{\alpha}] - \hat{K}_\Theta(\xi)\\ &+ 3\kappa(\Theta)\alpha'(\Theta)(\Theta - \Theta_{ref})\mathrm{tr}[\boldsymbol{\epsilon}^e - \boldsymbol{\alpha}] + \kappa'(\Theta)[\hat{e}(\Theta) - \hat{e}(\Theta_0)]\mathrm{tr}[\boldsymbol{\epsilon}^e - \boldsymbol{\alpha}]\\ &- \hat{W}_\Theta(\boldsymbol{\epsilon}^e, \Theta, \boldsymbol{\alpha}),\end{aligned}$$

ELSE

$$\begin{aligned}H^e &= \int_{\Theta_0}^{\Theta} [\rho_0 c_s(\bar{\Theta}) + L'(\bar{\Theta})]\frac{d\bar{\Theta}}{\bar{\Theta}} + \kappa(\Theta)[3\alpha(\Theta) + e^{ps}_{\Theta}(\Theta)]\ \mathrm{tr}[\boldsymbol{\epsilon}^e - \boldsymbol{\alpha}] - \hat{K}_\Theta(\xi)\\ &+ 3\kappa(\Theta)\alpha'(\Theta)(\Theta - \Theta_{ref})\mathrm{tr}[\boldsymbol{\epsilon}^e - \boldsymbol{\alpha}] + \kappa'(\Theta)[\hat{e}(\Theta) - \hat{e}(\Theta_0)]\mathrm{tr}[\boldsymbol{\epsilon}^e - \boldsymbol{\alpha}]\\ &- \hat{W}_\Theta(\boldsymbol{\epsilon}^e, \Theta, \boldsymbol{\alpha}),\end{aligned}$$

END IF

■ **Thermoviscous response**

i. Viscous stresses,

$$\boldsymbol{\beta} = \boldsymbol{\sigma}$$

ii. Evolution equations ($\bar{\eta}_v(\Theta) > 0, f_l(\Theta) \in [0,1]$),

$$\begin{aligned}\mathrm{dev}[\dot{\boldsymbol{\alpha}}] &= \frac{1}{\eta_v^{dev}}\ \boldsymbol{s} = \frac{f_l(\Theta)}{\bar{\eta}_v(\Theta)}\ \boldsymbol{s},\\ \mathrm{tr}[\dot{\boldsymbol{\alpha}}] &= \frac{1}{\eta_v^{vol}}\ 3\,p.\end{aligned}$$

2.3. Thermomechanical contact model

(A) *Contact kinematics.* Let $2 \leq n_{dim} \leq 3$ be the space dimension and $I := [0,T] \subset$

$\mathbb{R}_+$ the time interval of interest. Let the open sets $\Omega^{(1)} \subset \mathbb{R}^{n_{dim}}$ and $\Omega^{(2)} \subset \mathbb{R}^{n_{dim}}$ with smooth boundaries $\partial\Omega^{(1)}$ and $\partial\Omega^{(2)}$ and closures $\bar{\Omega}^{(1)} := \Omega^{(1)} \cup \partial\Omega^{(1)}$ and $\bar{\Omega}^{(2)} := \Omega^{(2)} \cup \partial\Omega^{(2)}$, be the reference placement of two continuum bodies $\mathcal{B}^{(1)}$ and $\mathcal{B}^{(2)}$, with material particles labeled $\boldsymbol{X} \in \bar{\Omega}^{(1)}$ and $\boldsymbol{Y} \in \bar{\Omega}^{(2)}$ respectively.

Denote by $\boldsymbol{\varphi}^{(i)} : \bar{\Omega}^{(i)} \times \mathbb{I} \to \mathbb{R}^{n_{dim}}$ the orientation preserving deformation map of the body $\mathcal{B}^{(i)}$, with material velocities $\boldsymbol{V}^{(i)} := \partial_t \boldsymbol{\varphi}^{(i)}$ and deformation gradients $\boldsymbol{F}^{(i)} := D\boldsymbol{\varphi}^{(i)}$. For each time $t \in I$, the mapping $t \in \mathbb{I} \mapsto \boldsymbol{\varphi}_t^{(i)} := \boldsymbol{\varphi}^{(i)}(\cdot, t)$ represents a one-parameter family of configurations indexed by time t, which maps the reference placement of body $\mathcal{B}^{(i)}$ onto its current placement $\mathcal{S}_t^{(i)} : \boldsymbol{\varphi}_t^{(i)}(\mathcal{B}^{(i)}) \subset \mathbb{R}^{n_{dim}}$.

We will denote as the *contact surface* $\Gamma^{(i)} \subset \partial\Omega^{(i)}$ the part of the boundary of the body $\mathcal{B}^{(i)}$ such that all material points where contact will occur at any time $t \in \mathbb{I}$ are included. The current placement of the contact surface $\Gamma^{(i)}$ is given by $\gamma^{(i)} := \boldsymbol{\varphi}_t^{(i)}(\Gamma^{(i)})$.

Attention will be focussed to material points on these surfaces denoted as $\boldsymbol{X} \in \Gamma^{(1)}$ and $\boldsymbol{Y} \in \Gamma^{(2)}$. Current placement of these particles is given by $\boldsymbol{x} = \boldsymbol{\varphi}_t^{(1)}(\boldsymbol{X}) \in \gamma^{(1)}$ and $\boldsymbol{y} = \boldsymbol{\varphi}_t^{(2)}(\boldsymbol{Y}) \in \gamma^{(2)}$.

Using a standard notation in contact mechanics we will assign to each pair of contact surfaces involved in the problem, the roles of *slave* and *master* surface. In particular, let $\Gamma^{(1)}$ be the *slave surface* and $\Gamma^{(2)}$ be the *master surface*. Additionally, we will denote *slave particles* and *master particles* to the material points of the slave and master surfaces, respectively. With this notation in hand, we will require that any slave particle may not penetrate the master surface, at any time $t \in \mathbb{I}$. Although in the continuum setting the slave-master notation plays no role, in the discrete setting this choice becomes important.

Contact surfaces parametrization. Let $\mathcal{A}^{(i)} \subset \mathbb{R}^{n_{dim}-1}$ be a parent domain for the contact surface of body $\mathcal{B}^{(i)}$. A parametrization of the contact surface for each body $\mathcal{B}^{(i)}$ is introduced by a family of (orientation preserving) one-parameter mappings indexed by time, $\boldsymbol{\psi}_t^{(i)} : \mathcal{A}^{(i)} \subset \mathbb{R}^{n_{dim}-1} \to \mathbb{R}^{n_{dim}}$ such that $\Gamma^{(i)} := \boldsymbol{\psi}_0^{(i)}(\mathcal{A}^{(i)})$ and $\gamma^{(i)} := \boldsymbol{\psi}_t^{(i)}(\mathcal{A}^{(i)})$. Using the mapping composition rule, it also follows that $\boldsymbol{\psi}_t^{(i)} = \boldsymbol{\varphi}_t^{(i)} \circ \boldsymbol{\psi}_0^{(i)}$. It will be assumed in what follows that these parametrizations have the required smoothness conditions.

Within the slave-master surface role, focuss will be placed on the parametrization of the master surface. Using the parametrization of the contact surfaces introduced above we consider a point $\boldsymbol{\xi} := (\xi^1, \xi^2) \in \mathcal{A}^{(2)}$ of the parent domain, such that

$$\begin{aligned} \boldsymbol{Y} &:= \boldsymbol{\psi}_0^{(2)}(\boldsymbol{\xi}) \,, \qquad & \boldsymbol{y} &:= \boldsymbol{\psi}_t^{(2)}(\boldsymbol{\xi}) \\ \boldsymbol{E}_\alpha &:= \boldsymbol{\psi}_{0,\alpha}^{(2)}(\boldsymbol{\xi}) \,, \qquad & \boldsymbol{e}_\alpha &:= \boldsymbol{\psi}_{t,\alpha}^{(2)}(\boldsymbol{\xi}) \end{aligned} \tag{15}$$

where $\boldsymbol{Y}$ and $\boldsymbol{y}$ are, respectively, the reference and current placement of a master particle and $\boldsymbol{E}_\alpha$ and $\boldsymbol{e}_\alpha$, $\alpha = 1, 2$ are the convected surface basis attached to the master particle $\boldsymbol{Y} \in \Gamma^{(2)}$, on the reference and current configuration, respectively. Here $(\cdot)_{,\alpha}$ denotes partial derivative with respect to ξ^α.

Closest-point-projection map and normal gap. Let $\hat{\hat{\boldsymbol{Y}}} : \Gamma^{(2)} \to \Gamma^{(1)}$ be the closest-

point-projection map defined as

$$\hat{\bar{\boldsymbol{Y}}}(\boldsymbol{X},t) := \arg \min_{\boldsymbol{Y}\in\Gamma^{(2)}} \{\|\boldsymbol{\varphi}_t^{(1)}(\boldsymbol{X}) - \boldsymbol{\varphi}_t^{(2)}(\boldsymbol{Y})\|\}, \tag{16}$$

and set

$$\bar{\boldsymbol{Y}} := \hat{\bar{\boldsymbol{Y}}}(\boldsymbol{X},t), \qquad \bar{\boldsymbol{y}} := \boldsymbol{\varphi}_t^{(2)}(\bar{\boldsymbol{Y}}) \tag{17}$$

where $\bar{\boldsymbol{y}} \in \gamma^{(2)}$ is the closest-point projection of the current position of the slave point $\boldsymbol{X}$ onto the current placement of the master surface $\Gamma^{(2)}$. Let $g_N := \hat{g}_N(\boldsymbol{X},t)$ be the normal gap function defined for any slave particle $\boldsymbol{X} \in \Gamma^{(1)}$ and for any time $t \in \mathbb{I}$ as

$$g_N := \hat{g}_N(\boldsymbol{X},t) := -[\![\boldsymbol{\varphi}]\!] \cdot \boldsymbol{\nu} \tag{18}$$

where $[\![\boldsymbol{\varphi}]\!] := \boldsymbol{\varphi}_t^{(1)}(\boldsymbol{X}) - \boldsymbol{\varphi}_t^{(2)}(\bar{\boldsymbol{Y}})$ gives the jump of the deformation map at the contact surface and $\boldsymbol{\nu} : \gamma^{(2)} \to S^2$ is the unit outward normal field to the current placement of the master surface particularized at the closest-point projection $\bar{\boldsymbol{y}} \in \gamma^{(2)}$.

Convected basis, metric and curvature tensors at the closest-point projection. Associated to the closest-point projection given by (16), for some point $\bar{\boldsymbol{\xi}} := (\bar{\xi}^1, \bar{\xi}^2) \in \mathcal{A}^{(2)}$ of the parent domain we will have

$$\bar{\boldsymbol{Y}} := \boldsymbol{\psi}_0^{(2)}(\bar{\boldsymbol{\xi}}) \,, \qquad \bar{\boldsymbol{y}} := \boldsymbol{\psi}_t^{(2)}(\bar{\boldsymbol{\xi}}) \tag{19}$$

Attached to the master particle $\bar{\boldsymbol{Y}} \in \Gamma^{(2)}$ we define the convected surface basis on the reference and current configurations, respectively, as

$$\boldsymbol{\tau}_\alpha^{ref} := \boldsymbol{E}_\alpha(\bar{\boldsymbol{\xi}}) \,, \qquad \boldsymbol{\tau}_\alpha := \boldsymbol{e}_\alpha(\bar{\boldsymbol{\xi}}) \tag{20}$$

Additionaly, the unit outward normals $\boldsymbol{\nu}^{ref} \in S^2$ and $\boldsymbol{\nu} \in S^2$ at the master particle $\bar{\boldsymbol{Y}}$ on the reference and current configurations, respectively, can be defined as

$$\boldsymbol{\nu}^{ref} := \frac{\boldsymbol{\tau}_1^{ref} \times \boldsymbol{\tau}_2^{ref}}{\|\boldsymbol{\tau}_1^{ref} \times \boldsymbol{\tau}_2^{ref}\|} \,, \qquad \boldsymbol{\nu} := \frac{\boldsymbol{\tau}_1 \times \boldsymbol{\tau}_2}{\|\boldsymbol{\tau}_1 \times \boldsymbol{\tau}_2\|} \tag{21}$$

The vectors $\boldsymbol{\tau}_\alpha^{ref} \in T_{\nu^{ref}}S^2$ and $\boldsymbol{\tau}_\alpha \in T_\nu S^2$, $\alpha = 1,2$ span the tangent spaces $T_{\nu^{ref}}S^2$ and $T_\nu S^2$ to the S^2 unit sphere at $\boldsymbol{\nu}^{ref}$ and $\boldsymbol{\nu}$, respectively. Here the tangent space to the S^2 unit sphere at $\boldsymbol{\nu} \in S^2$ is defined as

$$T_\nu S^2 := \{\delta\boldsymbol{\nu} \in \mathbb{R}^{n_{dim}} \;:\; \delta\boldsymbol{\nu} \cdot \boldsymbol{\nu} = 0\} \tag{22}$$

The convected surface basis vectors $\boldsymbol{\tau}_\alpha^{ref}$ and $\boldsymbol{\tau}_\alpha$, $\alpha = 1,2$, augmented with the unit outward normals $\boldsymbol{\nu}^{ref}$ and $\boldsymbol{\nu}$, provides local spatial frames at the master particle $\bar{\boldsymbol{Y}}(\boldsymbol{X},t)$ on the reference and current configurations, respectively.

The convected surface basis vectors $\boldsymbol{\tau}_\alpha^{ref}$ and $\boldsymbol{\tau}_\alpha$, $\alpha = 1,2$, induces a surface metric or first fundamental form on the reference and current configurations, defined respectively as

$$M_{\alpha\beta} := \boldsymbol{\tau}_\alpha^{ref} \cdot \boldsymbol{\tau}_\beta^{ref} \,, \qquad m_{\alpha\beta} := \boldsymbol{\tau}_\alpha \cdot \boldsymbol{\tau}_\beta \tag{23}$$

Inverse surface metrics $M^{\alpha\beta}$ and $m^{\alpha\beta}$ are defined in the usual manner. Additionally, dual surface basis on the reference and current configurations are straightforward defined respectively as

$$\boldsymbol{\tau}^{\alpha}_{ref} := M^{\alpha\beta}\boldsymbol{\tau}^{ref}_{\beta} \ , \qquad \boldsymbol{\tau}^{\alpha} := m^{\alpha\beta}\boldsymbol{\tau}_{\beta} \tag{24}$$

The variation of the convected surface basis along the convected coordinates, together with the unit normal, induces the second fundamental form or surface curvature defined, on the reference and current configurations, as

$$\kappa^{ref}_{\alpha\beta} := \boldsymbol{E}_{\alpha,\beta}(\bar{\boldsymbol{\xi}}) \cdot \boldsymbol{\nu}^{ref} \ , \qquad \kappa_{\alpha\beta} := \boldsymbol{e}_{\alpha,\beta}(\bar{\boldsymbol{\xi}}) \cdot \boldsymbol{\nu} \tag{25}$$

(B) *Local form of energy balance equation.* The local form of the energy balance equation at the contact surface take the form, see LAURSEN [1998],

$$\Theta_c \dot{H}_c = Q^{(1)}_c + Q^{(2)}_c + \mathcal{D}_{c,int} \qquad \text{on} \quad \Gamma^{(1)} \times \mathbb{I} \tag{26}$$

where $\Theta_c > 0$ is the absolute contact temperature, H_c the contact entropy per unit reference surface $\Gamma^{(1)}$, $Q^{(\alpha)}_c$, $\alpha = 1, 2$ are the outward normal nominal heat fluxes on the contact surface of bodies $\mathcal{B}^{\alpha}$, $\alpha = 1, 2$, per unit reference surface $\Gamma^{(1)}$ and $\mathcal{D}_{c,int}$ is the contact internal dissipation per unit reference surface $\Gamma^{(1)}$.

(C) *Dissipation inequalities.* The contact specific entropy H_c is defined via constitutive relations, typically formulated in terms of the contact internal energy E_c, and subjected to the following restriction on the contact internal dissipation, see LAURSEN [1998],

$$\mathcal{D}_{c,int} := -\boldsymbol{t}^{(1)} \cdot [\![\boldsymbol{V}]\!] + \Theta_c \dot{H}_c - \dot{E}_c \geq 0 \qquad \text{on} \quad \Gamma^{(1)} \times \mathbb{I} \tag{27}$$

where $[\![\boldsymbol{V}]\!] := \boldsymbol{V}^{(1)} - \boldsymbol{V}^{(2)}$ denotes the jump in the material velocities field accross the contact surface and $\boldsymbol{t}^{(1)}$ is the nominal contact traction on $\Gamma^{(1)}$.

Introducing the nominal contact pressure t_N, as the projection of the nominal traction $\boldsymbol{t}^{(1)}$ onto the unit normal $\boldsymbol{\nu}$, and nominal frictional tangent traction components $t_{T\alpha}$ on the convected dual basis $\boldsymbol{\tau}^{\alpha}$, $\alpha = 1, 2$, as (minus) the projection of the nominal traction $\boldsymbol{t}^{(1)}$ onto the convected basis $\boldsymbol{\tau}_{\alpha}$,

$$t_N := \boldsymbol{t}^{(1)} \cdot \boldsymbol{\nu}, \qquad t_{T\alpha} := -\boldsymbol{t}^{\flat\,(1)} \cdot \boldsymbol{\tau}_{\alpha} \tag{28}$$

and using the expressions

$$\dot{g}_N = -[\![\boldsymbol{V}]\!] \cdot \boldsymbol{\nu}, \qquad \dot{g}^{\alpha}_T|_{g_N=0} := [\![\boldsymbol{V}]\!] \cdot \boldsymbol{\tau}^{\alpha} \tag{29}$$

and the following relation holds

$$-\boldsymbol{t}^{(1)} \cdot [\![\boldsymbol{V}]\!] = t_N \dot{g}_N + t_{T\alpha} \dot{g}^{\alpha}_T \tag{30}$$

the contact internal dissipation given by (27) takes the form

$$\mathcal{D}_{c,int} := t_N \dot{g}_N + t_{T\alpha} \dot{g}^{\alpha}_T + \Theta_c \dot{H}_c - \dot{E}_c \geq 0 \qquad \text{on} \quad \Gamma^{(1)} \times \mathbb{I} \tag{31}$$

The outward normal nominal heat fluxes $Q^{(\alpha)}_c$, $\alpha = 1, 2$, are subjected to the following restriction on the dissipation by conduction

$$\mathcal{D}_{c,con} := \frac{Q^{(1)}_c}{\Theta^{(1)}}(\Theta^{(1)} - \Theta_c) + \frac{Q^{(2)}_c}{\Theta^{(2)}}(\Theta^{(2)} - \Theta_c) \geq 0 \qquad \text{on} \quad \Gamma^{(1)} \times \mathbb{I} \tag{32}$$

(D) *Thermofrictional contact constitutive equations.* Phenomenological frictional models adopt a local additive decomposition of the tangential gap into elastic and plastic parts. Frictional hardening mechanisms taking place at a microstructural level are characterized by an additional set of phenomenological internal variables collectively denoted here by $\zeta_{c\beta}$. Furthermore, an additive split of the local contact entropy into elastic and plastic has been adopted, following a parallel approach to the bulk continua case. The above considerations, motivate the following additive split of the tangential gap $g_{T\,\alpha} := g_T^{e\,\alpha} + g_T^{p\,\alpha}$, $\alpha = 1, 2$, and contact local entropy per unit reference surface $H_c := H_c^e + H_c^p$ and the following set of frictional internal variables $\boldsymbol{G}_c^p := \{g_{T\,\alpha}^p, H_c^p, \zeta_{c\beta}\}$.

The internal contact energy function $\hat{E}_c$ per unit contact surface $\Gamma^{(1)}$ depends on the normal gap, the elastic part of the tangential slip $g_T^{e\,\alpha}$, the frictional hardening internal variables $\zeta_{c\beta}$ and the configurational contact entropy H_c^e, taking the functional form $E_c = \hat{E}_c(g_T^{e\,\alpha}, H_c^e, \zeta_{c\beta})$. Introducing the functional form of the contact internal energy into the expression of the contact internal dissipation, taking the time derivative, applying the chain rule and using the additive split of the tangential gap and total contact entropy, a straightforward argument yields the following contact constitutive equations and reduced internal dissipation inequality

$$\left.\begin{aligned} t_N &= \partial_{g_N} \hat{E}_c(g_N, g_T^{e\,\alpha}, H_c^e, \zeta_{c\beta}), \\ t_{T\,\alpha} &= \partial_{g_T^{e\,\alpha}} \hat{E}_c(g_N, g_T^{e\,\alpha}, H_c^e, \zeta_{c\beta}), \\ \Theta_c &= \partial_{H_c^e} \hat{E}_c(g_N, g_T^{e\,\alpha}, H_c^e, \zeta_{c\beta}), \\ q_c^\beta &:= -\,\partial_{\zeta_{c\beta}} \hat{E}_c(g_N, g_T^{e\,\alpha}, H_c^e, \zeta_{c\beta}), \end{aligned}\right\} \tag{33}$$

$$\begin{aligned} \mathcal{D}_{c,int} &:= \mathcal{D}_{c,mech} + \mathcal{D}_{c,ther} \geq 0, \quad \text{with} \\ \mathcal{D}_{c,mech} &:= t_{T\,\alpha} \dot{g}_T^{p\,\alpha} + q_c^\beta \dot{\zeta}_{c\beta} \geq 0 \;\text{ and }\; \mathcal{D}_{c,ther} := \Theta_c \dot{H}_c^p. \end{aligned} \tag{34}$$

Using the Legendre transformation $\Psi_c = E_c - \Theta_c H_c^e$, the contact free energy function takes the functional form $\Psi_c = \hat{\Psi}_c(g_N, g_T^{e\,\alpha}, \Theta_c, \zeta_{c\beta})$. Taking the time derivative of the contact free energy function and applying the chain rule, a straightforward argument yields the following alternative expressions for the contact constitutive equations

$$\left.\begin{aligned} t_N &= \partial_{g_N} \hat{\psi}_c(g_N, g_T^{e\,\alpha}, \Theta_c, \zeta_{c\beta}), \\ t_{T\,\alpha} &= \partial_{g_T^{e\,\alpha}} \hat{\psi}_c(g_N, g_T^{e\,\alpha}, \Theta_c, \zeta_{c\beta}), \\ H_c^e &= -\,\partial_{\Theta_c} \hat{\psi}_c(g_N, g_T^{e\,\alpha}, \Theta_c, \zeta_{c\beta}), \\ q_c^\beta &:= -\,\partial_{\zeta_{c\beta}} \hat{\psi}_c(g_N, g_T^{e\,\alpha}, \Theta_c, \zeta_{c\beta}). \end{aligned}\right\} \tag{35}$$

Constitutive equations for the (nominal) normal heat conduction fluxes per unit reference contact surface $\Gamma^{(1)}$ are given by

$$\begin{aligned} Q_{c,cond}^{(1)} &= \hat{h}_{cond}^{(1)}(t_N, \Theta_c)\; g_\Theta^{(1)} \quad \text{with} \quad g_\Theta^{(1)} := \Theta^{(1)} - \Theta_c, \\ Q_{c,cond}^{(2)} &= \hat{h}_{cond}^{(2)}(t_N, \Theta_c)\; g_\Theta^{(2)} \quad \text{with} \quad g_\Theta^{(2)} := \Theta^{(2)} - \Theta_c, \end{aligned} \tag{36}$$

where $\hat{h}^{(\alpha)}_{cond}(t_N, \Theta_c) > 0$, $\alpha = 1, 2$, is the heat transfer coefficient of the surface $\Gamma^{(\alpha)}$, $\alpha = 1, 2$, assumed to be a function of the contact pressure and the contact temperature. Note that (36) allows that the contact dissipation by heat conduction restriction given by (32) is unconditionally satisfied.

Assuming a slip function of the form $\Phi_c = \hat{\Phi}_c(t_N, t_{T\alpha}, \Theta_c, q_c^\beta)$, the evolution laws of the plastic internal variables take the form

$$\left.\begin{aligned} \dot{g}_T^{p\,\alpha} &= \gamma_c\, \partial_{t_{T\alpha}} \hat{\Phi}_c(t_N, t_{T\alpha}, \Theta_c, q_c^\beta), \\ \dot{H}_c^p &= \gamma_c\, \partial_{\Theta_c} \hat{\Phi}_c(t_N, t_{T\alpha}, \Theta_c, q_c^\beta), \\ \dot{\zeta}_{c\beta} &= \gamma_c\, \partial_{q_c^\beta} \hat{\Phi}_c(t_N, t_{T\alpha}, \Theta_c, q_c^\beta), \end{aligned}\right\} \tag{37}$$

and the following Kuhn-Tucker $\gamma_c \geq 0, \Phi_c \leq 0, \gamma_c \Phi_c = 0$ and consistency $\gamma_c \dot{\Phi}_c = 0$ conditions must be satisfied for a rate-independent frictional model.

REMARK 4. *Equivalent forms of the energy balance equation.* Using the additive split of the total contact entropy into elastic and plastic parts and the additive split of the contact internal dissipation into mechanical and thermal, the reduced contact energy equation can be expressed as

$$\Theta_c \dot{H}_c^e = Q_c^{(1)} + Q_c^{(2)} + \mathcal{D}_{c,mech} \qquad \text{on} \quad \Gamma^{(1)} \times \mathbb{I} \tag{38}$$

Alternatively, using the constitutive equation of the contact elastic entropy, taking its time derivative and applying the chain rule, the temperature-form of the reduced contact energy equation can be written as

$$c_{c0}\, \dot{\Theta}_c = Q_c^{(1)} + Q_c^{(2)} + \mathcal{D}_{c,mech} - \mathcal{H}^{fc} \qquad \text{on} \quad \Gamma^{(1)} \times \mathbb{I} \tag{39}$$

where the reference contact heat capacity c_{c0} and the frictional contact heating $\mathcal{H}^{fc}$ take the form

$$c_{c0} := -\Theta_c \partial^2_{\Theta_c \Theta_c} \hat{\psi}_c(g_N, g_T^{e\,\alpha}, \Theta_c, \zeta_{c\beta}), \tag{40}$$

$$\begin{aligned} \mathcal{H}^{fc} := -\Theta_c \,[\; & \partial^2_{\Theta_c\, g_N} \hat{\psi}_c(g_N, g_T^{e\,\alpha}, \Theta_c, \zeta_{c\beta}) \cdot \dot{g}_n \\ & + \partial^2_{\Theta_c\, g_T^{e\,\alpha}} \hat{\psi}_c(g_N, g_T^{e\,\alpha}, \Theta_c, \zeta_{c\beta}) \cdot \dot{g}_T^{e\,\alpha} \\ & + \partial^2_{\Theta_c\, \zeta_{c\beta}} \hat{\psi}_c(g_N, g_T^{e\,\alpha}, \Theta_c, \zeta_{c\beta}) \cdot \dot{\zeta}_{c\beta} \;], \end{aligned} \tag{41}$$

or, alternatively, using the constitutive equations (35),

$$\begin{aligned} c_{c0} &:= \Theta_c\, \partial_{\Theta_c} H_c^e, \\ \mathcal{H}^{fc} &:= -\Theta_c\, \partial_{\Theta_c} (t_n \dot{g}_n + t_{T\alpha} \dot{g}_T^\alpha - \mathcal{D}_{c,mech}). \;\square \end{aligned} \tag{42}$$

2.4. A Thermofrictional constitutive model

Here the following thermofrictional constitutive model described in BOX 4 and BOX 5 is considered. Coupled thermofrictional behaviour is considered within the thermofrictional hardening potential.

BOX 4. Thermofrictional constitutive model. Free energy function

■ **Free energy function**

$$\hat{\psi}_c(g_N, g_T^{e\,\alpha}, \Theta_c, \zeta_c) = \hat{W}_c(g_N, g_T^{e\,\alpha}) + \hat{T}_c(\Theta_c) + \hat{K}_c(\zeta_c, \Theta_c)$$

i. Linear hyperelastic response ($\epsilon_N > 0$, $\epsilon_T > 0$),

$$\hat{W}_c(g_N, g_T^{e\,\alpha}) := \frac{1}{2}\epsilon_N \langle g_N \rangle^2 + \frac{1}{2}\epsilon_T g_T^{e\,\alpha} M_{\alpha\beta} g_T^{e\,\beta}.$$

ii. Thermal contribution ($c_c > 0$),

$$\hat{T}_c(\Theta_c) := c_c[(\Theta_c - \Theta_0) - \Theta_c \log(\Theta_c/\Theta_0)].$$

iii. Hardening potential,

$$\hat{K}_c(\zeta_c, \Theta_c) := \sum_{n=1}^{m} \frac{1}{n+1} \hat{\mu}_n(\Theta_c)\, \zeta_c^{n+1}.$$

2.5. Variational formulation

Using standard procedures, the weak form of the momentum balance (we will assume the quasi-static case for simplicity) and reduced energy balance equations in $\bar{\Omega} \times \mathbb{I}$ take the following expressions:

$$\begin{aligned} &\langle \boldsymbol{\sigma}, \mathrm{GRAD}[\boldsymbol{\eta}_0] \rangle - \langle \boldsymbol{B}, \boldsymbol{\eta}_0 \rangle - \langle \bar{\boldsymbol{t}}, \boldsymbol{\eta}_0 \rangle_{\Gamma_\sigma} - \langle \boldsymbol{t}^{(1)}, \boldsymbol{\eta}_0^{(1)} \rangle_{\Gamma^{(1)}} - \langle \boldsymbol{t}^{(2)}, \boldsymbol{\eta}_0^{(2)} \rangle_{\Gamma^{(2)}} = 0 \\ &\langle \Theta \dot{H}^e, \zeta_0 \rangle - \langle \boldsymbol{Q}, \mathrm{GRAD}[\zeta_0] \rangle - \langle R + \mathcal{D}_{mech}, \zeta_0 \rangle + \langle \bar{Q}, \zeta_0 \rangle_{\Gamma_Q} \\ &\qquad + \langle \boldsymbol{Q} \cdot \boldsymbol{N}^{(1)}, \zeta_0^{(1)} \rangle_{\Gamma^{(1)}} + \langle \boldsymbol{Q} \cdot \boldsymbol{N}^{(2)}, \zeta_0^{(2)} \rangle_{\Gamma^{(2)}} = 0 \end{aligned} \tag{43}$$

which must hold for any admissible displacement and temperature variations $\boldsymbol{\eta}_0$ and ζ_0, respectively. Here $\langle \cdot, \cdot \rangle$ denotes the $L_2(\bar{\Omega})$–inner product and with a slight abuse in notation $\langle \cdot, \cdot \rangle_{\Gamma_\sigma}$, $\langle \cdot, \cdot \rangle_{\Gamma_Q}$ and $\langle \cdot, \cdot \rangle_{\Gamma^{(\alpha)}}$ denote the $L_2(\Gamma_\sigma)$, $L_2(\Gamma_Q)$ and $L_2(\Gamma^{(\alpha)})$–inner products on the boundaries Γ_σ, Γ_Q and $\Gamma^{(\alpha)}$, respectively. For the sake of notation compactness, it is implicitly asssumed that $\bar{\Omega} := \cup_{\alpha=1}^{2} \bar{\Omega}^{(\alpha)}$, $\Gamma_\sigma := \cup_{\alpha=1}^{2} \Gamma_\sigma^{(\alpha)}$ and $\Gamma_Q := \cup_{\alpha=1}^{2} \Gamma_Q^{(\alpha)}$.

Using the equilibrium of forces at the contact interface and introducing the (nominal) contact heat fluxes $Q_c^{(1)}$ and $Q_c^{(2)}$ per *unit reference surface* $\Gamma^{(1)}$, the following expressions hold

$$\begin{aligned} \langle \boldsymbol{t}^{(1)}, \boldsymbol{\eta}_0^{(2)} \rangle_{\Gamma^{(1)}} + \langle \boldsymbol{t}^{(2)}, \boldsymbol{\eta}_0^{(2)} \rangle_{\Gamma^{(2)}} &= 0 \\ \langle \boldsymbol{Q} \cdot \boldsymbol{N}^{(1)}, \zeta_0^{(1)} \rangle_{\Gamma^{(1)}} - \langle Q_c^{(1)}, \zeta_0^{(1)} \rangle_{\Gamma^{(1)}} &= 0 \\ \langle \boldsymbol{Q} \cdot \boldsymbol{N}^{(2)}, \zeta_0^{(2)} \rangle_{\Gamma^{(2)}} - \langle Q_c^{(2)}, \zeta_0^{(2)} \rangle_{\Gamma^{(1)}} &= 0 \end{aligned} \tag{44}$$

BOX 5. Thermofrictional constitutive model. Thermofrictional response

■ **Thermoelastic response**

i. Contact pressure and frictional traction,

$$t_N = \epsilon_N \langle g_N \rangle,$$
$$t_{T\alpha} = \epsilon_T M_{\alpha\beta} g_T^{e\,\beta}.$$

ii. Elastic entropy,

$$H_c^e = c_c \log(\Theta_c/\Theta_0) - \sum_{n=1}^{m} \frac{1}{n+1} \hat{\mu}_n'(\Theta_c)\, \zeta_c^{n+1}.$$

■ **Thermoplastic response**

i. Slip function,

$$\hat{\Phi}_c(t_N, t_{T\alpha}, \Theta_c, q_c) := \|\boldsymbol{t}_T^\flat\|_{ref} - (\hat{\mu}_0(\Theta_c) - q_c)\, t_N,$$

where $\|\boldsymbol{t}_T^\flat\|_{ref} := (t_{T\alpha} M^{\alpha\beta} t_{T\beta})^{1/2}$.

ii. Hardening variable q_c conjugate to ζ_c,

$$q_c := -\partial_{\zeta_c} \hat{\psi}_c = -\sum_{n=1}^{m} \hat{\mu}_n(\Theta_c)\, \zeta_c^n.$$

iii. Linear thermal softening,

$$\hat{\mu}_n(\Theta_c) = \hat{\mu}_n(\Theta_0)[1 - w_n(\Theta_c - \Theta_0)], \quad n = 1, m.$$

iv. Frictional mechanical dissipation,

$$\mathcal{D}_{c,mech} = \gamma_c\, \hat{\mu}_0(\Theta_c)\, t_N.$$

Using (44) the weak form of the balance equations (43) take the form:

$$\begin{aligned} &\langle \boldsymbol{\sigma}, \mathrm{GRAD}[\boldsymbol{\eta}_0] \rangle - \langle \boldsymbol{B}, \boldsymbol{\eta}_0 \rangle - \langle \bar{\boldsymbol{t}}, \boldsymbol{\eta}_0 \rangle_{\Gamma_\sigma} - \langle \boldsymbol{t}^{(1)}, \boldsymbol{\eta}_0^{(1)} - \boldsymbol{\eta}_0^{(2)} \rangle_{\Gamma^{(1)}} = 0 \\ &\langle \Theta \dot{H}^e, \zeta_0 \rangle - \langle \boldsymbol{Q}, \mathrm{GRAD}[\zeta_0] \rangle - \langle R + \mathcal{D}_{mech}, \zeta_0 \rangle + \langle \bar{Q}, \zeta_0 \rangle_{\Gamma_Q} \\ &\qquad + \langle Q_c^{(1)}, \zeta_0^{(1)} \rangle_{\Gamma^{(1)}} + \langle Q_c^{(2)}, \zeta_0^{(2)} \rangle_{\Gamma^{(1)}} = 0 \end{aligned} \tag{45}$$

where it is pointed out that *all contact contributions* are parametrized in terms of the

contact surface $\Gamma^{(1)}$.

Similarly, the weak form of the reduced energy balance equation on $\Gamma^{(1)} \times \mathbb{I}$ take the form:

$$\langle \Theta_c \dot{H}_c^e, \zeta_{c0} \rangle_{\Gamma^{(1)}} - \langle Q_c^{(1)} + Q_c^{(2)}, \zeta_{c0} \rangle_{\Gamma^{(1)}} - \langle \mathcal{D}_{c,mech}, \zeta_{c0} \rangle_{\Gamma^{(1)}} = 0 \tag{46}$$

which must hold for any admissible contact temperature variation ζ_{c0}.

Adding the weak form of the energy balance on $\Gamma^{(1)} \times \mathbb{I}$ given by (46), to the weak form of the energy balance in $\bar{\Omega} \times \mathbb{I}$ given by $(45)_2$, the following alternative expressions are obtained

$$\begin{aligned} &\langle \boldsymbol{\sigma}, \mathrm{GRAD}[\boldsymbol{\eta}_0] \rangle - \langle \boldsymbol{B}, \boldsymbol{\eta}_0 \rangle - \langle \bar{\boldsymbol{t}}, \boldsymbol{\eta}_0 \rangle_{\Gamma_\sigma} - \langle \boldsymbol{t}^{(1)}, \boldsymbol{\eta}_0^{(1)} - \boldsymbol{\eta}_0^{(2)} \rangle_{\Gamma^{(1)}} = 0 \\ &\langle \Theta \dot{H}^e, \zeta_0 \rangle - \langle \boldsymbol{Q}, \mathrm{GRAD}[\zeta_0] \rangle - \langle R + \mathcal{D}_{mech}, \zeta_0 \rangle + \langle \bar{Q}, \zeta_0 \rangle_{\Gamma_Q} \\ &\qquad + \langle Q_c^{(1)}, \zeta_0^{(1)} - \zeta_{c0} \rangle_{\Gamma^{(1)}} + \langle Q_c^{(2)}, \zeta_0^{(2)} - \zeta_{c0} \rangle_{\Gamma^{(1)}} \\ &\qquad\qquad + \langle \Theta_c \dot{H}_c^e, \zeta_{c0} \rangle_{\Gamma^{(1)}} - \langle \mathcal{D}_{c,mech}, \zeta_{c0} \rangle_{\Gamma^{(1)}} = 0 \end{aligned} \tag{47}$$

3. TIME INTEGRATION OF THE COUPLED THERMOPLASTIC PROBLEM

The numerical solution of the coupled thermomechanical IBVP involves the transformation of an infinite dimensional dynamical system, governed by a system of quasi-linear partial differential equations into a sequence of discrete nonlinear algebraic problems by means of a Galerkin finite element projection and a time marching scheme for the advancement of the primary nodal variables, i.e. displacements and temperatures, together with a return mapping algorithm for the advancement of the internal variables.

Here, attention will be placed to the time integration schemes of the governing equations of the coupled thermoplastic problem. In particular, we are interested in a class of unconditionally stable staggered solution schemes, based on a *product formula algorithm* arising from an operator split of the governing evolution equations. These methods fall within the classical *fractional step methods.*

3.1. Local evolution problem

Consider the following (homogeneous) first order dissipative local problems of evolution, see Simo [1994], Agelet de Saracibar *et al.* [1997], Laursen [1998],

i. *Evolution problem in* $\bar{\Omega} \times \mathbb{I}$. Consider the local dissipative problem of evolution for the (homogeneous) thermoplastic problem, written as

$$\left.\begin{aligned} \frac{d}{dt}\boldsymbol{Z} &= \boldsymbol{A}[\boldsymbol{Z}, \boldsymbol{\Gamma}] \quad \text{in} \quad \bar{\Omega} \times \mathbb{I}, \\ \boldsymbol{Z}|_{t=0} &= \boldsymbol{Z}_0 \qquad \text{in} \quad \bar{\Omega}, \end{aligned}\right\} \tag{48}$$

along with

$$\left.\begin{aligned} \frac{d}{dt}\boldsymbol{\Gamma}^p &= \gamma\, \boldsymbol{G}^p[\boldsymbol{Z}, \boldsymbol{\Gamma}] \quad \text{in} \quad \bar{\Omega} \times \mathbb{I}, \\ \boldsymbol{\Gamma}^p|_{t=0} &= 0 \qquad\qquad \text{in} \quad \bar{\Omega}, \end{aligned}\right\} \quad \text{and} \quad \left.\begin{aligned} \frac{d}{dt}\boldsymbol{\Gamma}^v &= \boldsymbol{G}^v[\boldsymbol{Z}, \boldsymbol{\Gamma}] \quad \text{in} \quad \bar{\Omega} \times \mathbb{I}, \\ \boldsymbol{\Gamma}^v|_{t=0} &= 0 \qquad\qquad \text{in} \quad \bar{\Omega}, \end{aligned}\right\} \tag{49}$$

where $\boldsymbol{Z}$, lying in a suitable Sobolev space $\mathcal{Z}$, is a set of primary independent variables, $\boldsymbol{\Gamma} := \{\boldsymbol{\Gamma}^p, \boldsymbol{\Gamma}^v\}$ is a set of internal variables, $\boldsymbol{A}[\boldsymbol{Z}, \boldsymbol{\Gamma}]$ and $\boldsymbol{G}[\boldsymbol{Z}, \boldsymbol{\Gamma}]$ are nonlinear operators and $\gamma \geq 0$ is a plastic multiplier.

ii. *Evolution problem on* $\Gamma^{(1)} \times \mathbb{I}$. Consider the dissipative local problem of evolution for the frictional contact problem, written as

$$\left.\begin{aligned} \frac{d}{dt}\boldsymbol{Z}_c &= \boldsymbol{A}_c[\bar{\boldsymbol{Z}}, \bar{\boldsymbol{\Gamma}}] \quad \text{on} \quad \Gamma^{(1)} \times \mathbb{I}, \\ \boldsymbol{Z}_c|_{t=0} &= \boldsymbol{Z}_{c0} \qquad\quad \text{on} \quad \Gamma^{(1)}, \end{aligned}\right\} \tag{50}$$

along with

$$\left.\begin{aligned} \frac{d}{dt}\boldsymbol{\Gamma}_c &= \gamma_c\, \boldsymbol{G}_c[\bar{\boldsymbol{Z}}, \bar{\boldsymbol{\Gamma}}] \quad \text{on} \quad \Gamma^{(1)} \times \mathbb{I}, \\ \boldsymbol{\Gamma}_c|_{t=0} &= 0 \qquad\qquad\quad \text{on} \quad \Gamma^{(1)}, \end{aligned}\right\} \tag{51}$$

where $\boldsymbol{Z}_c$, lying in a suitable Sobolev space $\mathcal{Z}_c$, is a set of primary independent variables, $\boldsymbol{\Gamma}_c$ is a set of internal variables, $\boldsymbol{A}_c[\bar{\boldsymbol{Z}}, \bar{\boldsymbol{\Gamma}}]$ and $\boldsymbol{G}_c[\bar{\boldsymbol{Z}}, \bar{\boldsymbol{\Gamma}}]$ are nonlinear operators and $\gamma_c \geq 0$ is a frictional multiplier. Additionally, collecting variables and using a compact notation, we introduce the following set of variables, $\bar{\boldsymbol{Z}} := \{\boldsymbol{Z}, \boldsymbol{Z}_c\}$ and $\bar{\boldsymbol{\Gamma}} := \{\boldsymbol{\Gamma}, \boldsymbol{\Gamma}_c\}$, and nonlinear operators, $\bar{\boldsymbol{A}}[\bar{\boldsymbol{Z}}, \bar{\boldsymbol{\Gamma}}] := \{\boldsymbol{A}[\boldsymbol{Z}, \boldsymbol{\Gamma}], \boldsymbol{A}_c[\bar{\boldsymbol{Z}}, \bar{\boldsymbol{\Gamma}}]\}$ and $\bar{\boldsymbol{G}}[\bar{\boldsymbol{Z}}, \bar{\boldsymbol{\Gamma}}] := \{\boldsymbol{G}[\boldsymbol{Z}, \boldsymbol{\Gamma}], \boldsymbol{G}_c[\bar{\boldsymbol{Z}}, \bar{\boldsymbol{\Gamma}}]\}$.

In the formulation of the fractional step method described below, it is essential to regard the set of internal variables $\bar{\boldsymbol{\Gamma}}$ as *implicitly defined* in terms of the variables $\bar{\boldsymbol{Z}}$ via the evolution equations. Therefore $\bar{\boldsymbol{Z}}$ are the only independent variables and their choice becomes a crucial aspect in the formulation of the fractional step method. We refer to SIMO [1994], AGELET DE SARACIBAR *et al.* [1997] and LAURSEN [1998] for further details.

Motivated by the structure and the design constraints of the isentropic split described below, we consider the following set of *conservation/entropy/latent heat* variables $\bar{\boldsymbol{Z}}$

$$\bar{\boldsymbol{Z}} := \{\boldsymbol{Z}, \boldsymbol{Z}_c\}, \tag{52}$$

where

$$\boxed{\begin{aligned} \boldsymbol{Z} &:= \{\boldsymbol{\varphi}, \boldsymbol{p}, H^e, H^p, L\} \quad \text{in} \quad \Omega \times \mathbb{I}, \\ \boldsymbol{Z}_c &:= \{H_c^e, H_c^p\} \qquad\quad \text{on} \quad \Gamma^{(1)} \times \mathbb{I}, \end{aligned}} \tag{53}$$

along with the set of plastic strain/hardening/viscous and frictional slip/hardening variables $\bar{\boldsymbol{\Gamma}}$ defined as

$$\bar{\boldsymbol{\Gamma}} := \{\boldsymbol{\Gamma}, \boldsymbol{\Gamma}_c\} \quad \text{with} \quad \boldsymbol{\Gamma} := \{\boldsymbol{\Gamma}^p, \boldsymbol{\Gamma}^v\}, \tag{54}$$

where

$$\boxed{\begin{aligned} \boldsymbol{\Gamma}^p := \{\boldsymbol{\epsilon}^p, \xi_\alpha\} \text{ and } \boldsymbol{\Gamma}^v := \{\mathrm{dev}[\boldsymbol{\alpha}], \mathrm{tr}[\boldsymbol{\alpha}]\} \quad &\text{in} \quad \Omega \times \mathbb{I}, \\ \boldsymbol{\Gamma}_c := \{g_T^{p\,\alpha}, \zeta_{c\beta}\} \qquad\qquad &\text{on} \quad \Gamma^{(1)} \times \mathbb{I}. \end{aligned}} \tag{55}$$

Here $\boldsymbol{\varphi}$ is the deformation map, $\boldsymbol{p} := \rho_0 \boldsymbol{V}$ denotes the material linear momentum, H^e and H^p are the elastic entropy (including phase change contributions) and plastic entropy

per unit reference volume, respectively, L is the latent heat per unit reference volume, $\boldsymbol{\epsilon}^p$ the plastic strain, ξ_α the strain-like hardening variables and $\boldsymbol{\alpha}$ the viscous strains. Additionaly, H_c^e and H_c^p are the elastic and plastic contact entropy per unit reference surface, $g_T^{p\,\alpha}$ the plastic slip and $\zeta_{c\beta}$ the frictional hardening variables.

All the remaining variables in the problem can be defined in terms of $\bar{\boldsymbol{Z}}$ and $\bar{\boldsymbol{\Gamma}}$ by kinematic and constitutive equations. In particular,

i. The elastic strain $\boldsymbol{\epsilon}^e := \boldsymbol{\epsilon} - \boldsymbol{\epsilon}^p$.
ii. The Cauchy stress tensor $\boldsymbol{\sigma} := \partial_{\boldsymbol{\epsilon}^e} \hat{E}(\boldsymbol{\epsilon}^e, H^e, \xi_\alpha, \boldsymbol{\alpha})$ and stress-like hardening variables $\beta^\alpha := -\partial_{\xi_\alpha} \hat{E}(\boldsymbol{\epsilon}^e, H^e, \xi_\alpha, \boldsymbol{\alpha})$.
iii. The temperature $\Theta := \partial_{H^e} \hat{E}(\boldsymbol{\epsilon}^e, H^e, \xi_\alpha, \boldsymbol{\alpha})$ and nominal heat flux $\boldsymbol{Q} = -K\ \mathrm{GRAD}[\Theta]$.
iv. The normal gap $g_N := -[\![\boldsymbol{\varphi}]\!] \cdot \boldsymbol{\nu}$ and tangential gap g_T^α given by the time integration of $\dot{g}_T^\alpha := [\![\boldsymbol{V}]\!] \cdot \boldsymbol{\tau}^\alpha$.
v. The nominal contact pressure $t_N := \partial_{g_N} \hat{E}_c(g_N, g_T^{e\,\alpha}, H_c^e, \zeta_{c\beta})$, nominal frictional traction $t_{T\alpha} := \partial_{g_T^{e\,\alpha}} \hat{E}_c(g_N, g_T^{e\,\alpha}, H_c^e, \zeta_{c\beta})$ and conjugate of the frictional hardening variable $q_c^\beta := -\partial_{\zeta_c} \hat{E}_c(g_N, g_T^{e\,\alpha}, H_c^e, \zeta_{c\beta})$.
vi. The contact temperature $\Theta_c = \partial_{H_c^e} \hat{E}_c(g_N, g_T^{e\,\alpha}, H_c^e, \zeta_{c\beta})$.

(A) *Thermoplastic/viscous nonlinear operators in* $\bar{\Omega} \times \mathbb{I}$. With these definitions in hand, and assuming zero body forces and zero heat sources, the governing evolution equations of the thermoplastic/viscous problem can be written in the form given by (48) and (49) where the thermoplastic/viscous nonlinear operators $\boldsymbol{A}[\boldsymbol{Z}, \boldsymbol{\Gamma}]$ and $\boldsymbol{G}[\boldsymbol{Z}, \boldsymbol{\Gamma}] = \{\boldsymbol{G}^p[\boldsymbol{Z}, \boldsymbol{\Gamma}], \boldsymbol{G}^v[\boldsymbol{Z}, \boldsymbol{\Gamma}]\}$ take the form

$$\boxed{\begin{aligned} \boldsymbol{A}[\boldsymbol{Z}, \boldsymbol{\Gamma}] &:= \left\{ \begin{array}{c} \frac{1}{\rho_0}\boldsymbol{p} \\ \mathrm{DIV}[\boldsymbol{\sigma}] \\ -\frac{1}{\Theta}\mathrm{DIV}[\boldsymbol{Q}] + \frac{1}{\Theta}\mathcal{D}_{mech} \\ \frac{1}{\Theta}\mathcal{D}_{ther} \\ \mathcal{H}^{pc} \end{array} \right\}, \\ \boldsymbol{G}^p[\boldsymbol{Z}, \boldsymbol{\Gamma}] :&= \left\{ \begin{array}{c} \partial_\sigma \hat{\Phi}(\boldsymbol{\sigma}, q^\alpha, \Theta) \\ \partial_{q^\alpha} \hat{\Phi}(\boldsymbol{\sigma}, q^\alpha, \Theta) \end{array} \right\}, \qquad \boldsymbol{G}^v[\boldsymbol{Z}, \boldsymbol{\Gamma}] := \left\{ \begin{array}{c} \frac{1}{\eta_v^{dev}} \mathrm{dev}[\boldsymbol{\beta}] \\ \frac{1}{\eta_v^{vol}} \mathrm{tr}[\boldsymbol{\beta}] \end{array} \right\}, \end{aligned}} \tag{56}$$

where the phase-change heating $\mathcal{H}^{pc}$ is given by

$$\mathcal{H}^{pc} := -\Theta \partial^2_{\Theta\Theta} \hat{\Psi}_{tpc}(\Theta) \cdot \dot{\Theta}, \tag{57}$$

and the mechanical dissipation $\mathcal{D}_{mech}$ and thermal dissipation $\mathcal{D}_{ther}$ are given by

$$\mathcal{D}_{mech} := \gamma \boldsymbol{\Sigma}^p : \boldsymbol{G}^p[\boldsymbol{Z}, \boldsymbol{\Gamma}] + \boldsymbol{\Sigma}^v : \boldsymbol{G}^v[\boldsymbol{Z}, \boldsymbol{\Gamma}] \geq 0, \qquad \mathcal{D}_{ther} := \gamma \Theta \partial_\Theta \hat{\Phi}(\boldsymbol{\sigma}, \beta^\alpha, \Theta), \tag{58}$$

where, using a compact notation, we have denoted as $\boldsymbol{\Sigma}^{p\,T} := [\boldsymbol{\sigma}^T, \beta^\alpha]$ and $\boldsymbol{\Sigma}^{v\,T} := [\mathrm{dev}[\boldsymbol{\beta}]^T, \frac{1}{3}\mathrm{tr}[\boldsymbol{\beta}]]$ the generalized plastic and viscous stress tensors, respectively.

(B) *Thermofrictional nonlinear operators on* $\Gamma^{(1)} \times \mathbb{I}$. With the above definitions in hand the governing evolution equations of the thermofrictional problem can be written in the form given by (50) and (51) where the thermofrictional nonlinear operators $\boldsymbol{A}_c[\bar{\boldsymbol{Z}}, \bar{\boldsymbol{\Gamma}}]$ and $\boldsymbol{G}_c[\bar{\boldsymbol{Z}}, \bar{\boldsymbol{\Gamma}}]$ take the form

$$\boxed{\begin{aligned} \boldsymbol{A}_c[\bar{\boldsymbol{Z}}, \bar{\boldsymbol{\Gamma}}] &:= \left\{ \begin{array}{c} \frac{1}{\Theta_c}(Q_c^{(1)} + Q_c^{(2)}) + \frac{1}{\Theta_c}\mathcal{D}_{c,mech} \\ \frac{1}{\Theta_c}\mathcal{D}_{c,ther} \end{array} \right\}, \\ \boldsymbol{G}_c[\bar{\boldsymbol{Z}}, \bar{\boldsymbol{\Gamma}}] &:= \left\{ \begin{array}{c} \partial_{t_{T\alpha}} \hat{\Phi}_c(t_N, t_{T\alpha}, \Theta_c, q_c^\beta) \\ \partial_{q_c^\beta} \hat{\Phi}_c(t_N, t_{T\alpha}, \Theta_c, q_c^\beta) \end{array} \right\}, \end{aligned}} \tag{59}$$

where the contact mechanical dissipation $\mathcal{D}_{c,mech}$ and thermal dissipation $\mathcal{D}_{c,ther}$ are given by

$$\mathcal{D}_{c,mech} := t_{T\alpha} \dot{g}_T^{p\,\alpha} + q_c^\beta \dot{\zeta}_{c\beta} \geq 0, \qquad \mathcal{D}_{c,ther} := \gamma_c \, \Theta_c \, \partial_{\Theta_c} \hat{\Phi}_c(t_N, t_{T\alpha}, \Theta_c, q_c^\beta). \tag{60}$$

3.2. A-priori stability estimate

For nonlinear *dissipative* problems of evolution *nonlinear stability* can be phrased in terms of an *a-priori estimate* on the dynamics of the form

$$\boxed{\frac{d}{dt}\mathcal{L}(\bar{\boldsymbol{Z}}, \bar{\boldsymbol{\Gamma}}) \leq 0 \quad \text{for} \quad t \in [0, T]} \tag{61}$$

where $\mathcal{L}(\cdot)$ is a *non-negative Lyapunov*-like function.

For nonlinear thermoplasticity featuring frictional contact behavior, see ARMERO & SIMO [1993] and LAURSEN [1998], consider an extended canonical free energy functional $\mathcal{L}(\cdot)$ defined as

$$\boxed{\begin{aligned} \mathcal{L}(\bar{\boldsymbol{Z}}, \bar{\boldsymbol{\Gamma}}) = &\int_\Omega [\frac{|\boldsymbol{p}|^2}{2\rho_0} + \hat{E}(\boldsymbol{\epsilon}^e, H^e, \xi_\alpha, \boldsymbol{\alpha}) - \Theta_0 H^e] d\Omega + V_{ext}(\boldsymbol{\varphi}) \\ &+ \int_{\Gamma^{(1)}} [\hat{E}_c(g_N, g_T^{e\,\alpha}, H_c^e, \zeta_{c\beta}) - \Theta_0 H_c^e] \, d\Gamma, \end{aligned}} \tag{62}$$

and assume that the following conditions hold,

i. Zero heat sources, i.e., $R = 0$,

ii. Conservative mechanical loading with potential $V_{ext}(\boldsymbol{\varphi})$, i.e., $DV_{ext} \cdot \boldsymbol{\eta}_0 := -\langle \boldsymbol{B}, \boldsymbol{\eta}_0 \rangle - \langle \bar{\boldsymbol{t}}, \boldsymbol{\eta}_0 \rangle_{\Gamma_\sigma}$,

iii. Dirichlet boundary conditions for the temperature field with prescribed constant temperature $\Theta_0 > 0$, i.e., $\Theta = \Theta_0$ on $\Gamma_\Theta \times \mathbb{I}$ and $\Gamma_Q = \emptyset$, or Von-Neuman boundary conditions for the heat flux with zero heat flux, i.e., $\bar{Q} = 0$ on $\Gamma_Q \times \mathbb{I}$ and $\Gamma_\Theta = \emptyset$, or in general mixed boundary conditions satisfying $\bar{Q}(\Theta - \Theta_0) = 0$ on $\Gamma_\Theta \cup \Gamma_Q \times \mathbb{I}$.

Then, $\mathcal{L}(\cdot)$ is a *non-increasing Lyapunov*-like function along the flow generated by the thermoplastic problem and a straightforward computation shows that the following *a-priori stability estimate* holds in $\mathbb{I}$:

$$\boxed{\begin{aligned}\frac{d}{dt}\mathcal{L}(\bar{\boldsymbol{Z}},\bar{\boldsymbol{\Gamma}}) = &-\int_{\Omega}\frac{\Theta_0}{\Theta}[\mathcal{D}_{mech}+\mathcal{D}_{con}]\,d\Omega\\ &-\int_{\Gamma^{(1)}}\frac{\Theta_0}{\Theta_c}[\mathcal{D}_{c,mech}+\mathcal{D}_{c,con}]\,d\Gamma\leq 0.\end{aligned}} \tag{63}$$

This condition is regarded, see ARMERO & SIMO [1993], LAURSEN [1998], as a *fundamental a-priori stability estimate* for the thermoplastic problem of evolution which *must be preserved* by the time-stepping algorithm.

3.3. Operator splits

Consider the dissipative problem of evolution given by (48)-(51) with the associated non-increasing Lyapunov-like function $\mathcal{L}(\cdot)$ given by (62). Consider an additive operator split of the vector field $\bar{\boldsymbol{A}} = \bar{\boldsymbol{A}}^{(1)}+\bar{\boldsymbol{A}}^{(2)}$, with $\bar{\boldsymbol{A}}^{(\alpha)} := \{\boldsymbol{A}^{(\alpha)}, \boldsymbol{A}_c^{(\alpha)}\}$, leading to the following two sub-problems

$$\begin{array}{ll}\underline{\text{Problem 1}} & \underline{\text{Problem 2}}\\ \left.\begin{aligned}\dot{\bar{\boldsymbol{Z}}} &= \bar{\boldsymbol{A}}^{(1)}[\bar{\boldsymbol{Z}},\bar{\boldsymbol{\Gamma}}],\\ \dot{\boldsymbol{\Gamma}}^p &= \gamma\ \boldsymbol{G}^p[\boldsymbol{Z},\boldsymbol{\Gamma}],\\ \dot{\boldsymbol{\Gamma}}^v &= \ \ \boldsymbol{G}^v[\boldsymbol{Z},\boldsymbol{\Gamma}],\\ \dot{\boldsymbol{\Gamma}}_c &= \gamma_c\ \boldsymbol{G}_c[\bar{\boldsymbol{Z}},\bar{\boldsymbol{\Gamma}}],\end{aligned}\right\} & \left.\begin{aligned}\dot{\bar{\boldsymbol{Z}}} &= \bar{\boldsymbol{A}}^{(2)}[\bar{\boldsymbol{Z}},\bar{\boldsymbol{\Gamma}}],\\ \dot{\boldsymbol{\Gamma}}^p &= \gamma\ \boldsymbol{G}^p[\boldsymbol{Z},\boldsymbol{\Gamma}],\\ \dot{\boldsymbol{\Gamma}}^v &= \ \ \boldsymbol{G}^v[\boldsymbol{Z},\boldsymbol{\Gamma}],\\ \dot{\boldsymbol{\Gamma}}_c &= \gamma_c\ \boldsymbol{G}_c[\bar{\boldsymbol{Z}},\bar{\boldsymbol{\Gamma}}].\end{aligned}\right\}\end{array} \tag{64}$$

The *critical restriction on the design of the operator split* is that each one of the sub-problems *must preserve the underlying dissipative structure of the original problem*, i.e.,

$$\boxed{\frac{d}{dt}\mathcal{L}(\bar{\boldsymbol{Z}}^{(\alpha)},\bar{\boldsymbol{\Gamma}}^{(\alpha)})\leq 0,\quad \alpha=1,2} \tag{65}$$

where $t\mapsto(\bar{\boldsymbol{Z}}^{(\alpha)},\bar{\boldsymbol{\Gamma}}^{(\alpha)})$ denotes the flow generated by the vector field $\bar{\boldsymbol{A}}^{(\alpha)}$, $\alpha=1,2$.

Two different operator splits will be considered here. First, following ARMERO & SIMO [1992A,1992B,1993], see also LAURSEN [1998] for frictional contact problems, an isentropic operator split, which satisfies the critical design restriction mentioned above, is considered. This split is compared next with an isothermal operator split, which does not satisfy the design restriction.

(A) *The isentropic operator split.* Consider the following additive *isentropic*-based operator split of the vector field $\bar{\boldsymbol{A}}[\bar{\boldsymbol{Z}},\bar{\boldsymbol{\Gamma}}]$:

$$\bar{\boldsymbol{A}}[\bar{\boldsymbol{Z}},\bar{\boldsymbol{\Gamma}}] := \bar{\boldsymbol{A}}^{(1)}_{ise}[\bar{\boldsymbol{Z}},\bar{\boldsymbol{\Gamma}}]+\bar{\boldsymbol{A}}^{(2)}_{ise}[\bar{\boldsymbol{Z}},\bar{\boldsymbol{\Gamma}}], \tag{66}$$

where we define the vector fields $\bar{\boldsymbol{A}}^{(1)}_{ise} := \{\boldsymbol{A}^{(1)}_{ise}, \boldsymbol{A}^{(1)}_{c,ise}\}$ and $\bar{\boldsymbol{A}}^{(2)}_{ise} := \{\boldsymbol{A}^{(2)}_{ise}, \boldsymbol{A}^{(2)}_{c,ise}\}$ as

$$\boxed{\boldsymbol{A}^{(1)}_{ise}[\boldsymbol{Z},\boldsymbol{\Gamma}] := \left\{\begin{array}{c} \frac{1}{\rho_0}\boldsymbol{p} \\ \mathrm{DIV}[\boldsymbol{\sigma}] \\ 0 \\ 0 \\ 0 \end{array}\right\}, \quad \boldsymbol{A}^{(2)}_{ise}[\boldsymbol{Z},\boldsymbol{\Gamma}] := \left\{\begin{array}{c} 0 \\ 0 \\ -\frac{1}{\Theta}\mathrm{DIV}[\boldsymbol{Q}] + \frac{1}{\Theta}\mathcal{D}_{mech} \\ \frac{1}{\Theta}\mathcal{D}_{ther} \\ \mathcal{H}^{pc} \end{array}\right\}, \tag{67}}$$

$$\boxed{\boldsymbol{A}^{(1)}_{c,ise}[\bar{\boldsymbol{Z}},\bar{\boldsymbol{\Gamma}}] := \left\{\begin{array}{c} 0 \\ 0 \end{array}\right\}, \quad \boldsymbol{A}^{(2)}_{c,ise}[\bar{\boldsymbol{Z}},\bar{\boldsymbol{\Gamma}}] := \left\{\begin{array}{c} \frac{1}{\Theta_c}(Q^{(1)}_c + Q^{(2)}_c) + \frac{1}{\Theta_c}\mathcal{D}_{c,mech} \\ \frac{1}{\Theta_c}\mathcal{D}_{c,ther} \end{array}\right\}, \tag{68}}$$

and consider the following two problems of evolution:

$$\begin{array}{ll} \underline{\textit{Problem 1}} & \underline{\textit{Problem 2}} \\ \left.\begin{array}{l} \dot{\bar{\boldsymbol{Z}}} = \bar{\boldsymbol{A}}^{(1)}_{ise}[\bar{\boldsymbol{Z}},\bar{\boldsymbol{\Gamma}}], \\ \dot{\boldsymbol{\Gamma}}^p = \gamma\ \boldsymbol{G}^p[\boldsymbol{Z},\boldsymbol{\Gamma}], \\ \dot{\boldsymbol{\Gamma}}^v = \ \boldsymbol{G}^v[\boldsymbol{Z},\boldsymbol{\Gamma}], \\ \dot{\boldsymbol{\Gamma}}_c = \gamma_c\ \boldsymbol{G}_c[\bar{\boldsymbol{Z}},\bar{\boldsymbol{\Gamma}}], \end{array}\right\} & \left.\begin{array}{l} \dot{\bar{\boldsymbol{Z}}} = \bar{\boldsymbol{A}}^{(2)}_{ise}[\boldsymbol{Z},\boldsymbol{\Gamma}], \\ \dot{\boldsymbol{\Gamma}}^p = \gamma\ \boldsymbol{G}^p[\boldsymbol{Z},\boldsymbol{\Gamma}], \\ \dot{\boldsymbol{\Gamma}}^v = \ \boldsymbol{G}^v[\boldsymbol{Z},\boldsymbol{\Gamma}], \\ \dot{\boldsymbol{\Gamma}}_c = \gamma_c\ \boldsymbol{G}_c[\bar{\boldsymbol{Z}},\bar{\boldsymbol{\Gamma}}]. \end{array}\right\} \end{array} \tag{69}$$

Within this operator split, *Problem* 1 defines a mechanical phase at fixed entropy and *Problem* 2 defines a thermal phase at fixed configuration. Note that a strong condition has been placed in the *Problem* 1, by the additional requirement that not only the total specific entropy must remain fixed, but also the elastic and plastic entropy, as well as the latent heat. Note also that the evolution of the plastic internal variables $\boldsymbol{\Gamma}$ is imposed in both problems.

Denoting by $t \mapsto (\bar{\boldsymbol{Z}}^{(\alpha)}, \bar{\boldsymbol{\Gamma}}^{(\alpha)})$ the flow generated by the vector field $\bar{\boldsymbol{A}}^{(\alpha)}_{ise}$, $\alpha = 1, 2$, a straightforward computation shows that the following stability estimates hold:

$$\boxed{\begin{aligned} \frac{d}{dt}\mathcal{L}(\bar{\boldsymbol{Z}}^{(1)}, \bar{\boldsymbol{\Gamma}}^{(1)}) &= -\int_{\Omega} \mathcal{D}^{(1)}_{mech} d\Omega \\ &\quad -\int_{\Gamma^{(1)}} \mathcal{D}^{(1)}_{c,mech} d\Gamma \leq 0, \\ \frac{d}{dt}\mathcal{L}(\bar{\boldsymbol{Z}}^{(2)}, \bar{\boldsymbol{\Gamma}}^{(2)}) &= -\int_{\Omega} \frac{\Theta_0}{\Theta^{(2)}}[\mathcal{D}^{(2)}_{mech} + \mathcal{D}^{(2)}_{con}] d\Omega \\ &\quad -\int_{\Gamma^{(1)}} \frac{\Theta_0}{\Theta^{(2)}_c}[\mathcal{D}^{(2)}_{c,mech} + \mathcal{D}^{(2)}_{c,con}] d\Gamma \leq 0, \end{aligned}} \tag{70}$$

where $\mathcal{D}^{(\alpha)}_{mech}$, $\mathcal{D}^{(\alpha)}_{con}$ and $\Theta^{(\alpha)}$ are the mechanical dissipation, thermal heat conduction dissipation and absolute temperature, respectively, and $\mathcal{D}^{(\alpha)}_{c,mech}$, $\mathcal{D}^{(\alpha)}_{c,con}$ and $\Theta^{(\alpha)}_c$ are the contact frictional mechanical dissipation, contact heat conduction dissipation and contact temperature, respectively, in *Problem* α, $\alpha = 1, 2$.

Thus, the isentropic split preserves the underlying dissipative structure of the original problem.

(B) *The isothermal operator split.* Consider the following additive *isothermal*-based operator split of the vector field $\bar{\boldsymbol{A}}[\bar{\boldsymbol{Z}}, \bar{\boldsymbol{\Gamma}}]$:

$$\bar{\boldsymbol{A}}[\bar{\boldsymbol{Z}}, \bar{\boldsymbol{\Gamma}}] := \bar{\boldsymbol{A}}^{(1)}_{iso}[\bar{\boldsymbol{Z}}, \bar{\boldsymbol{\Gamma}}] + \bar{\boldsymbol{A}}^{(2)}_{iso}[\bar{\boldsymbol{Z}}, \bar{\boldsymbol{\Gamma}}], \tag{71}$$

where we define the vector fields $\bar{\boldsymbol{A}}^{(1)}_{iso} := \{\boldsymbol{A}^{(1)}_{iso}, \boldsymbol{A}^{(1)}_{c,iso}\}$ and $\bar{\boldsymbol{A}}^{(2)}_{iso} := \{\boldsymbol{A}^{(2)}_{iso}, \boldsymbol{A}^{(2)}_{c,iso}\}$ as

$$\boxed{\boldsymbol{A}^{(1)}_{iso}[\boldsymbol{Z}, \boldsymbol{\Gamma}] := \left\{ \begin{array}{c} \frac{1}{\rho_0}\boldsymbol{p} \\ \mathrm{DIV}[\boldsymbol{\sigma}] \\ \frac{1}{\Theta}\mathcal{H}^{ep} \\ 0 \\ 0 \end{array} \right\}, \quad \boldsymbol{A}^{(2)}_{iso}[\boldsymbol{Z}, \boldsymbol{\Gamma}] := \left\{ \begin{array}{c} 0 \\ 0 \\ -\frac{1}{\Theta}\mathrm{DIV}[\boldsymbol{Q}] + \frac{1}{\Theta}(\mathcal{D}_{mech} - \mathcal{H}^{ep}) \\ \frac{1}{\Theta}\mathcal{D}_{ther} \\ \mathcal{H}^{pc} \end{array} \right\},} \tag{72}$$

$$\boxed{\boldsymbol{A}^{(1)}_{c,iso}[\bar{\boldsymbol{Z}}, \bar{\boldsymbol{\Gamma}}] := \left\{ \begin{array}{c} \frac{1}{\Theta_c}\mathcal{H}^{fc} \\ 0 \end{array} \right\}, \quad \boldsymbol{A}^{(2)}_{c,iso}[\bar{\boldsymbol{Z}}, \bar{\boldsymbol{\Gamma}}] := \left\{ \begin{array}{c} \frac{1}{\Theta_c}(Q^{(1)}_c + Q^{(2)}_c) + \frac{1}{\Theta_c}(\mathcal{D}_{c,mech} - \mathcal{H}^{fc}) \\ \frac{1}{\Theta_c}\mathcal{D}_{c,ther} \end{array} \right\},} \tag{73}$$

and consider the following two problems of evolution:

$$\begin{array}{ll} \underline{\textit{Problem 1}} & \underline{\textit{Problem 2}} \\ \left. \begin{array}{l} \dot{\bar{\boldsymbol{Z}}} = \bar{\boldsymbol{A}}^{(1)}_{iso}[\bar{\boldsymbol{Z}}, \bar{\boldsymbol{\Gamma}}], \\ \dot{\boldsymbol{\Gamma}}^p = \gamma\, \boldsymbol{G}^p[\boldsymbol{Z}, \boldsymbol{\Gamma}], \\ \dot{\boldsymbol{\Gamma}}^v = \quad \boldsymbol{G}^v[\boldsymbol{Z}, \boldsymbol{\Gamma}], \\ \dot{\boldsymbol{\Gamma}}_c = \gamma_c\, \boldsymbol{G}_c[\bar{\boldsymbol{Z}}, \bar{\boldsymbol{\Gamma}}], \end{array} \right\} & \left. \begin{array}{l} \dot{\bar{\boldsymbol{Z}}} = \bar{\boldsymbol{A}}^{(2)}_{iso}[\bar{\boldsymbol{Z}}, \bar{\boldsymbol{\Gamma}}], \\ \dot{\boldsymbol{\Gamma}}^p = \gamma\, \boldsymbol{G}^p[\boldsymbol{Z}, \boldsymbol{\Gamma}], \\ \dot{\boldsymbol{\Gamma}}^v = \quad \boldsymbol{G}^v[\boldsymbol{Z}, \boldsymbol{\Gamma}], \\ \dot{\boldsymbol{\Gamma}}_c = \gamma_c\, \boldsymbol{G}_c[\bar{\boldsymbol{Z}}, \bar{\boldsymbol{\Gamma}}]. \end{array} \right\} \end{array} \tag{74}$$

Within this operator split, *Problem* 1 defines a mechanical phase at fixed temperature and *Problem* 2 defines a thermal phase at fixed configuration. Note also, that the evolution of the plastic internal variables $\boldsymbol{\Gamma}$ is imposed in both problems.

Denoting by $t \mapsto (\bar{\boldsymbol{Z}}^{(\alpha)}, \bar{\boldsymbol{\Gamma}}^{(\alpha)})$ the flow generated by the vector field $\bar{\boldsymbol{A}}^{(\alpha)}_{iso}$, $\alpha = 1, 2$, a straightforward computation shows that the following stability estimates hold:

$$\boxed{\begin{aligned} \frac{d}{dt}\mathcal{L}(\bar{\boldsymbol{Z}}^{(1)}, \bar{\boldsymbol{\Gamma}}^{(1)}) = &- \int_\Omega \mathcal{D}^{(1)}_{mech} d\Omega + \int_\Omega (1 - \frac{\Theta_0}{\Theta^{(1)}})\mathcal{H}^{ep(1)} d\Omega \\ &- \int_{\Gamma^{(1)}} \mathcal{D}^{(1)}_{c,mech} d\Gamma + \int_{\Gamma^{(1)}} (1 - \frac{\Theta_0}{\Theta^{(1)}_c})\mathcal{H}^{fc(1)} d\Gamma \not\leq 0, \\ \frac{d}{dt}\mathcal{L}(\bar{\boldsymbol{Z}}^{(2)}, \bar{\boldsymbol{\Gamma}}^{(2)}) = &- \int_\Omega \frac{\Theta_0}{\Theta^{(2)}}[\mathcal{D}^{(2)}_{mech} + \mathcal{D}^{(2)}_{con}] d\Omega - \int_\Omega (1 - \frac{\Theta_0}{\Theta^{(2)}})\mathcal{H}^{ep(2)} d\Omega \\ &- \int_{\Gamma^{(1)}} \frac{\Theta_0}{\Theta^{(2)}_c}[\mathcal{D}^{(2)}_{c,mech} + \mathcal{D}^{(2)}_{c,con}] d\Gamma - \int_{\Gamma^{(1)}} (1 - \frac{\Theta_0}{\Theta^{(2)}_c})\mathcal{H}^{fc(2)} d\Gamma \not\leq 0, \end{aligned}} \tag{75}$$

where $\mathcal{D}^{(\alpha)}_{mech}$, $\mathcal{D}^{(\alpha)}_{con}$, $\mathcal{H}^{ep(\alpha)}$ and $\Theta^{(\alpha)}$ are the mechanical dissipation, thermal heat conduction dissipation, structural elastoplastic heating and absolute temperature, respectively, and $\mathcal{D}^{(\alpha)}_{c,mech}$, $\mathcal{D}^{(\alpha)}_{c,con}$, $\mathcal{H}^{fc(\alpha)}$ and $\Theta^{(\alpha)}_c$ are the contact frictional mechanical dissipation, contact heat conduction dissipation, frictional hardening heating and contact temperature, respectively, in *Problem* α, $\alpha = 1, 2$.

The contribution of the *structural elastoplastic heating* and *frictional hardening heating* to the evolution equations of each one of the problems arising from the isothermal operator split, *breaks the underlying dissipative structure of the original problem.*

3.4. Product formula algorithms

The additive operator split of the governing evolution equations leads to a product formula algorithm and to a staggered solution scheme of the coupled problem, in which each one of the subproblems is solved sequentially. Remember that the set of internal variables $\bar{\boldsymbol{\Gamma}}$ is viewed as implicitly defined in terms of the set of variables $\bar{\boldsymbol{Z}}$, which are considered to be the only independent variables. Therefore, our interest here is placed on the time discrete version of the evolution equations (48) and (50), and the update in time of the variables $\bar{\boldsymbol{Z}}$ using a time-stepping algorithm.

Consider algorithms $\mathbb{K}^{(\alpha)}_{\Delta t}[\cdot]$ being *consistent* with the flows $t \mapsto (\bar{\boldsymbol{Z}}^{(\alpha)}, \bar{\boldsymbol{\Gamma}}^{(\alpha)})$, $\alpha = 1, 2$, and *dissipative stable*, i.e. which inherit the a-priori stability estimate on the dynamics given by (63). Then the algorithm defined by the *product formula*:

$$\mathbb{K}_{\Delta t}[\cdot] = \left(\mathbb{K}^{(2)}_{\Delta t} \circ \mathbb{K}^{(1)}_{\Delta t}\right)[\cdot] \tag{76}$$

is also *consistent* and *dissipative stable*. For *dissipative dynamical systems* if each of the algorithms is unconditionally dissipative stable, then the *product formula algorithm* is also unconditionally dissipative stable. This product formula algorithm is only *first order accurate*. A second order accurate product formula algorithm can be defined through a *double pass technique* given by, see STRANG [1969],

$$\mathbb{K}_{\Delta t}[\cdot] = \left(\mathbb{K}^{(1)}_{\Delta t/2} \circ \mathbb{K}^{(2)}_{\Delta t} \circ \mathbb{K}^{(1)}_{\Delta t/2}\right)[\cdot]. \tag{77}$$

Note that, according to (75), algorithms based on the isothermal operator split will result in staggered schemes at best only conditionally stables and only an isentropic operator split leads to unconditionally (dissipative) stable product formula algorithms.

3.5. Time discrete variational formulation

The use of an *operator split*, applied to the coupled system of nonlinear ordinary differential equations, and a *product formula algorithm*, leads to a *staggered algorithm* in which each one of the subproblems defined by the partition is solved sequentially, within the framework of classical *fractional step methods*. We note that contrary to common practice, the evolution equations for the microstructural internal variables are enforced in both phases of the operator split, as in ARMERO & SIMO [1992B,1993] and SIMO [1994].

A Backward-Euler (BE) time stepping algorithm has been used and two different operator splits have been considered:

(A) *Isentropic split.* In the *isentropic split*, first introduced by ARMERO & SIMO [1992A,1992B,1993], the coupled problem is partitioned into a mechanical phase at constant entropy, followed by a thermal phase at fixed configuration, leading to an unconditionally stable staggered scheme. Additional design constraints of constant elastic and plastic entropy and latent heat in $\bar{\Omega}$ and constant elastic and plastic contact entropy on $\Gamma^{(1)}$ have been introduced in the isentropic mechanical phase. An efficient implementation of the split can be done using the temperature as primary variable. See ARMERO & SIMO [1992A,1992B,1993] and SIMO [1994] for further details.

i. *Mechanical phase.* The mechanical problem is solved at constant entropy. For the sake of simplicity, only the quasi-static case will be considered here. According to the definition of $\bar{\boldsymbol{Z}}$ given by (52)-(53) and the operator split given by (66)-(69), the additional design constraints of constant elastic and plastic entropy and latent heat in $\bar{\Omega}$ and constant contact elastic and plastic entropy on $\Gamma^{(1)}$, have been introduced. The evolution of the temperature and contact temperature can be computed locally. The time discrete weak form of the momentum balance, local updates of elastic and plastic entropy, latent heat and internal variables in $\bar{\Omega}$ and elastic and plastic contact entropy and internal variables on $\Gamma^{(1)}$, take the form:

$$\left.\begin{aligned} &\langle \tilde{\boldsymbol{\sigma}}_{n+1}, \mathrm{GRAD}[\boldsymbol{\eta}_0]\rangle - \langle \boldsymbol{B}, \boldsymbol{\eta}_0\rangle - \langle \bar{\boldsymbol{t}}_{n+1}, \boldsymbol{\eta}_0\rangle_{\Gamma_\sigma} - \langle \tilde{\boldsymbol{t}}^{(1)}_{n+1}, \boldsymbol{\eta}^{(1)}_0 - \boldsymbol{\eta}^{(2)}_0\rangle_{\Gamma^{(1)}} = 0,\\ &\tilde{H}^e_{n+1} = H^e_n,\\ &\tilde{H}^p_{n+1} = H^p_n,\\ &\tilde{L}_{n+1} = L_n,\\ &\tilde{\boldsymbol{\Gamma}}^p_{n+1} = \boldsymbol{\Gamma}^p_n + \tilde{\gamma}_{n+1}\, \tilde{\boldsymbol{G}}^p_{n+1},\\ &\tilde{\boldsymbol{\Gamma}}^v_{n+1} = \boldsymbol{\Gamma}^v_n + \Delta t\, \tilde{\boldsymbol{G}}^v_{n+1}, \end{aligned}\right\} \text{ in } \bar{\Omega} \quad (78a)$$

$$\left.\begin{aligned} &\tilde{H}^e_{c_{n+1}} = H^e_{c\,n},\\ &\tilde{H}^p_{c_{n+1}} = H^p_{c\,n},\\ &\tilde{\boldsymbol{\Gamma}}_{c_{n+1}} = \boldsymbol{\Gamma}_{cn} + \tilde{\gamma}_{c_{n+1}}\, \tilde{\boldsymbol{G}}_{c_{n+1}}, \end{aligned}\right\} \text{ on } \Gamma^{(1)} \quad (78b)$$

and the temperature and contact temperature are locally updated according to $\tilde{\Theta}_{n+1} = \partial_{H^e}\hat{E}(\tilde{\boldsymbol{\epsilon}}^e_{n+1}, H^e_n, \tilde{\xi}_{\alpha_{n+1}}, \tilde{\boldsymbol{\alpha}}_{n+1})$ and $\tilde{\Theta}_{c_{n+1}} = \partial_{H^e_c}\hat{E}_c(\tilde{g}_{N_{n+1}}, \tilde{\boldsymbol{g}}^{e\,\alpha}_{T_{n+1}}, H^e_{c\,n}, \tilde{\zeta}_{c_{n+1}})$, respectively.

ii. *Thermal phase.* Using a BE scheme the time discrete weak form of the energy balance equation, updated elastic and plastic entropy, latent heat and internal variables in $\bar{\Omega}$ and elastic and plastic contact entropy and contact internal variables on $\Gamma^{(1)}$, in the

thermal phase, take the form:

$$\left.\begin{aligned}
&\frac{1}{\Delta t}\langle \Theta_{n+1}(H^e_{n+1}-H^e_n),\zeta_0\rangle - \langle \boldsymbol{Q}_{n+1},\mathrm{GRAD}[\zeta_0]\rangle - \langle R+\mathcal{D}_{mech\,n+1},\zeta_0\rangle \\
&\quad + \langle \bar{Q}_{n+1},\zeta_0\rangle_{\Gamma_Q} + \langle Q^{(1)}_{c\,n+1},\zeta^{(1)}_0-\zeta_{c0}\rangle_{\Gamma^{(1)}} + \langle Q^{(2)}_{c\,n+1},\zeta^{(2)}_0-\zeta_{c0}\rangle_{\Gamma^{(1)}} \\
&\quad + \frac{1}{\Delta t}\langle \Theta_{c\,n+1}(H^e_{c\,n+1}-H^e_{c\,n}),\zeta_{c0}\rangle_{\Gamma^{(1)}} - \langle \mathcal{D}_{c,mech\,n+1},\zeta_{c0}\rangle_{\Gamma^{(1)}} = 0, \\
&\qquad H^e_{n+1} = -\partial_\Theta \hat{\Psi}(\boldsymbol{\epsilon}^e_{n+1},\Theta_{n+1},\xi_{\alpha n+1},\boldsymbol{\alpha}_{n+1}), \\
&\qquad H^p_{n+1} = H^p_n + \frac{\Delta t}{\Theta_{n+1}}\mathcal{D}_{ther\,n+1}, \\
&\qquad L_{n+1} = L(\Theta_{n+1}), \\
&\qquad \boldsymbol{\Gamma}^p_{n+1} = \boldsymbol{\Gamma}^p_n + \gamma_{n+1}\,\boldsymbol{G}^p_{n+1}, \\
&\qquad \boldsymbol{\Gamma}^v_{n+1} = \boldsymbol{\Gamma}^v_n + \Delta t\,\boldsymbol{G}^v_{n+1},
\end{aligned}\right\} \text{ in } \bar{\Omega} \tag{79a}$$

$$\left.\begin{aligned}
H^e_{c\,n+1} &= H^e_{c\,n} + \frac{\Delta t}{\Theta_{c\,n+1}}\,(Q^{(1)}_{c_{n+1}} + Q^{(2)}_{c_{n+1}}) + \frac{\Delta t}{\Theta_{c\,n+1}}\mathcal{D}_{c,mech\,n+1}, \\
H^p_{c\,n+1} &= H^p_{c\,n} + \frac{\Delta t}{\Theta_{c\,n+1}}\mathcal{D}_{c,ther\,n+1}, \\
\boldsymbol{\Gamma}_{c\,n+1} &= \boldsymbol{\Gamma}_{c\,n} + \gamma_{c\,n+1}\,\boldsymbol{G}_{c\,n+1},
\end{aligned}\right\} \text{ on } \Gamma^{(1)} \tag{79b}$$

where $\Theta_{c\,n+1} = \partial_{H^e_c}\hat{E}_c(g_{N\,n+1}, g_{T\,n+1}^{e\,\alpha}, H^e_{c\,n+1}, \zeta_{c\,n+1})$.

(B) *Isothermal split.* In the isothermal split the coupled system of equations is partitioned into a mechanical phase at constant temperature in $\bar{\Omega}$ and constant contact temperature on $\Gamma^{(1)}$, followed by a thermal phase at fixed configuration. Note that, within the context of the product formula algorithm, using the entropy form of the energy equation, the elastic entropy and elastic contact entropy computed at the end of the mechanical partition is used as initial condition for the solution of the thermal partition.

i. *Mechanical phase.* Noting that under isothermal conditions the plastic entropy, latent heat and plastic contact entropy remain constant, the time discrete weak form of the momentum balance equation, updated elastic and plastic entropy, latent heat and internal variables in $\bar{\Omega}$ and updated elastic and plastic contact entropy and contact internal variables on $\Gamma^{(1)}$ take the form:

$$\left.\begin{aligned}
&\langle \tilde{\boldsymbol{\sigma}}_{n+1},\mathrm{GRAD}[\boldsymbol{\eta}_0]\rangle - \langle \boldsymbol{B},\boldsymbol{\eta}_0\rangle - \langle \bar{\boldsymbol{t}}_{n+1},\boldsymbol{\eta}_0\rangle_{\Gamma_\sigma} - \langle \tilde{\boldsymbol{t}}^{(1)}_{n+1},\boldsymbol{\eta}^{(1)}_0-\boldsymbol{\eta}^{(2)}_0\rangle_{\Gamma^{(1)}} = 0, \\
&\qquad \tilde{H}^e_{n+1} = -\partial_\Theta \hat{\Psi}(\tilde{\boldsymbol{\epsilon}}^e_{n+1},\Theta_n,\tilde{\xi}_{\alpha_{n+1}},\tilde{\boldsymbol{\alpha}}_{n+1}), \\
&\qquad \tilde{H}^p_{n+1} = H^p_n, \\
&\qquad \tilde{L}_{n+1} = L_n, \\
&\qquad \tilde{\boldsymbol{\Gamma}}^p_{n+1} = \boldsymbol{\Gamma}^p_n + \tilde{\gamma}_{n+1}\,\tilde{\boldsymbol{G}}^p_{n+1}, \\
&\qquad \tilde{\boldsymbol{\Gamma}}^v_{n+1} = \boldsymbol{\Gamma}^v_n + \Delta t\,\tilde{\boldsymbol{G}}^v_{n+1},
\end{aligned}\right\} \text{ in } \bar{\Omega} \tag{80a}$$

$$\left.\begin{aligned}
\tilde{H}^{e}_{c_{n+1}} &= -\partial_{\Theta_c}\hat{\Psi}_c(\tilde{g}_{N_{n+1}}, \tilde{g}^{e\,\alpha}_{T_{n+1}}, \Theta_{cn}, \tilde{\zeta}_{c_{n+1}}),\\
\tilde{H}^{p}_{c_{n+1}} &= H^{p}_{c\,n},\\
\tilde{\boldsymbol{\Gamma}}_{c_{n+1}} &= \boldsymbol{\Gamma}_{cn} + \tilde{\gamma}_{c_{n+1}}\,\tilde{\boldsymbol{G}}_{c_{n+1}}.
\end{aligned}\right\} \text{ on } \Gamma^{(1)} \tag{80b}$$

It is pointed out that the design conditions $\tilde{\Theta}_{n+1} = \Theta_n$ and $\tilde{\Theta}_{c_{n+1}} = \Theta_{cn}$ have been introduced in $(8oa)_2$ and $(80b)_1$, respectively.

ii. *Thermal phase.* Using a BE scheme the time discrete weak form of the energy balance equation, updated elastic and plastic entropy, latent heat and internal variables in $\bar{\Omega}$ and updated elastic and plastic contact entropy and contact internal variables on $\Gamma^{(1)}$ take the form:

$$\left.\begin{aligned}
&\frac{1}{\Delta t}\langle\Theta_{n+1}(H^{e}_{n+1} - \tilde{H}^{e}_{n+1}), \zeta_0\rangle - \langle \boldsymbol{Q}_{n+1}, \mathrm{GRAD}[\zeta_0]\rangle - \langle R + \mathcal{D}_{mech\,n+1}, \zeta_0\rangle\\
&\quad + \langle \bar{Q}_{n+1}, \zeta_0\rangle_{\Gamma_Q} + \langle Q^{(1)}_{c_{n+1}}, \zeta^{(1)}_0 - \zeta_{c0}\rangle_{\Gamma^{(1)}} + \langle Q^{(2)}_{c_{n+1}}, \zeta^{(2)}_0 - \zeta_{c0}\rangle_{\Gamma^{(1)}}\\
&\quad + \frac{1}{\Delta t}\langle\Theta_{cn+1}(H^{e}_{c\,n+1} - \tilde{H}^{e}_{c_{n+1}}), \zeta_{c0}\rangle_{\Gamma^{(1)}} - \langle \mathcal{D}_{c,mech\,n+1}, \zeta_{c0}\rangle_{\Gamma^{(1)}} = 0,\\
&\qquad H^{e}_{n+1} = -\partial_{\Theta}\hat{\Psi}(\boldsymbol{\epsilon}^{e}_{n+1}, \Theta_{n+1}, \xi_{\alpha n+1}, \boldsymbol{\alpha}_{n+1}),\\
&\qquad H^{p}_{n+1} = H^{p}_{n} + \frac{\Delta t}{\Theta_{n+1}}\mathcal{D}_{ther\,n+1},\\
&\qquad L_{n+1} = L(\Theta_{n+1}),\\
&\qquad \boldsymbol{\Gamma}^{p}_{n+1} = \boldsymbol{\Gamma}^{p}_{n} + \gamma_{n+1}\,\boldsymbol{G}^{p}_{n+1},\\
&\qquad \boldsymbol{\Gamma}^{v}_{n+1} = \boldsymbol{\Gamma}^{v}_{n} + \Delta t\,\boldsymbol{G}^{v}_{n+1},
\end{aligned}\right\} \text{ in } \bar{\Omega} \tag{81a}$$

$$\left.\begin{aligned}
H^{e}_{c\,n+1} &= \tilde{H}^{e}_{c_{n+1}} + \frac{\Delta t}{\Theta_{cn+1}}\,(Q^{(1)}_{c_{n+1}} + Q^{(2)}_{c_{n+1}}) + \frac{\Delta t}{\Theta_{cn+1}}(\mathcal{D}_{c,mech\,n+1} - \mathcal{H}^{fc}_{n+1}),\\
H^{p}_{c\,n+1} &= H^{p}_{c\,n} + \frac{\Delta t}{\Theta_{cn+1}}\mathcal{D}_{c,ther\,n+1},\\
\boldsymbol{\Gamma}_{cn+1} &= \boldsymbol{\Gamma}_{cn} + \gamma_{cn+1}\,\boldsymbol{G}_{cn+1}.
\end{aligned}\right\} \text{ on } \Gamma^{(1)} \tag{81b}$$

where $\Theta_{cn+1} = \partial_{H^{e}_{c}}\hat{E}_c(g_{N\,n+1}, g^{e\,\alpha}_{T\,n+1}, H^{e}_{c\,n+1}, \zeta_{cn+1})$.

4. NUMERICAL SIMULATIONS

The formulation presented in the previous Sections is illustrated here in a number of representative numerical simulations. The goals are to provide a practical accuracy assessment of the thermomechanical model and to demonstrate the robustness of the overall coupled thermomechanical formulation in a number of solidification examples, including industrial processes. The computations are performed with the finite element code COMET developed by the authors. The Newton-Raphson method, combined with a line search optimization procedure, is used to solve the nonlinear system of equations arising from the spatial and temporal discretization of the weak form of the momentum and reduced

dissipation balance equations. Convergence of the incremental iterative solution procedure was monitored by requiring a tolerance of 0.1% in the residual based error norm.

4.1. Solidification of an aluminium ring into an steel mould

This example deals with the numerical simulation of the solidification of an aluminium ring into an steel mould. FIGURE 1 shows the initial geometry of the part and the mould. Assumed starting conditions in the numerical simulation of the casting process are given by a completely filled mould with aluminium in liquid state at uniform temperature. The initial temperatures of the aluminium part and the steel mould were 700°C and 200°C, respectively. Only gravitational forces have been assumed. The aluminium used for the part presents a sharp liquid-solid phase change between 659°C and 660°C.

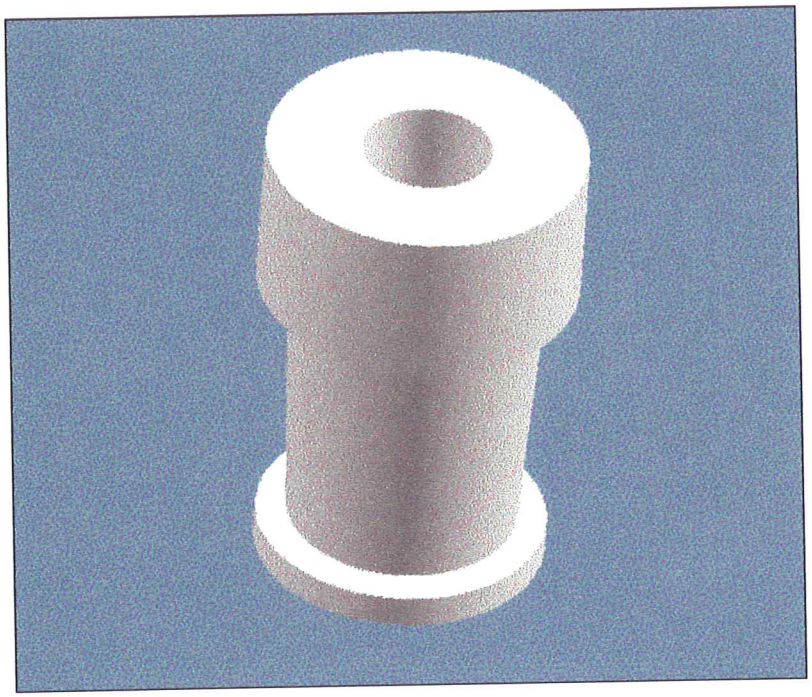

FIGURE 1. Solidification of an aluminium ring into an steel mould. Initial geometry of the part and the mould.

FIGURE 2A shows the four-noded axisymmetric finite element meshes, for both the part and the mould, used in the analysis. FIGURE 2B shows the deformed configuration at 90 s. of the analysis. A detail of the deformed mesh at the corner areas is shown in FIGURE 3.

FIGURES 4, 5 and 6 show the distribution of temperature, solid volume fraction and Von Mises effective stress, at different time steps. FIGURE 7 shows the location of different selected points of the part and the mould, where the time evolution of different variables has been monitored. FIGURES 8 and 9 show the time evolution of the temperature and radial and vertical displacements, respectively, at the selected points shown in FIGURE 7.

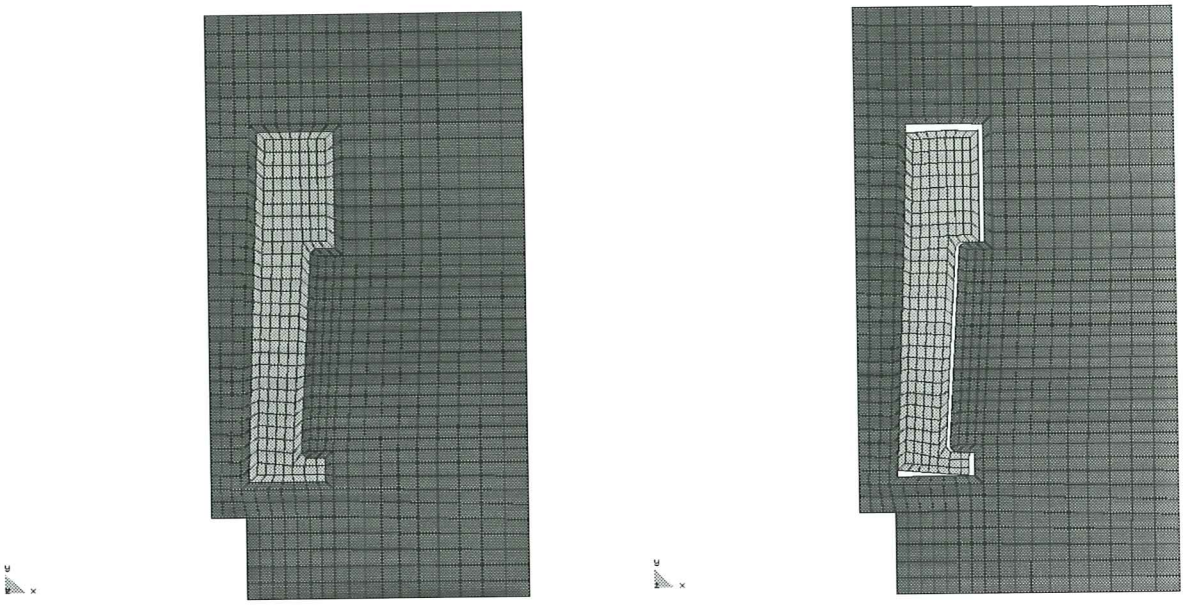

FIGURE 2. Solidification of an aluminium ring into an steel mould. (A) Four-noded axisymmteric finite element meshes for the part and the mould at the initial configuration; (B) Deformed finite element mesh at 90 s.

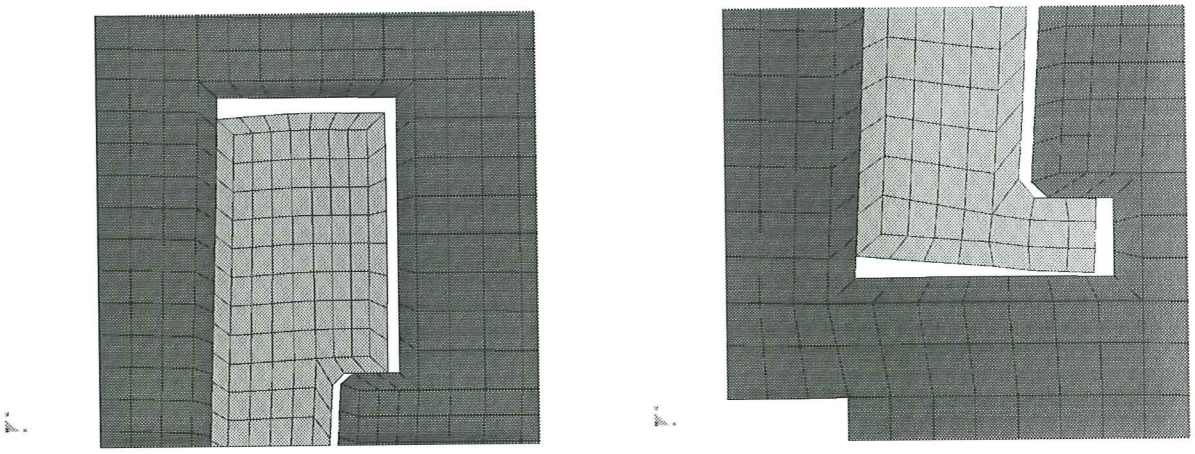

FIGURE 3. Solidification of an aluminium ring into an steel mould. Finite element mesh at a deformed configuration of t=90 s. Detail of the deformed mesh at the corner areas.

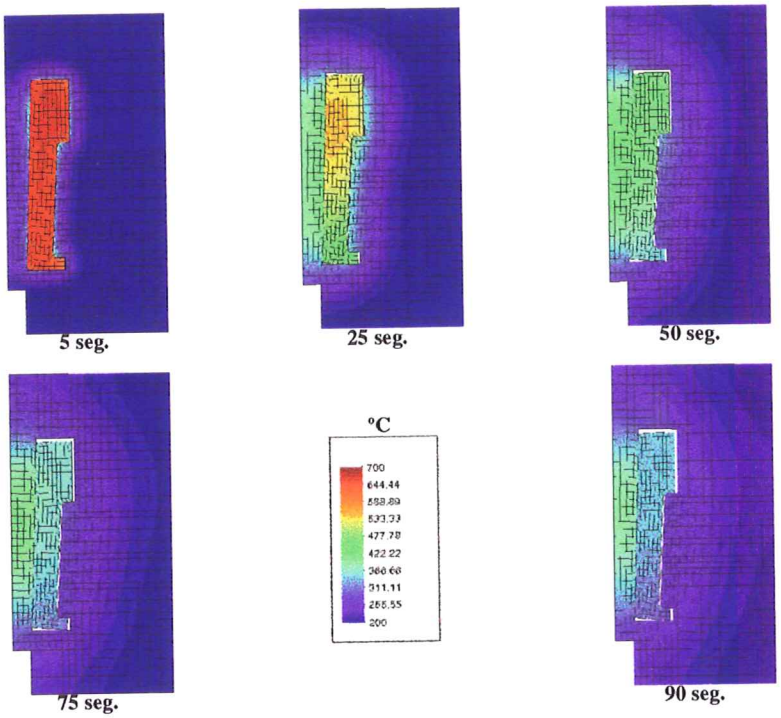

FIGURE 4. Solidification of an aluminium ring into an steel mould. Temperature distribution at different time steps.

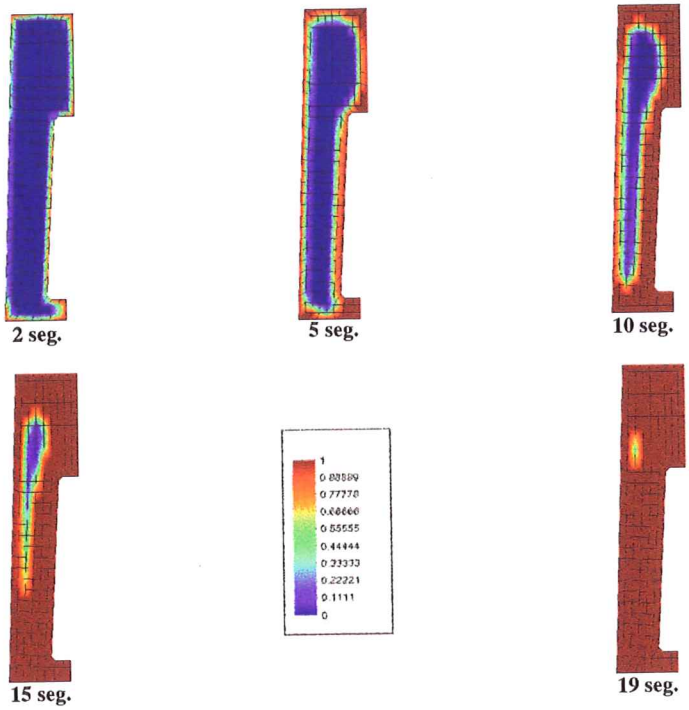

FIGURE 5. Solidification of an aluminium ring into an steel mould. Solid volume fraction distribution at different time steps.

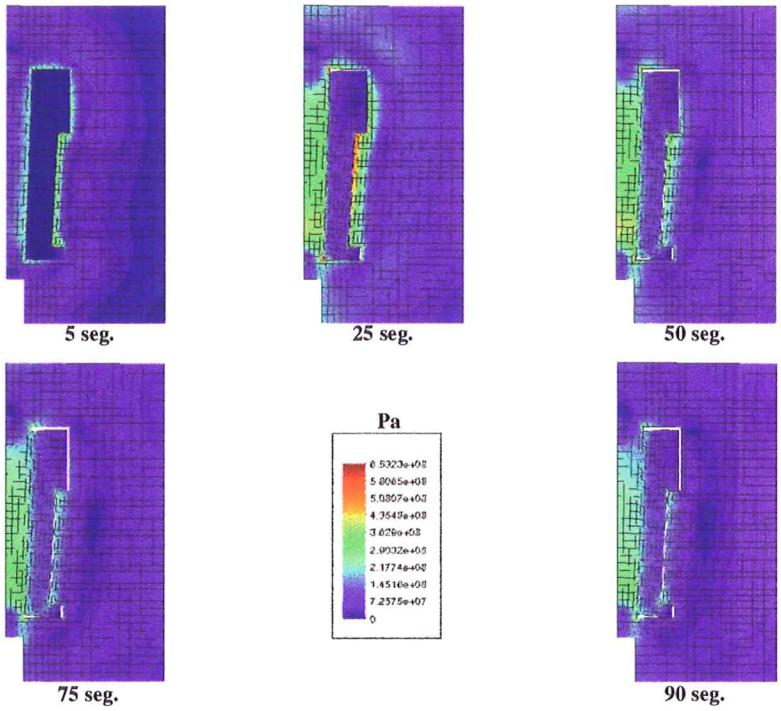

FIGURE 6. Solidification of an aluminium ring into an steel mould. Von Mises effective stress distribution at different time steps.

A	Node 424	Mould
B	Node 965	Mould
C	Node 314	Mould
D	Node 11	Part
E	Node 141	Part
F	Node 55	Part
G	Node 270	Mould
H	Node 661	Mould
I	Node 360	Mould

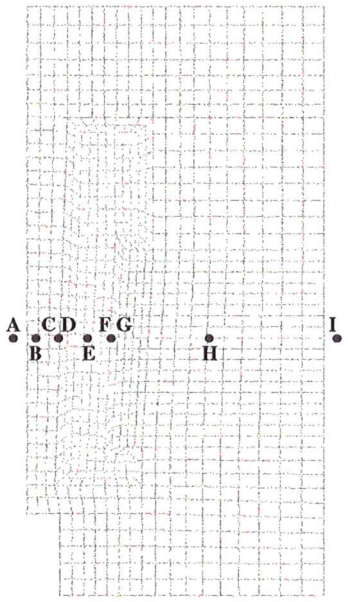

FIGURE 7. Solidification of an aluminium ring into an steel mould. Location of the selected points at the part and the mould.

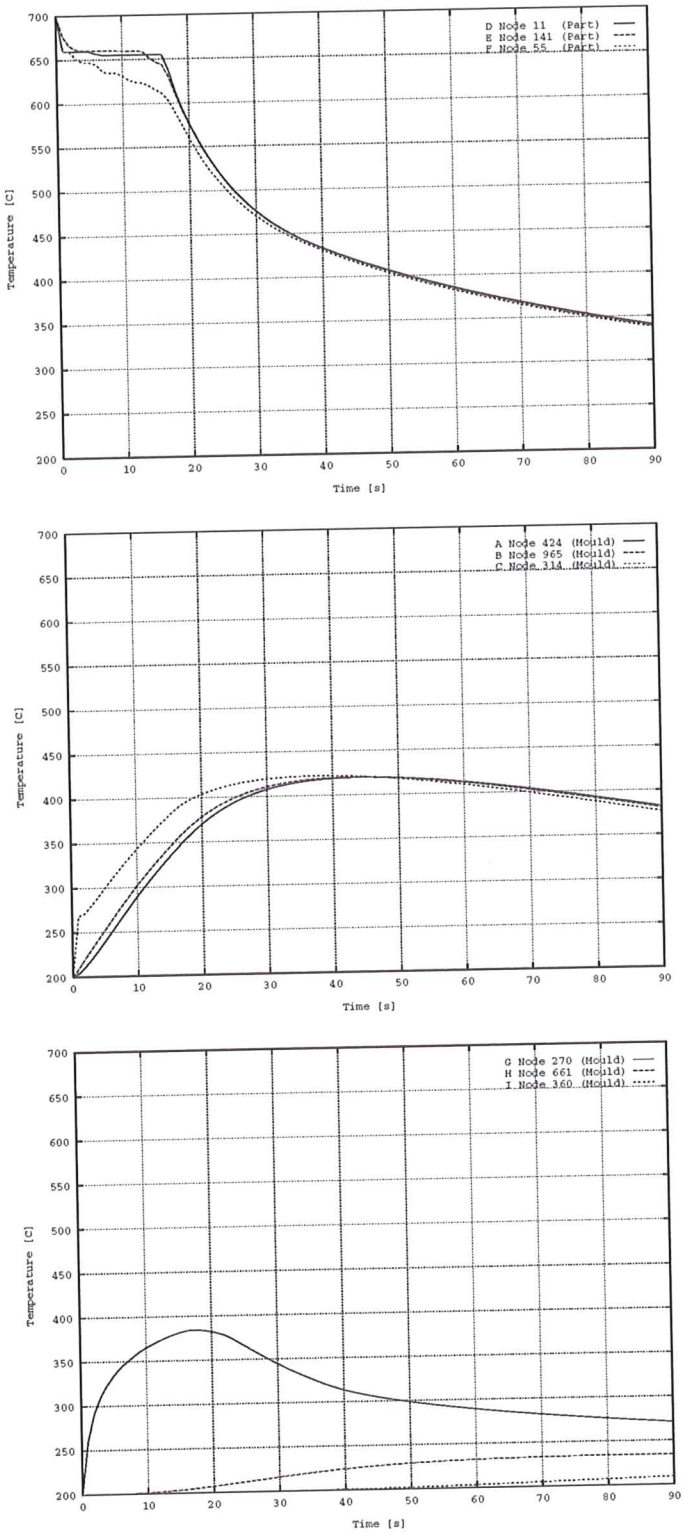

FIGURE 8. Solidification of an aluminium ring into an steel mould. Time evolution of the temperature at some selected points of the part and the mould.

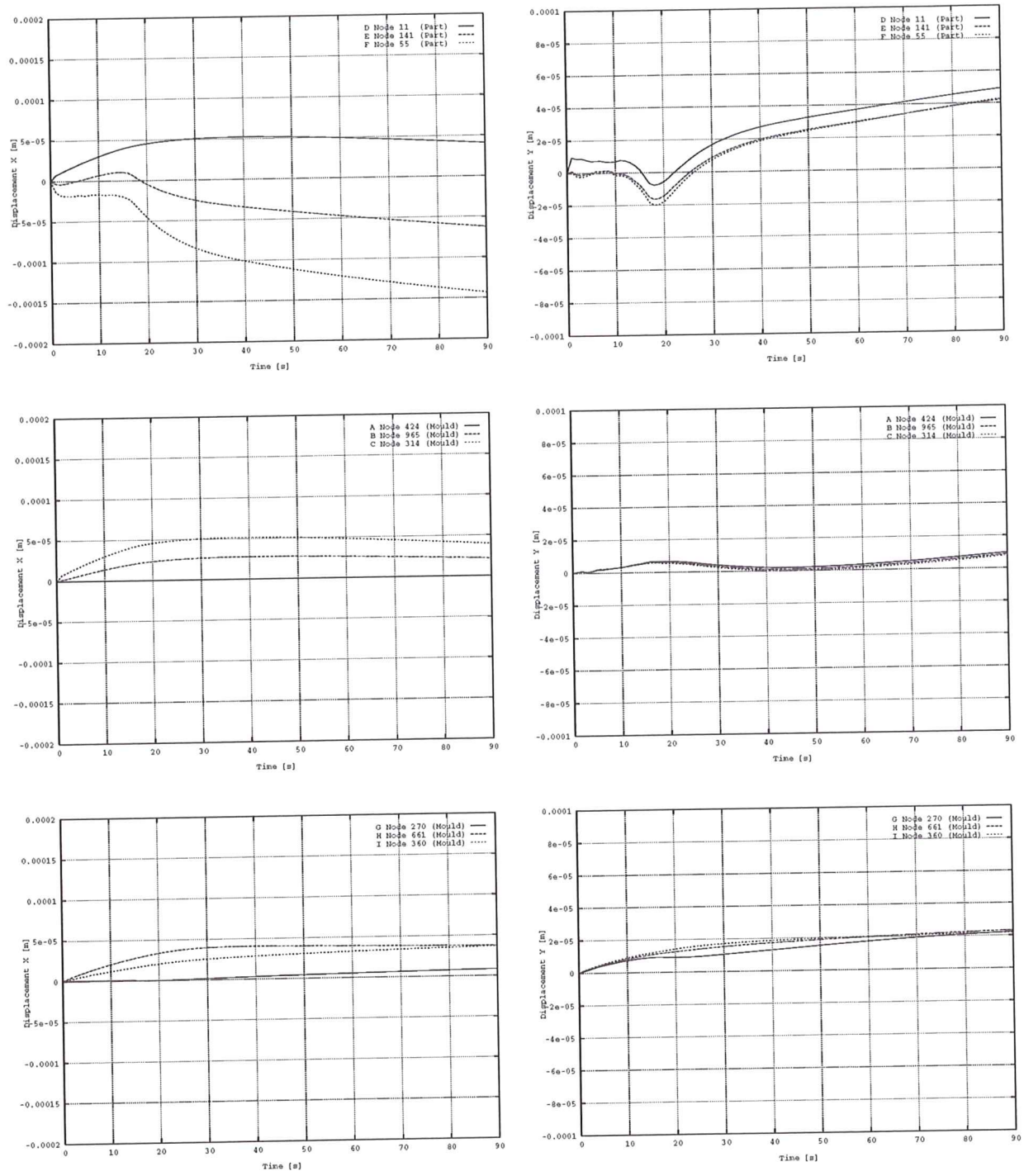

FIGURE 9. Solidification of an aluminium ring into an steel mould. Time evolution of the radial and vertical displacement at some selected points of the part and the mould.

4.2. Solidification of an Al-3Mg Si alloy driving wheel into a green sand mould

This example deals with the numerical simulation of the solidification of an Al-3Mg Si alloy driving wheel into a green sand mould. FIGURE 10 shows the geometry of the part. Assumed starting conditions in the numerical simulation of the casting process are given by a completely filled mould with an Al-3Mg Si alloy in liquid state at uniform temperature. The initial temperatures of the alloy part and the green sand mould were 700°C and 20°C, respectively. Only gravitational forces have been assumed. The Al-3Mg Si alloy used for the part presents a liquid-solid phase change between 590°C and 640°C. Due to the geometry of the weel, only a 1/5 section of the part and the mould has been discretized, using around 25000 tetrahedral elements and 6400 nodes. FIGURE 11 shows a view of the finite element mesh used in the analysis. The analysis has been carried out in 56 time steps of 15 s. each.

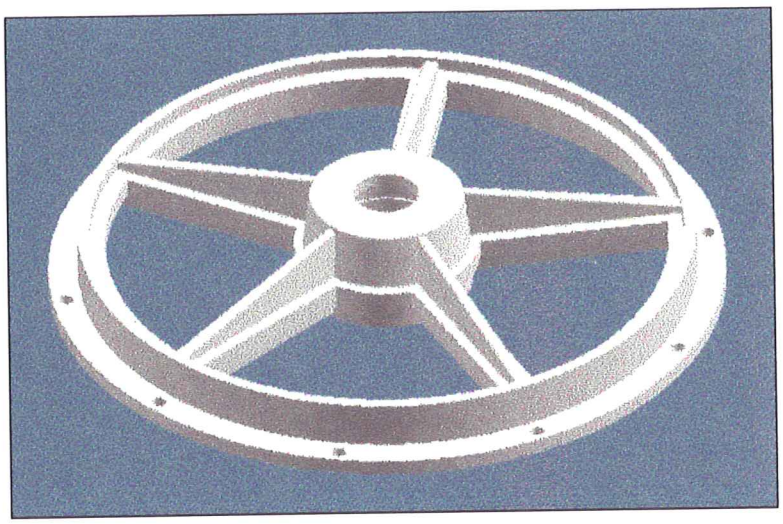

FIGURE 10. Solidification of an Al-3Mg Si alloy driving wheel into a green sand mould. Geometry of the solidified part.

Two different solidification positions, shown in FIGURE 12, have been analysed. FIGURES 13 and 14 show the distribution of the temperature and Von Mises equivalent stress in the part at 840 s., respectively, for the solidification process on positions 1 and 2. As it is shown in these figures, a faster solidification process is obtained using position 1, giving a lower temperature distribution and higher Von Mises stresses. It is pointed out that the actual manufacturing process corresponds to position 2 and the remaining of the results will be presented only for this position.

FIGURE 15 shows the temperature evolution at selected points of the part and the mould. A typical temperature plateau due to the release of latent heat during solidification can be observed in these figures. It can also be shown that the points located at the core (points D, E and F), take more time to solidify, up to 225 s. approximately, than the

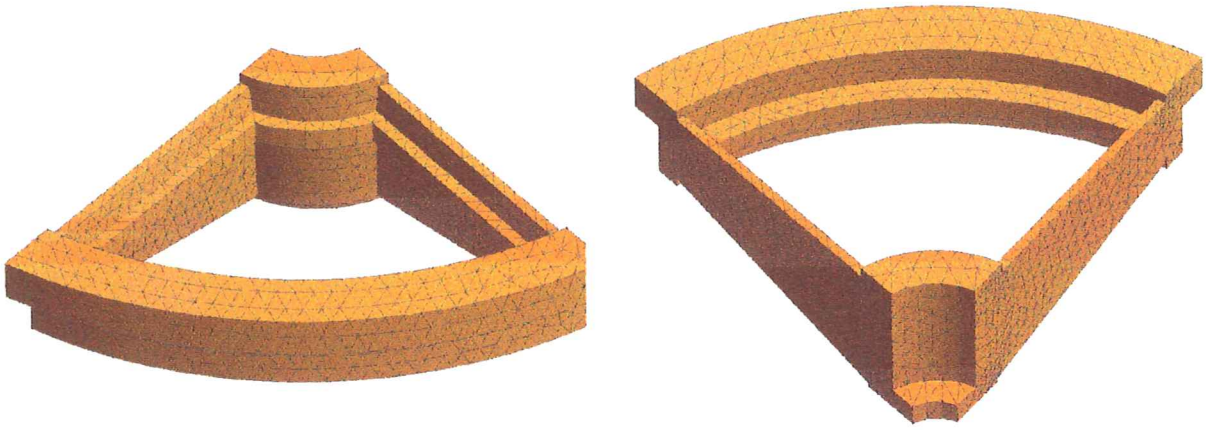

FIGURE 11. Solidification of an Al-3Mg Si alloy driving wheel into a green sand mould. Different views of the finite element mesh used in the discretization of the part.

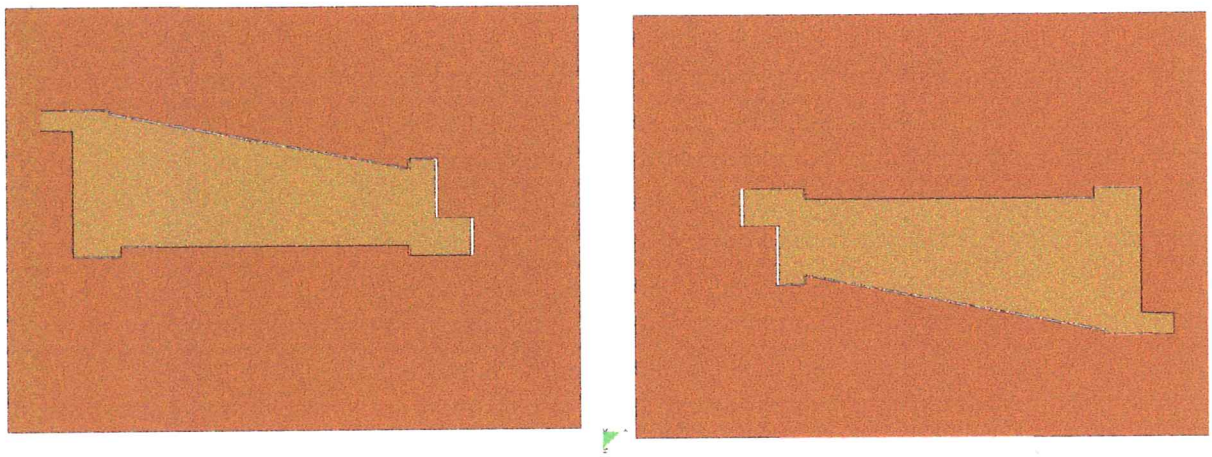

FIGURE 12. Solidification of an Al-3Mg Si alloy driving wheel into a green sand mould. Solidification positions 1 and 2.

at the core (points D, E and F), take more time to solidify, up to 225 s. approximately, than the points located at the rim and at the external part (points A, B, J and K), which take up to 125 s. approximately.

FIGURE 17 shows the location of the sections AA' and BB' selected to show the plot contours of different results at various time steps. FIGURE 18 shows the solidification time on sections AA' and BB'.FIGURES 19 and 20 show the temperature distribution on sections AA' and BB', respectively, at different time steps. FIGURES 21 and 22 show the solid volume fraction distribution on sections AA' and BB', respectively, at different time steps. It can be shown that the mushy zone occupes a vast area and there is not any internal area with metal in liquid state. This is due to a very high initial cooling rate and a large difference between the solidus and liquidus temperatures. FIGURES 23 and 24 show the distribution of the Von Mises equivalent stress on sections AA' and BB' respectively,

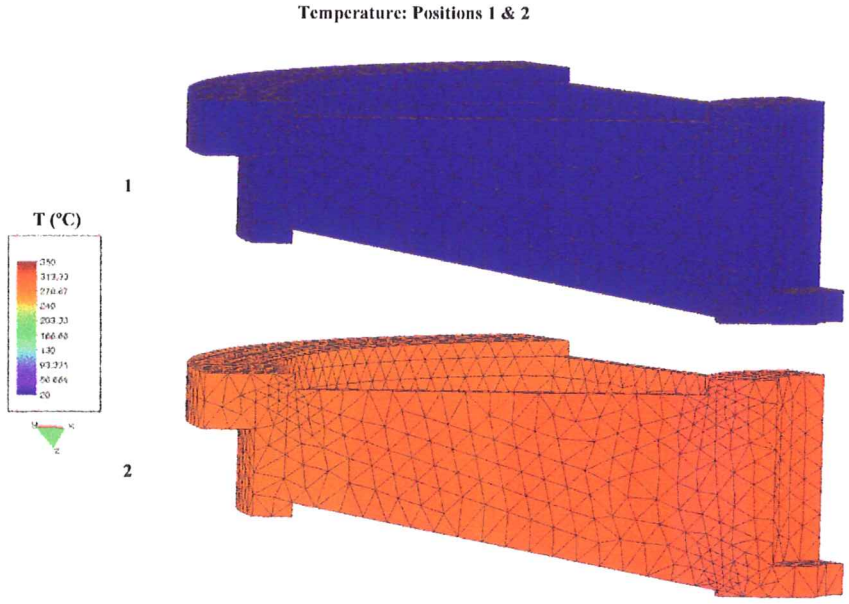

FIGURE 13. Solidification of an Al-3Mg Si alloy driving wheel into a green sand mould. Temperature in the part, at t=840 s., for solidification positions 1 and 2.

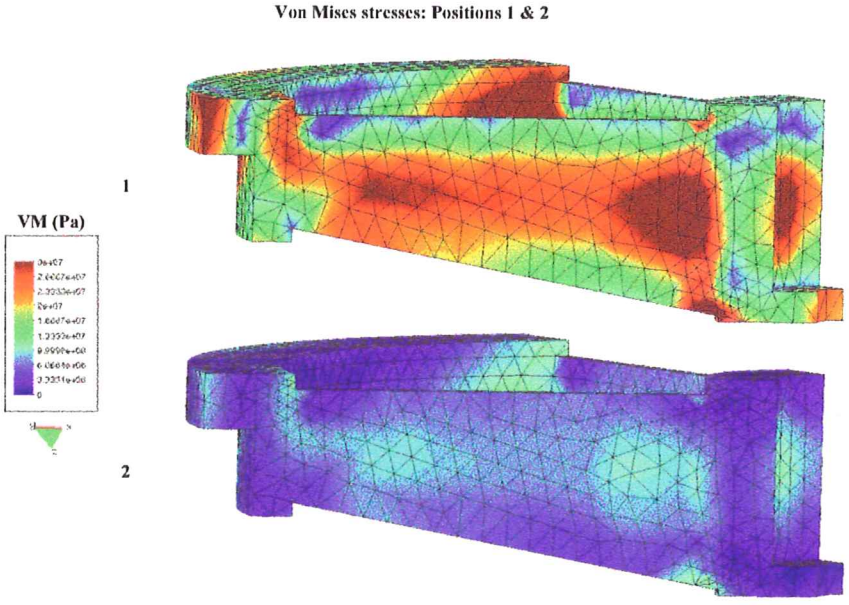

FIGURE 14. Solidification of an Al-3Mg Si alloy driving wheel into a green sand mould. Von Mises equivalent stress in the part, at t=840 s., for solidification positions 1 and 2.

A	**Node 275 Pieza**	**Node 276 Mould**
B	**Node 610 Pieza**	**Node 609 Mould**
C	**Node 1846 Pieza**	
D	**Node 4230 Pieza**	**Node 4231 Mould**
E	**Node 4239 Pieza**	**Node 4238 Mould**
F	**Node 3068 Pieza**	**Node 3069 Mould**
G	**Node 2425 Pieza**	**Node 2426 Mould**
H		**Node 154 Mould**
I		**Node 5835 Mould**
J	**Node 2369 Pieza**	**Node 2368 Mould**
K	**Node 2430 Pieza**	**Node 2431 Mould**

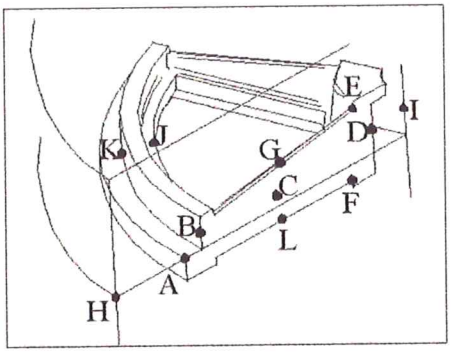

FIGURE 15. Solidification of an Al-3Mg Si alloy driving wheel into a green sand mould. Location of the selected points at the part and the mould to plot the time evolution of selected results.

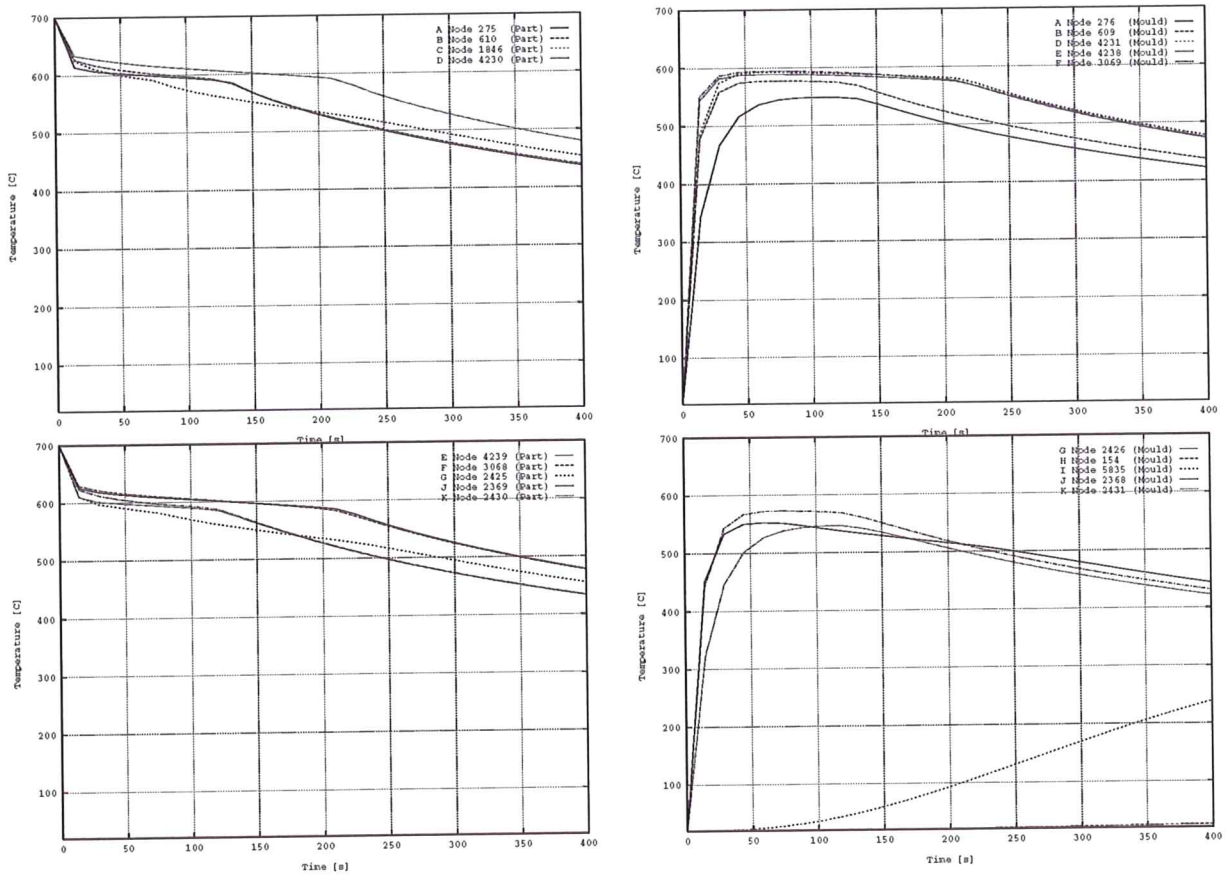

FIGURE 16. Solidification of an Al-3Mg Si alloy driving wheel into a green sand mould. Temperature time evolution at selected points of the part and the mould.

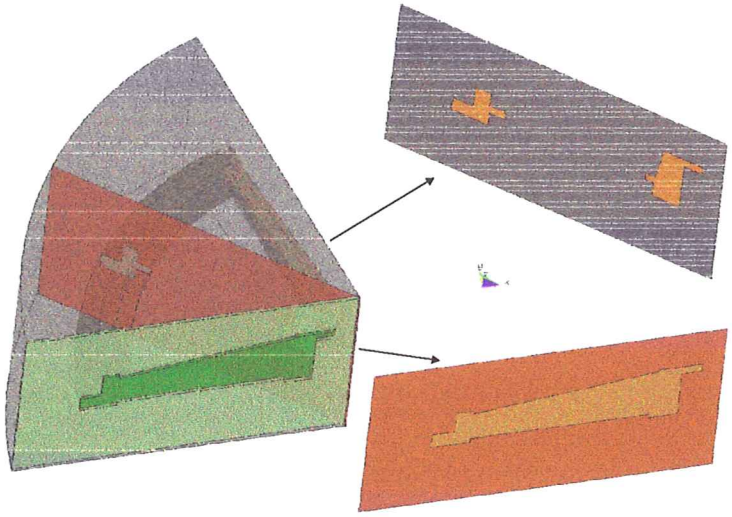

FIGURE 17. Solidification of an Al-3Mg Si alloy driving wheel into a green sand mould. Location of the sections AA' and BB' selected to show the contours of different results at various time steps.

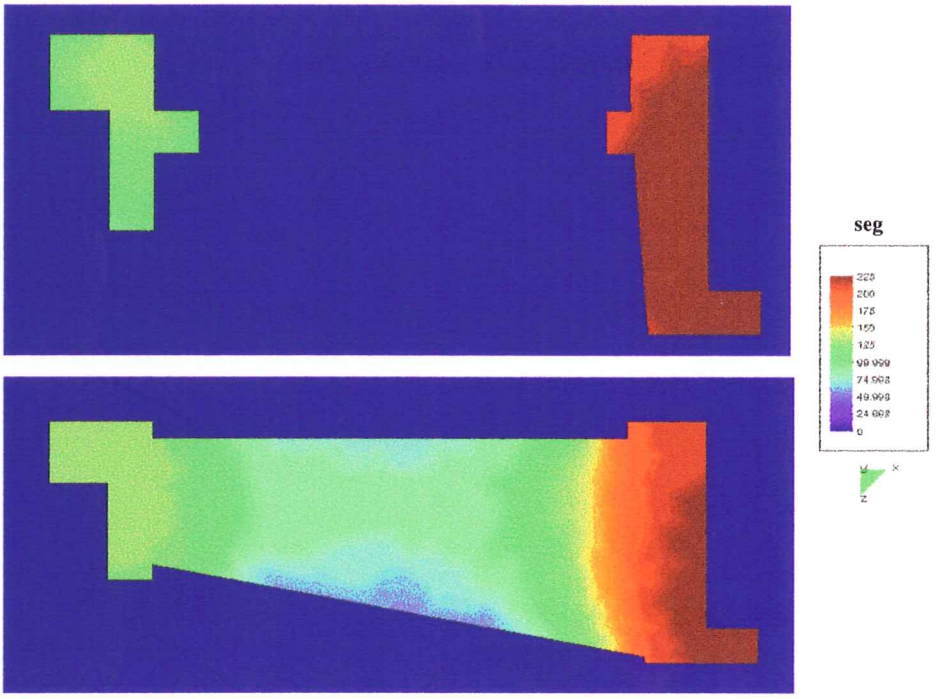

FIGURE 18. Solidification of an Al-3Mg Si alloy driving wheel into a green sand mould. (A) Solidification time on section AA'; (B) Solidification time on section BB'.

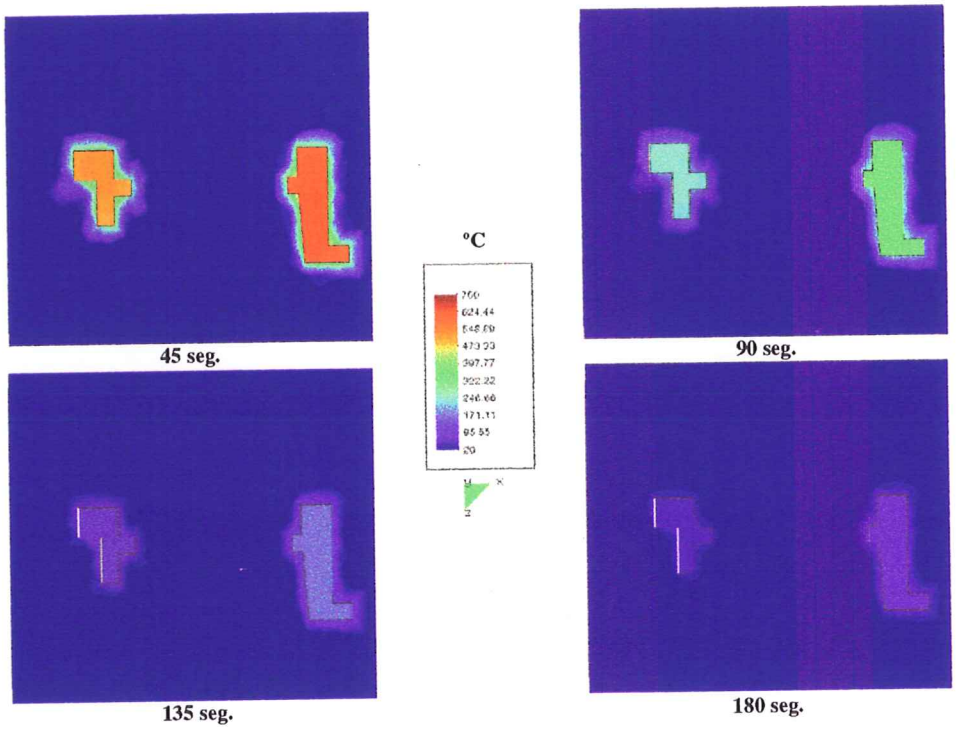

FIGURE 19. Solidification of an Al-3Mg Si alloy driving wheel into a green sand mould. Temperature distribution on section AA' at different time steps.

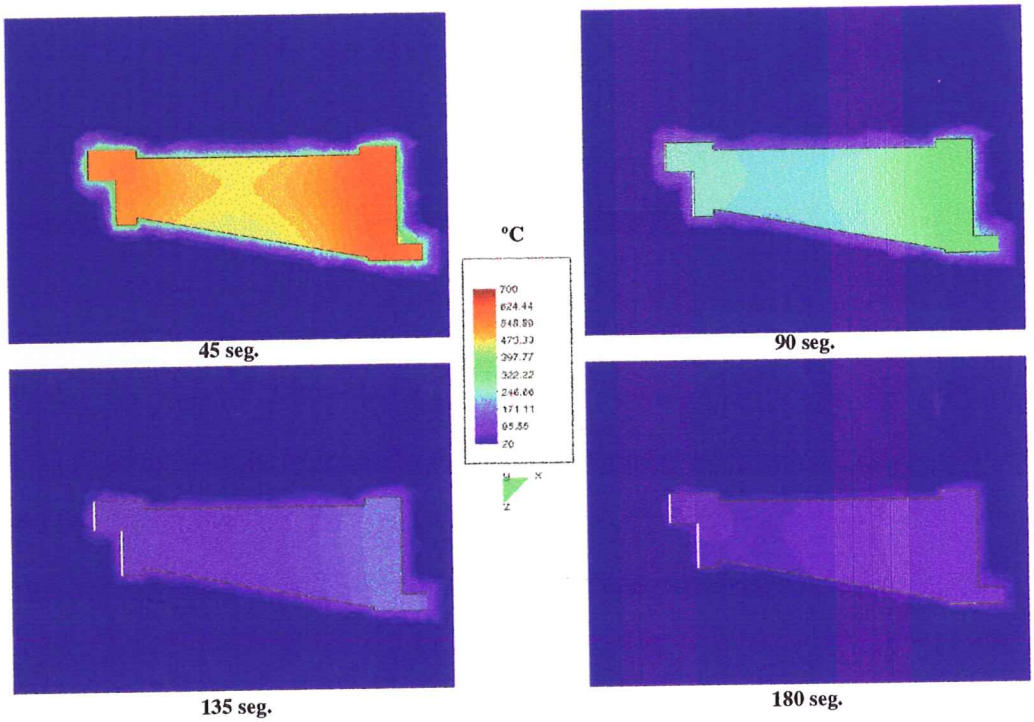

FIGURE 20. Solidification of an Al-3Mg Si alloy driving wheel into a green sand mould. Temperature distribution on section BB' at different time steps.

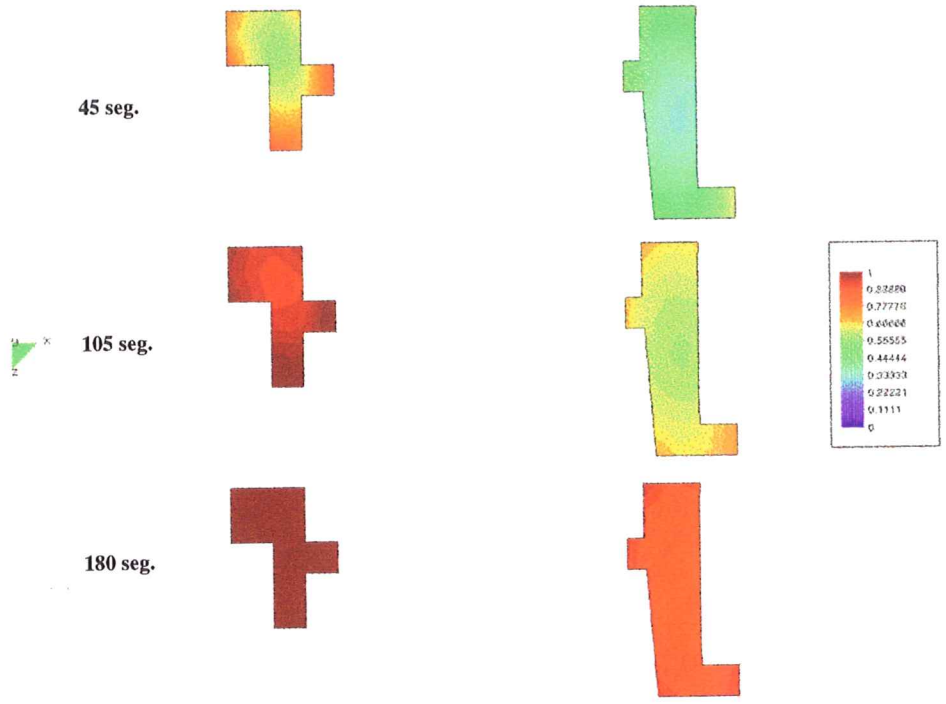

FIGURE 21. Solidification of an Al-3Mg Si alloy driving wheel into a green sand mould. Solid volume fraction distribution on section AA' at different time steps.

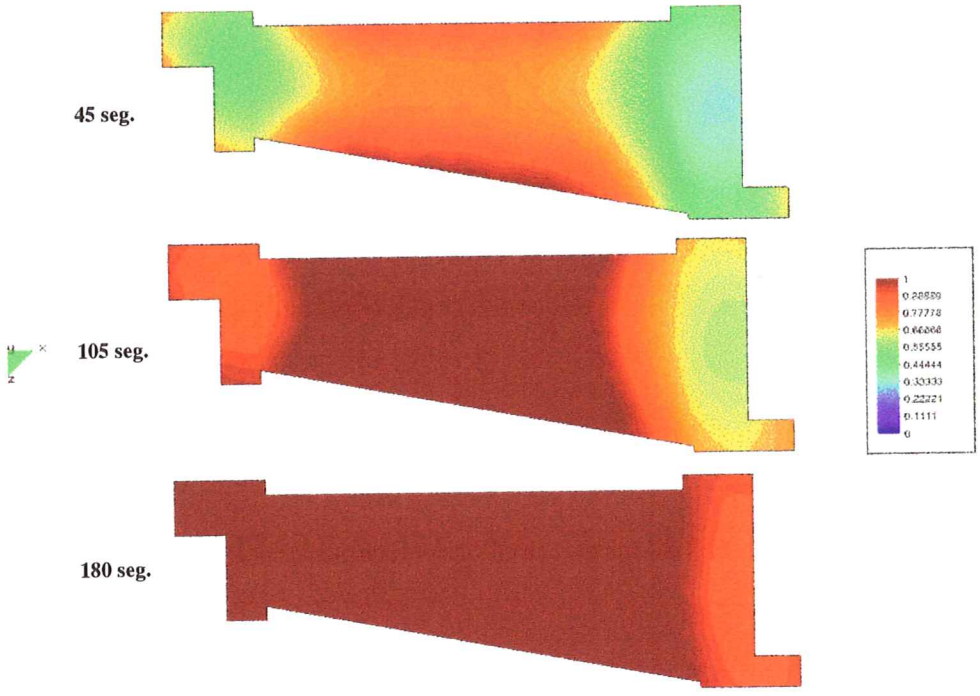

FIGURE 22. Solidification of an Al-3Mg Si alloy driving wheel into a green sand mould. Solid volume fraction distribution on section BB' at different time steps.

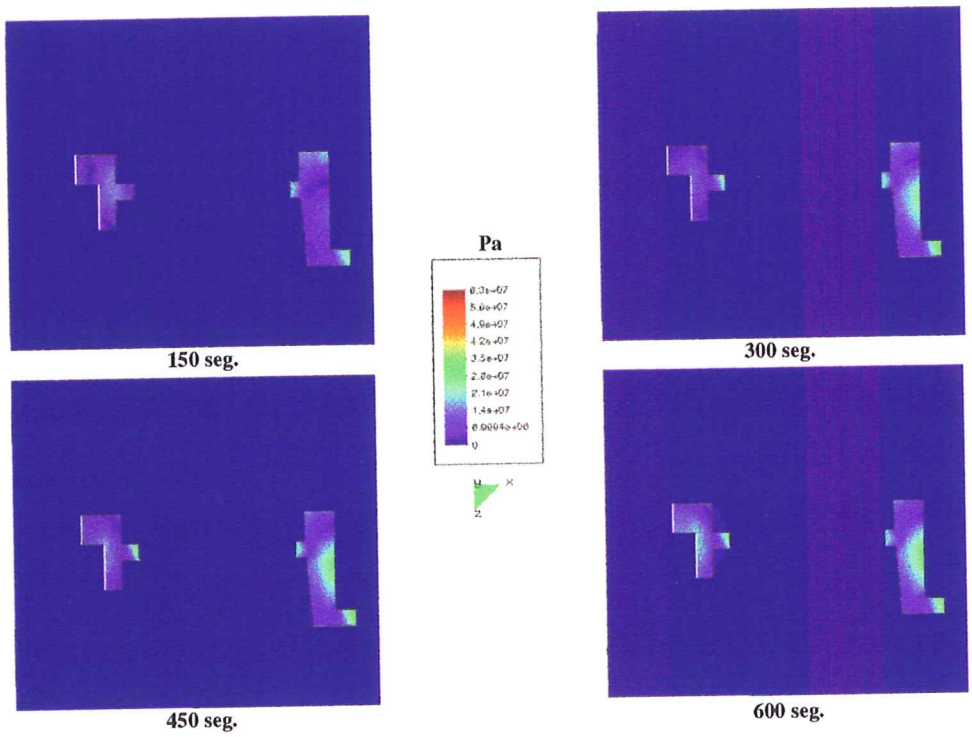

FIGURE 23. Solidification of an Al-3Mg Si alloy driving wheel into a green sand mould. Von Mises stress distribution on section AA' at different time steps.

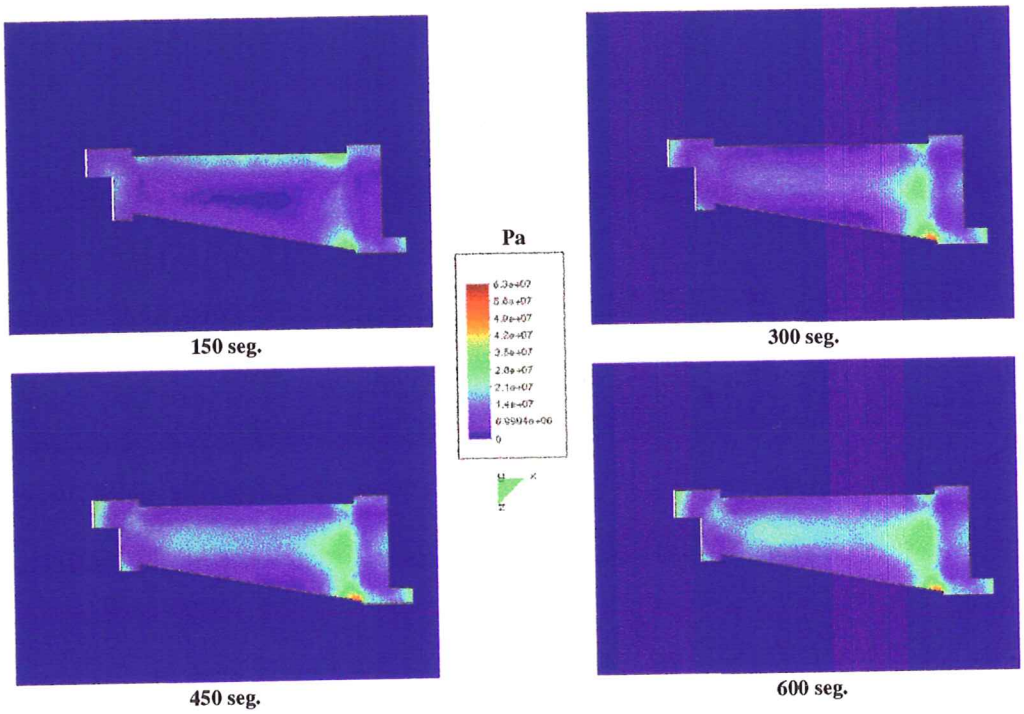

FIGURE 24. Solidification of an Al-3Mg Si alloy driving wheel into a green sand mould. Von Mises stress distribution on section BB' at different time steps.

at different time steps.

5. CONCLUDING REMARKS

A formulation of coupled thermoplastic problems with phase-change and thermofrictional contact has been presented. The formulation has been consistenly derived within a thermodynamic framework. Viscous strains and phase-change straining have been taken into account. A particular J2 thermoplastic model has been considered in which the material properties have been assumed to be temperature dependent. Operator splits of the governing differential equations, and their nonlinear stability properties, have been discussed. Within the isentropic operator split, additional split design constraints have been introduced. The formulation developed has been applied in a number of representative numerical examples, including industrial solidification processes.

ACKNOWLEDGEMENTS

Financial support for this work has been provided by the CEE through the Esprit project EP 28144 (DECAST) and the Brite-Euram projects BE97-4614 (FORMAS) and BES2-5637 (DARCAST). These financial supports are gratefully acknowledged. The financial support provided by the ETS Ingenieros de Caminos, Canales y Puertos de Barcelona to participate at the Seventh International Symposium on Plasticity and its Current Applications, held in Cancun, on January 5-13, 1999, is also gratefully acknowledged. The support provided by F. Aleman and J.M. Rodriguez, in the computational examples and the postprocess of the results, is gratefully acknowledged.

REFERENCES

AGELET DE SARACIBAR, C. [1998], "Numerical Analysis of Coupled Thermomechanical Contact Problems. Computational Model and Applications", *Archives of Computational Methods in Engineering*, **5**, 3, 243.

AGELET DE SARACIBAR, C. [1997], "A New Frictional Time Integration Algorithm for Multi-Body Large Slip Frictional Contact Problems", *Computer Methods in Applied Mechanics and Engineering*, **142**, 303-334.

AGELET DE SARACIBAR, C. & M. CHIUMENTI [1999], "On the Numerical Modeling of Frictional Wear Phenomena", *Computer Methods in Applied Mechanics and Engineering*, to appear.

AGELET DE SARACIBAR, C. & M. CHIUMENTI [1995], "Numerical Analysis of Frictional Wear Contact Problems. Computational Model and Applications", *Research Report no. 70*, CIMNE.

AGELET DE SARACIBAR, C., M. CERVERA & M. CHIUMENTI [1999], "On the Constitutive Modeling of Thermoplastic Phase-change Problems", *Proc. of The 7th Int. Symp. on Plasticity and its Current Applications, January 5-13, 1999, Cancun, Mexico*, A.S. Khan, ed., 1999.

AGELET DE SARACIBAR, C., M. CERVERA & M. CHIUMENTI [1999], "On the Formulation of Coupled Thermoplastic Problems with Phase-change", *International Journal of Plasticity*, **15**, 1, 1-34.

AGELET DE SARACIBAR, C., M. CERVERA & M. CHIUMENTI [1997], "Current Issues in the Numerical Simulation of Casting Processes.", *Physics and Mechanics of Finite Plastic and Viscoplastic Deformation, Proc. of The 6th Int. Symp. on Plasticity and its Current Applications, July 14-18, 1997, Juneau, Alaska, USA*, A.S. Khan, ed., 1997

AGELET DE SARACIBAR, C., M. CERVERA & M. CHIUMENTI [1997], "Current Issues in the Numerical Simulation of Casting Processes.", *Proc. Proc. Int. Conf. on Computational Engineering and Sciences, ICES'97, May 4-9, 1997, San Jose, Costa Rica.*

AGELET DE SARACIBAR, C., M. CERVERA & M. CHIUMENTI [1997], "VULCAN 2000: A Finite Element System for the Simulation of Casting Processes.", *Proc. 5th Int. Conf. on Computational Plasticity, COMPLAS V, March 17-20, 1997, Barcelona, Spain*, D.R.J. Owen, E. Oñate and E. Hinton, eds., CIMNE.

ARMERO F. & J.C. SIMO [1993], "A Priori Stability Estimates and Unconditionally Stable Product Algorithms for Nonlinear Coupled Thermoplasticity", *International Journal of Plasticity*, **9**, 749-782.

ARMERO, F. & J.C. SIMO [1992A], "A new Unconditionally Stable Fractional Step Method for Nonlinear Coupled Thermomechanical Problems", *International Journal for Numerical Methods in Engineering*, **35**, 737-766.

ARMERO F. & J.C. SIMO [1992B], "Product Formula Algorithms for Nonlinear Coupled Thermoplasticity: Formulation and Nonlinear Stability Analysis", *Division of Applied Mechanics, Department of Mechanical Engineering, Stanford University, Stanford, California*, SUDAM Report no. 92-4, March 1992.

CERVERA, M., C. AGELET DE SARACIBAR & M. CHIUMENTI [1998], "Thermo-mechanical analysis of industrial solidification processes", *International Journal for Numerical Methods in Engineering*, to appear.

CERVERA, M., C. AGELET DE SARACIBAR & M. CHIUMENTI [1998], "Thermo-mechanical analysis of industrial solidification processes", *Computational Mechanics, New Trends and Applications, Proc. of the Fourth World Congress on Computational Mechanics, Buenos Aires, Argentina, 29 June - 2 July, 1998*, E. Oñate and S. Idelsohn, eds., CIMNE.

CERVERA, M., C. AGELET DE SARACIBAR & M. CHIUMENTI [1998], "Coupled Thermo-mechanical simulation of industrial solidification processes", *Proc. Int. Conf. Modeling of Casting, Welding and Advanced Solidification Processes VIII, San Diego, CA, USA, 1998.*

CHIUMENTI, M. [1998], "Constitutive Modeling and Numerical Analysis of Thermomechanical Phase-change Systems", *Ph.D. Dissertation*, Departamento de Resistencia de Materiales y Estructuras en la Ingeniería, ETS de Ingenieros de Caminos, Canales y Puertos de Barcelona, UPC, September 1998.

CHIUMENTI, M., C. AGELET DE SARACIBAR & M. CERVERA [1998], "Un Modelo Constitutivo Termomecánico para Sistemas Multifase", *Proc. IV Congreso Métodos Num'ericos en Ingeniería, Sevilla, España, 7-10 Junio, 1999*, to appear.

LAURSEN, T.A. [1998], "On the Development of Thermodynamically Consistent Algorithms for Thermomechanical Frictional Contact", *Computer Methods in Applied Mechanics and Engineering*, to appear.

LAURSEN, T.A. [1992], "Formulation and Treatment of Frictional Contact Problems Using Finite Elements", *Ph.D. Dissertation*, Stanford University, Division of Applied Mechanics, Report no. 92-6.

LAURSEN, T.A. & S. GOVINDJEE [1994], "A Note on the Treatment of Frictionless Contact Between Non-smooth Surfaces in Fully Non-linear Problems", *Communications in Applied Numerical Methods*, **10**, 869-878

LAURSEN, T.A. & J.C. SIMO [1993A], "A Continuum-Based Finite Element Formulation for the Implicit Solution of Multi-Body, Large Deformation Frictional Contact Problems", *International Journal for Numerical Methods in Engineering*, **36**(20), 3451-3485.

LAURSEN, T.A. & J.C. SIMO [1993B], "Algorithmic Symmetrization of Coulomb Frictional Problems Using Augmented Lagrangians", *Computer Methods in Applied Mechanics and Engineering*, **108**, 133-146.

LAURSEN, T.A. & J.C. SIMO [1992], "Formulation and Regularization of Frictional Contact Problems for Lagrangian Finite Element Computations", in *Proc. of The Third International Conference on Computational Plasticity: Fundamentals and Applications, COMPLAS III*, D.R.J. Owen, E. Oñate & E. Hinton, eds., Pineridge Press, Swansea, pp. 395-407.

LAURSEN, T.A. & J.C. SIMO [1991], "On the Formulation and Numerical Treatment of Finite Deformation Frictional Contact Problems", in *Nonlinear Computational Mechanics–State of the Art*, P. Wriggers & W. Wagner, eds., Springer-Verlag, Berlin, pp. 716-736.

NIYAMA, E., T. UCHIDA, M. MORIKAWA & S. SAITO [1982], "A method of shrinkage prediction and its application to steel casting practice", *AFS Int. Cast Metals J.*, **52**

SIMO, J.C. [1994], "Numerical Analysis Aspects of Plasticity", in *Handbook of Numerical Analysis, Volume IV*, P.G. Ciarlet and J.J. Lions, eds., Nort-Holland.

SIMO, J.C. & F. ARMERO [1991], "Recent Advances in the Formulation and Numerical Analysis of Thermoplasticity at Finite Strains", in *Finite Inelastic Deformations - Theory and Applications*, E. Stein and D. Besdo, eds., IUTAM/IACM Symposium, Hannover, FRG, August, 19-23, 1991 Springer-Verlag, Berlin, 1991.

SIMO, J.C. & C. MIEHE [1992], "Associative Coupled Thermoplasticity at Finite Strains: Formulation, Numerical Analysis and Implementation", *Computer Methods in Applied Mechanics and Engineeering*, **98**, 41-104.

STRANG, G. [1969], "Approximating Semigroups and the Consistency of Difference Schemes", *Proc. American Mathematical Society*, **20**, 1-7.

TRUESDELL, C. & W. NOLL [1965], "The nonlinear field theories of mechanics", in *Handbuch der Physics Bd. III/3*, ed. by S. Fluegge, Springer-Verlag, Berlin.

WRIGGERS, P. & C. MIEHE [1994], "Contact Constraints within Coupled Thermomechanical Analysis. A Finite Element Model", *Computer Methods in Applied Mechanics and Engineering*, **113**, 301-319.

WRIGGERS, P. & C. MIEHE [1992], "Recent Advances in the Simulation of Thermomechanical Contact Processes", in *Proc. of The Third International Conference on Computational Plasticity: Fundamentals and Applications, COMPLAS III*, D.R.J. Owen, E. Oñate & E. Hinton, eds., Pineridge Press, Swansea, pp. 325-347.

WRIGGERS, P. & G. ZAVARISE [1993], "Thermomechanical Contact. A Rigorous but Simple Numerical Approach", *Computers and Structures*, **46**, 47-53.

ZDEBEL, U. & T. LEHMANN [1987], "Some theoretical considerations and experimental investigations on a constitutive law in thermoplasticity", *International Journal of Plasticity*, **3**, 369-389.

APPENDIX I. THERMOPLASTIC RETURN MAPPING ALGORITHMS

In this appendix we summarize the main steps involved in the thermoplastic return mapping algorithms for the mechanical and thermal problems arising from the isentropic operator split. Note that for the mechanical problem an isentropic return mapping algorithm is performed, while for the thermal problem the classical isothermal return mapping is performed.

I.A. Mechanical problem

Step 1. *Trial state (kinematics).* Given the initial data $\{\boldsymbol{\epsilon}_n, \Theta_n\}$ and database $\{\boldsymbol{\epsilon}^p_n, \xi_n, \boldsymbol{\alpha}_n\}$ at time t_n and prescribed $\boldsymbol{\epsilon}_{n+1}$ at time t_{n+1}, set:

$$\begin{aligned}
\boldsymbol{\epsilon}^{p\,trial}_{n+1} &:= \boldsymbol{\epsilon}^p_n, \\
\xi^{trial}_{n+1} &:= \xi_n, \\
\boldsymbol{\epsilon}^{e\,trial}_{n+1} &:= \boldsymbol{\epsilon}_{n+1} - \boldsymbol{\epsilon}^{p\,trial}_{n+1},
\end{aligned}$$

and

$$\mathrm{dev}[\boldsymbol{\alpha}_{n+1}^{trial}] := \mathrm{dev}[\boldsymbol{\alpha}_n] + \frac{\Delta t}{\tau_{\mu\,n+1}^{trial} + \Delta t}\mathrm{dev}[\boldsymbol{\epsilon}_{n+1}^{e\,trial} - \boldsymbol{\alpha}_n],$$

$$\mathrm{tr}[\boldsymbol{\alpha}_{n+1}^{trial}] := \mathrm{tr}[\boldsymbol{\alpha}_n] + \frac{\Delta t}{\tau_{\kappa\,n+1}^{trial} + \Delta t}\mathrm{tr}[\boldsymbol{\epsilon}_{n+1} - \boldsymbol{\alpha}_n] - \frac{\Delta t}{\tau_{\kappa\,n+1}^{trial} + \Delta t}[\hat{e}(\Theta_{n+1}^{trial}) - \hat{e}(\Theta_0)],$$

where

$$\tau_{\mu\,n+1}^{trial} := \eta_{v\,n+1}^{dev\;trial}/2\mu_{n+1}^{trial},$$
$$\tau_{\kappa\,n+1}^{trial} := \eta_{v\,n+1}^{vol\;trial}/3\kappa_{n+1}^{trial},$$

and

$$\hat{e}(\Theta_{n+1}^{trial}) = 3\alpha(\Theta_{n+1}^{trial})(\Theta_{n+1}^{trial} - \Theta_{ref}) + e^{ps}(\Theta_{n+1}^{trial}),$$
$$\hat{e}(\Theta_0) = 3\alpha(\Theta_0)(\Theta_0 - \Theta_{ref}) + e^{ps}(\Theta_0).$$

Step 2. *Trial temperature.* Compute trial (isentropic) temperature at time t_{n+1} at constant elastic entropy H_n^e.

IF (constant material properties) THEN

$$\Theta_{n+1}^{trial} := \hat{\Theta}(\boldsymbol{\epsilon}_{n+1}^{e\,trial}, H_n^e, \xi_{n+1}^{trial}, \boldsymbol{\alpha}_{n+1}^{trial}),$$
$$\text{with}\quad H_n^e := \hat{H}^e(\boldsymbol{\epsilon}_n^e, \Theta_n, \xi_n, \boldsymbol{\alpha}_n),$$

ELSE

Solve for Θ_{n+1}^{trial} the implicit nonlinear equation:

$$\hat{H}^e(\boldsymbol{\epsilon}_{n+1}^{e\,trial}, \Theta_{n+1}^{trial}, \xi_{n+1}^{trial}, \boldsymbol{\alpha}_{n+1}^{trial}) - H_n^e = 0,$$
$$\text{with}\quad H_n^e := \hat{H}^e(\boldsymbol{\epsilon}_n^e, \Theta_n, \xi_n, \boldsymbol{\alpha}_n).$$

END IF

Step 3. *Trial (generalized) stresses.* Compute trial generalized stresses at trial temperature Θ_{n+1}^{trial}.

$$\boldsymbol{s}_{n+1}^{trial} := \mathrm{dev}[\boldsymbol{\sigma}_{n+1}^{trial}] = 2\hat{\mu}_{n+1}^{trial}\mathrm{dev}[\boldsymbol{\epsilon}_{n+1}^{e\,trial} - \boldsymbol{\alpha}_n],$$
$$p_{n+1}^{trial} := \hat{\kappa}_{n+1}^{trial}\mathrm{tr}[\boldsymbol{\epsilon}_{n+1} - \boldsymbol{\alpha}_n] - \hat{\kappa}_{n+1}^{trial}[\hat{e}(\Theta_{n+1}^{trial}) - \hat{e}(\Theta_0)],$$
$$q_{n+1}^{trial} := -\hat{K}_\xi(\xi_{n+1}^{trial}, \Theta_{n+1}^{trial}),$$

where

$$\hat{\mu}_{n+1}^{trial} := \frac{\tau_{\mu\,n+1}^{trial}}{\tau_{\mu\,n+1}^{trial} + \Delta t}\mu_{n+1}^{trial},$$

$$\hat{\kappa}_{n+1}^{trial} := \frac{\tau_{\kappa\,n+1}^{trial}}{\tau_{\kappa\,n+1}^{trial} + \Delta t}\kappa_{n+1}^{trial},$$

with

$$\tau_{\mu n+1}^{trial} := \eta_{v n+1}^{dev\ trial} / 2\mu_{n+1}^{trial},$$
$$\tau_{\kappa n+1}^{trial} := \eta_{v n+1}^{vol\ trial} / 3\kappa_{n+1}^{trial},$$

and

$$\hat{e}(\Theta_{n+1}^{trial}) = 3\alpha(\Theta_{n+1}^{trial})(\Theta_{n+1}^{trial} - \Theta_{ref}) + e^{ps}(\Theta_{n+1}^{trial}),$$
$$\hat{e}(\Theta_0) = 3\alpha(\Theta_0)(\Theta_0 - \Theta_{ref}) + e^{ps}(\Theta_0).$$

Step 4. *Trial yield function.* Compute trial yield function at constant temperature Θ_n, as a consequence of the additional design constraint of constant plastic entropy.

$$\Phi_{n+1}^{trial} := \hat{\Phi}(\boldsymbol{\sigma}_{n+1}^{trial}, q_{n+1}^{trial}, \Theta_n) = \|\boldsymbol{s}_{n+1}^{trial}\| - \sqrt{\frac{2}{3}}[y_0(\Theta_n) - q_{n+1}^{trial}]$$

IF $\Phi_{n+1}^{trial} \leq 0$ THEN

Set $(\cdot)_{n+1} := (\cdot)_{n+1}^{trial}$ and update database

RETURN

END IF

Step 5. *Isentropic return mapping.* Perform an isentropic return mapping algorithm at constant elastic and plastic entropy.

IF (constant material properties) THEN

Solve for γ_{n+1} the implicit nonlinear equation:

$$\Phi_{n+1} := \hat{\Phi}(\boldsymbol{\sigma}_{n+1}, q_{n+1}, \Theta_n) = 0 \quad \text{with}$$
$$\Theta_{n+1} = \hat{\Theta}(\boldsymbol{\epsilon}_{n+1}^e, H_n^e, \xi_{n+1}, \boldsymbol{\alpha}_{n+1}),$$

ELSE

Solve for γ_{n+1} and Θ_{n+1} the implicit nonlinear set of equations:

$$\left.\begin{aligned} \Phi_{n+1} := \hat{\Phi}(\boldsymbol{\sigma}_{n+1}, q_{n+1}, \Theta_n) = 0, \\ \hat{H}^e(e_{n+1}, \Theta_{n+1}, \xi_{n+1}, \boldsymbol{\alpha}_{n+1}) - H_n^e = 0, \end{aligned}\right\}$$

END IF

where

$$\Phi_{n+1} := \frac{\hat{\mu}_{n+1}}{\hat{\mu}_{n+1}^{trial}} \|\boldsymbol{s}_{n+1}^{trial}\| - 2\hat{\mu}_{n+1}\gamma_{n+1} - \sqrt{\frac{2}{3}}[y_0(\Theta_n) - q_{n+1}],$$

$$q_{n+1} = -\hat{K}_\xi(\xi_{n+1}, \Theta_{n+1}),$$

$$\xi_{n+1} = \xi_{n+1}^{trial} + \sqrt{\frac{2}{3}}\gamma_{n+1},$$

$$\boldsymbol{s}_{n+1} = \frac{\hat{\mu}_{n+1}}{\hat{\mu}^{trial}_{n+1}} \boldsymbol{s}^{trial}_{n+1} - 2\hat{\mu}_{n+1}\gamma_{n+1}\boldsymbol{n}^{trial}_{n+1},$$
$$p_{n+1} = \hat{\kappa}_{n+1}\mathrm{tr}[\boldsymbol{\epsilon}_{n+1} - \boldsymbol{\alpha}_n] - \hat{\kappa}_{n+1}[\hat{e}(\Theta_{n+1}) - \hat{e}(\Theta_0)],$$

$$\mathrm{dev}[\boldsymbol{\alpha}_{n+1}] = \mathrm{dev}[\boldsymbol{\alpha}_n] + \frac{\Delta t}{\eta_{v\,n+1}^{dev}} \boldsymbol{s}_{n+1},$$
$$\mathrm{tr}[\boldsymbol{\alpha}_{n+1}] = \mathrm{tr}[\boldsymbol{\alpha}_n] + \frac{\Delta t}{\eta_{v\,n+1}^{vol}} 3p_{n+1},$$

with

$$\hat{\mu}_{n+1} := \frac{\tau_{\mu n+1}}{\tau_{\mu n+1} + \Delta t}\mu_{n+1}, \quad \hat{\mu}^{trial}_{n+1} := \frac{\tau^{trial}_{\mu n+1}}{\tau^{trial}_{\mu n+1} + \Delta t}\mu^{trial}_{n+1},$$
$$\hat{\kappa}_{n+1} := \frac{\tau_{\kappa n+1}}{\tau_{\kappa n+1} + \Delta t}\kappa_{n+1},$$

and

$$\tau_{\mu n+1} := \eta_{v\,n+1}^{dev}/2\mu_{n+1}, \quad \tau^{trial}_{\mu n+1} := \eta_{v\,n+1}^{dev\ trial}/2\mu^{trial}_{n+1},$$
$$\tau_{\kappa n+1} := \eta_{v\,n+1}^{vol}/3\kappa_{n+1},$$

and

$$\hat{e}(\Theta_{n+1}) = 3\alpha(\Theta_{n+1})(\Theta_{n+1} - \Theta_{ref}) + e^{ps}(\Theta_{n+1}),$$
$$\hat{e}(\Theta_0) = 3\alpha(\Theta_0)(\Theta_0 - \Theta_{ref}) + e^{ps}(\Theta_0).$$

Step 6. *Update database and compute stresses.*

$$\boldsymbol{\epsilon}^{p}_{n+1} = \boldsymbol{\epsilon}^{p\ trial}_{n+1} + \gamma_{n+1}\boldsymbol{n}^{trial}_{n+1},$$
$$\xi_{n+1} = \xi^{trial}_{n+1} + \sqrt{\frac{2}{3}}\gamma_{n+1},$$
$$\boldsymbol{\alpha}_{n+1} = \boldsymbol{\alpha}_n + \frac{\Delta t}{\eta_{v\,n+1}^{dev}}\ \boldsymbol{s}_{n+1} + \frac{\Delta t}{\eta_{v\,n+1}^{vol}}\ p_{n+1}\ \mathbf{1}_3,$$

$$\boldsymbol{s}_{n+1} = \frac{\hat{\mu}_{n+1}}{\hat{\mu}^{trial}_{n+1}} \boldsymbol{s}^{trial}_{n+1} - 2\hat{\mu}_{n+1}\gamma_{n+1}\boldsymbol{n}^{trial}_{n+1},$$
$$p_{n+1} = \hat{\kappa}_{n+1}\mathrm{tr}[\boldsymbol{\epsilon}_{n+1} - \boldsymbol{\alpha}_n] - \hat{\kappa}_{n+1}[\hat{e}(\Theta_{n+1}) - \hat{e}(\Theta_0)],$$
$$\boldsymbol{\sigma}_{n+1} = p_{n+1}\ \mathbf{1}_3 + \boldsymbol{s}_{n+1},$$

where

$$\boldsymbol{n}^{trial}_{n+1} := \boldsymbol{s}^{trial}_{n+1}/\|\boldsymbol{s}^{trial}_{n+1}\|,$$

$$\hat{e}(\Theta^{trial}_{n+1}) = 3\alpha(\Theta^{trial}_{n+1})(\Theta^{trial}_{n+1} - \Theta_{ref}) + e^{ps}(\Theta^{trial}_{n+1}),$$
$$\hat{e}(\Theta_0) = 3\alpha(\Theta_0)(\Theta_0 - \Theta_{ref}) + e^{ps}(\Theta_0),$$

and

$$\hat{\mu}_{n+1} := \frac{\tau_{\mu n+1}}{\tau_{\mu n+1} + \Delta t}\mu_{n+1}, \quad \hat{\mu}^{trial}_{n+1} := \frac{\tau^{trial}_{\mu n+1}}{\tau^{trial}_{\mu n+1} + \Delta t}\mu^{trial}_{n+1},$$
$$\hat{\kappa}_{n+1} := \frac{\tau_{\kappa n+1}}{\tau_{\kappa n+1} + \Delta t}\kappa_{n+1},$$

with

$$\tau_{\mu n+1} := \eta^{dev}_{v n+1}/2\mu_{n+1}, \quad \tau^{trial}_{\mu n+1} := \eta^{dev\ trial}_{v n+1}/2\mu^{trial}_{n+1},$$
$$\tau_{\kappa n+1} := \eta^{vol}_{v n+1}/3\kappa_{n+1}.$$

I.B. Thermal problem

Step 1. *Trial state (kinematics).* Given the initial data $\{\boldsymbol{\epsilon}_n, \Theta_n\}$ and database $\{\boldsymbol{\epsilon}^p_n, \xi_n, \boldsymbol{\alpha}_n\}$ at time t_n and prescribed $\{\boldsymbol{\epsilon}_{n+1}, \Theta_{n+1}\}$ at time t_{n+1}, set:

$$\boldsymbol{\epsilon}^{p\ trial}_{n+1} := \boldsymbol{\epsilon}^p_n,$$
$$\xi^{trial}_{n+1} := \xi_n,$$
$$\boldsymbol{\epsilon}^{e\ trial}_{n+1} := \boldsymbol{\epsilon}_{n+1} - \boldsymbol{\epsilon}^{p\ trial}_{n+1},$$

and

$$\mathrm{dev}[\boldsymbol{\alpha}^{trial}_{n+1}] := \mathrm{dev}[\boldsymbol{\alpha}_n] + \frac{\Delta t}{\tau_{\mu n+1} + \Delta t}\mathrm{dev}[\boldsymbol{\epsilon}^{e\ trial}_{n+1} - \boldsymbol{\alpha}_n],$$

where

$$\tau_{\mu n+1} := \eta^{dev}_{v n+1}/2\mu_{n+1}.$$

Step 2. *Trial (generalized) stresses.* Compute trial generalized stresses at current temperature Θ_{n+1}.

$$\boldsymbol{s}^{trial}_{n+1} := \mathrm{dev}[\boldsymbol{\sigma}^{trial}_{n+1}] = 2\mu_{n+1}\mathrm{dev}[\boldsymbol{\epsilon}^{e\ trial}_{n+1} - \boldsymbol{\alpha}^{trial}_{n+1}],$$
$$q^{trial}_{n+1} := -K_\xi(\xi^{trial}_{n+1}, \Theta_{n+1}).$$

Step 3. *Trial yield function.* Compute trial yield function at current temperature Θ_{n+1}.

$$\Phi^{trial}_{n+1} := \hat{\Phi}(\boldsymbol{\sigma}^{trial}_{n+1}, q^{trial}_{n+1}, \Theta_{n+1}) = \|\boldsymbol{s}^{trial}_{n+1}\| - \sqrt{\frac{2}{3}}[y_0(\Theta_{n+1}) - q^{trial}_{n+1}]$$

IF $\Phi^{trial}_{n+1} \leq 0$ THEN

Set $(\cdot)_{n+1} := (\cdot)^{trial}_{n+1}$ and update database

RETURN

END IF

Step 4. *Isothermal return mapping.* Solve for γ_{n+1} the implicit nonlinear equation:

$$\Phi_{n+1} := \hat{\Phi}(\boldsymbol{\sigma}_{n+1}, q_{n+1}, \Theta_{n+1}) = 0 \quad \text{with}$$

$$\Phi_{n+1} := \|\boldsymbol{s}^{trial}_{n+1}\| - 2\mu_{n+1}\gamma_{n+1} - \sqrt{\frac{2}{3}}[y_0(\Theta_{n+1}) - q_{n+1}],$$

$$\xi_{n+1} = \xi^{trial}_{n+1} + \sqrt{\frac{2}{3}}\gamma_{n+1},$$

$$q_{n+1} = -\hat{K}_\xi(\xi_{n+1}, \Theta_{n+1}).$$

Step 5. *Update database.*

$$\boldsymbol{\epsilon}^p_{n+1} = \boldsymbol{\epsilon}^{p\ trial}_{n+1} + \gamma_{n+1}\boldsymbol{n}^{trial}_{n+1},$$

$$\xi_{n+1} = \xi^{trial}_{n+1} + \sqrt{\frac{2}{3}}\gamma_{n+1},$$

$$\boldsymbol{\alpha}_{n+1} = \boldsymbol{\alpha}_n + \frac{\Delta t}{\eta_{v\,n+1}^{dev}}\,\boldsymbol{s}_{n+1} + \frac{\Delta t}{\eta_{v\,n+1}^{vol}}\,p_{n+1}\,\mathbf{1}_3,$$

where

$$\boldsymbol{n}^{trial}_{n+1} := \boldsymbol{s}^{trial}_{n+1}/\|\boldsymbol{s}^{trial}_{n+1}\|,$$

$$\boldsymbol{s}_{n+1} = \boldsymbol{s}^{trial}_{n+1} - 2\hat{\mu}_{n+1}\gamma_{n+1}\boldsymbol{n}^{trial}_{n+1},$$

$$p_{n+1} = \hat{\kappa}_{n+1}\mathrm{tr}[\boldsymbol{\epsilon}_{n+1} - \boldsymbol{\alpha}_n] - \hat{\kappa}_{n+1}[\hat{e}(\Theta_{n+1}) - \hat{e}(\Theta_0)],$$

$$\hat{e}(\Theta^{trial}_{n+1}) = 3\alpha(\Theta^{trial}_{n+1})(\Theta^{trial}_{n+1} - \Theta_{ref}) + e^{ps}(\Theta^{trial}_{n+1}),$$

$$\hat{e}(\Theta_0) = 3\alpha(\Theta_0)(\Theta_0 - \Theta_{ref}) + e^{ps}(\Theta_0),$$

with

$$\hat{\mu}_{n+1} := \frac{\tau_{\mu n+1}}{\tau_{\mu n+1} + \Delta t}\mu_{n+1},$$

$$\hat{\kappa}_{n+1} := \frac{\tau_{\kappa n+1}}{\tau_{\kappa n+1} + \Delta t}\kappa_{n+1},$$

and

$$\tau_{\mu n+1} := \eta_{v\,n+1}^{dev}/2\mu_{n+1},$$

$$\tau_{\kappa n+1} := \eta_{v\,n+1}^{vol}/3\kappa_{n+1}.$$

Step 6. *Plastic mechanical dissipation.*

$$\mathcal{D}_{mech\,n+1} = \sqrt{\frac{2}{3}}\gamma_{n+1}\ y_0(\Theta_{n+1})/\Delta t + \frac{1}{\eta_{v\,n+1}^{dev}}\|\boldsymbol{s}_{n+1}\|^2 + \frac{3}{\eta_{v\,n+1}^{vol}}p^2_{n+1}.$$

APPENDIX II. THERMOFRICTIONAL RETURN MAPPING ALGORITHMS

In this appendix we summarize the main steps involved in the thermofrictional return mapping algorithms for the mechanical and thermal problems arising from the isentropic operator split.

II.A. Mechanical problem

Step 1. *Trial state (kinematics)* Given the initial data $\{g_{N\,n}, g_{T\,n}^{\alpha}\}$ and the database $\{g_{T\,n}^{p\,\alpha}, \Theta_{c\,n}, \zeta_{c\,n}\}$ at time t_n, and prescribed data $\{g_{N\,n+1}, g_{T\,n+1}^{\alpha}\}$ at time t_{n+1}, set:

$$
\begin{aligned}
g_{T\,n+1}^{p\,\alpha\,trial} &:= g_{T\,n}^{p\,\alpha}, \\
\zeta_{c\,n+1}^{trial} &:= \zeta_{c\,n}, \\
g_{T\,n+1}^{e\,\alpha\,trial} &:= g_{T\,n+1}^{\alpha} - g_{T\,n+1}^{p\,\alpha\,trial}.
\end{aligned}
$$

Step 2. *Trial contact temperature.* Solve for $\Theta_{c\,n+1}^{trial}$ the implicit nonlinear equation:

$$
\begin{aligned}
&\hat{H}_c^e(g_{N\,n+1}, g_{T\,n+1}^{e\,\alpha\,trial}, \Theta_{c\,n+1}^{trial}, \zeta_{c\,n+1}^{trial}) - H_{c\,n}^e = 0, \\
&\text{with } H_{c\,n}^e := \hat{H}_c^e(g_{N\,n}, g_{T\,n}^{e\,\alpha}, \Theta_{c\,n}, \zeta_{c\,n}).
\end{aligned}
$$

Step 3. *Trial (generalized) traction.*

$$
\begin{aligned}
t_{N\,n+1} &:= \begin{cases} \frac{1}{2}\epsilon_N \frac{\langle g_{N\,n+1}\rangle^2 - \langle g_{N\,n}\rangle^2}{g_{N\,n+1} - g_{N\,n}}; & \text{if } g_{N\,n+1} \neq g_{N\,n}, \\ \epsilon_N \langle g_{N\,n+1}\rangle; & \text{if } g_{N\,n+1} = g_{N\,n}, \end{cases} \\
t_{T\,\alpha\,n+1}^{trial} &:= \epsilon_T M_{\alpha\beta\,n+1} g_{T\,n+1}^{e\,\beta\,trial}, \\
q_{c\,n+1}^{trial} &:= -\partial_{\zeta_c} \hat{K}_c(\zeta_{c\,n+1}^{trial}, \Theta_{c\,n+1}^{trial}).
\end{aligned}
$$

Step 4. *Trial slip function.* Compute trial slip function at fixed contact temperature $\Theta_{c\,n}$, to satisfy the design constraint of constant plastic contact entropy.

$$
\begin{aligned}
\Phi_{c\,n+1}^{trial} &:= \hat{\Phi}_c(t_{N\,n+1}, t_{T\,\alpha\,n+1}^{trial}, \Theta_{c\,n}, q_{c\,n+1}^{trial}) \\
&= \|\boldsymbol{t}_{T\,n+1}^{\flat\,trial}\|_{ref} - (\hat{\mu}_0(\Theta_{c\,n}) - q_{c\,n+1}^{trial})\, t_{N\,n+1}
\end{aligned}
$$

with $\|\boldsymbol{t}_{T\,n+1}^{\flat\,trial}\|_{ref} = (t_{T\,\alpha\,n+1}^{trial} M_{n+1}^{\alpha\beta} t_{T\,\beta\,n+1}^{trial})^{1/2}$.

IF $\Phi_{c\,n+1}^{trial} \leq 0$ THEN

Set $(\cdot)_{n+1} := (\cdot)_{n+1}^{trial}$ and update database

RETURN

END IF

Step 5. *Isentropic return mapping.* Solve for γ_{cn+1} and Θ_{cn+1} the implicit nonlinear set of equations:

$$\left.\begin{aligned} \Phi_{cn+1} &:= \hat{\Phi}_c(t_{Nn+1}, t_{T\alpha\, n+1}, \Theta_{cn}, q_{cn+1}) = 0, \\ \hat{H}^e_c(g_{Nn+1}, g^{e\,\alpha}_{T\,n+1}, \Theta_{cn+1}, \zeta_{cn+1}) &- H^e_{c\,n} = 0, \end{aligned}\right\}$$

where

$$\begin{aligned} \Phi_{cn+1} &= \|\boldsymbol{t}^{\flat}_{Tn+1}\|_{ref} - (\hat{\mu}_0(\Theta_{cn}) - q_{cn+1})\, t_{Nn+1}, \\ t_{T\alpha\, n+1} &= t^{trial}_{T\alpha\, n+1} - \gamma_{cn+1}\, \epsilon_T\, t^{trial}_{T\alpha\, n+1} / \|\boldsymbol{t}^{\flat\, trial}_{Tn+1}\|_{ref}, \\ g^{p\,\alpha}_{Tn+1} &= g^{p\,\alpha\, trial}_{Tn+1} + \gamma_{cn+1}\, M^{\alpha\beta}_{n+1}\, t^{trial}_{T\beta\, n+1} / \|\boldsymbol{t}^{\flat\, trial}_{Tn+1}\|_{ref}, \\ \zeta_{cn+1} &= \zeta^{trial}_{cn+1} + \gamma_{cn+1}\, t_{Nn+1}, \\ q_{cn+1} &= -\partial_{\zeta_c} \hat{K}_c(\zeta_{cn+1}, \Theta_{cn+1}), \end{aligned}$$

with $\|\boldsymbol{t}^{\flat}_{Tn+1}\|_{ref} = (t_{T\alpha\, n+1} M^{\alpha\beta}_{n+1} t_{T\beta\, n+1})^{1/2}$.

Step 6. *Update database and compute contact traction.*

$$\begin{aligned} g^{p\,\alpha}_{Tn+1} &= g^{p\,\alpha\, trial}_{Tn+1} + \gamma_{cn+1}\, M^{\alpha\beta}_{n+1}\, t^{trial}_{T\beta\, n+1} / \|\boldsymbol{t}^{\flat\, trial}_{Tn+1}\|_{ref}, \\ \zeta_{cn+1} &= \zeta^{trial}_{cn+1} + \gamma_{cn+1}\, t_{Nn+1}, \\ t_{T\alpha\, n+1} &:= \epsilon_T\, M_{\alpha\beta_{n+1}}\, g^{e\,\beta}_{Tn+1}, \\ q_{cn+1} &:= -\partial_{\zeta_c} \hat{K}_c(\zeta_{cn+1}, \Theta_{cn+1}). \end{aligned}$$

II.B. Thermal problem

Step 1. *Trial state (kinematics).* Given the initial data $\{g_{Nn}, g^{\alpha}_{Tn}\}$ and the database $\{g^{p\,\alpha}_{Tn}, \Theta_{cn}, \zeta_{cn}\}$ at time t_n, and prescribed data $\{g_{Nn+1}, g^{\alpha}_{Tn+1}\}$ at time t_{n+1}, set:

$$\begin{aligned} g^{p\,\alpha\, trial}_{Tn+1} &:= g^{p\,\alpha}_{Tn}, \\ \zeta^{trial}_{cn+1} &:= \zeta_{cn}, \\ g^{e\,\alpha\, trial}_{Tn+1} &:= g^{\alpha}_{Tn+1} - g^{p\,\alpha\, trial}_{Tn+1}. \end{aligned}$$

Step 2. *Trial contact temperature.* Solve for Θ^{trial}_{cn+1} the implicit nonlinear equation:

$$H^{e\, trial}_{c\,n+1} - H^e_{c\,n} = \frac{\Delta t}{\Theta^{trial}_{cn+1}} (Q^{(1)\, trial}_{c\;n+1} + Q^{(2)\, trial}_{c\;n+1}),$$

where

$$\begin{aligned} H^{e\, trial}_{c\,n+1} &:= \hat{H}^e_c(g_{Nn+1}, g^{e\,\alpha\, trial}_{Tn+1}, \Theta^{trial}_{cn+1}, \zeta^{trial}_{cn+1}), \\ H^e_{c\,n} &:= \hat{H}^e_c(g_{Nn}, g^{e\,\alpha}_{Tn}, \Theta_{cn}, \zeta_{cn}), \\ Q^{(1)\, trial}_{c\;n+1} &:= \hat{h}^{(1)}_{cond}(t_{Nn+1}, \Theta^{trial}_{cn+1})(\Theta^{(1)}_{n+1} - \Theta^{trial}_{cn+1}), \\ Q^{(2)\, trial}_{c\;n+1} &:= \hat{h}^{(2)}_{cond}(t_{Nn+1}, \Theta^{trial}_{cn+1})(\Theta^{(2)}_{n+1} - \Theta^{trial}_{cn+1}). \end{aligned}$$

Step 3. *Trial (generalized) traction.*

$$t_{N\,n+1} := \begin{cases} \frac{1}{2}\epsilon_N \frac{\langle g_{N\,n+1}\rangle^2 - \langle g_{N\,n}\rangle^2}{g_{N\,n+1} - g_{N\,n}}; & \text{if } g_{N\,n+1} \neq g_{N\,n}, \\ \epsilon_N \langle g_{N\,n+1}\rangle; & \text{if } g_{N\,n+1} = g_{N\,n}, \end{cases}$$

$$t_{T\,\alpha\,n+1}^{trial} := \epsilon_T M_{\alpha\beta\,n+1} g_{T\,n+1}^{e\,\beta\,trial},$$

$$q_{c\,n+1}^{trial} := -\partial_{\zeta_c} \hat{K}_c(\zeta_{c\,n+1}^{trial}, \Theta_{c\,n+1}^{trial}).$$

Step 4. *Trial slip function.*

$$\begin{aligned} \Phi_{c\,n+1}^{trial} &:= \hat{\Phi}_c(t_{N\,n+1}, t_{T\,\alpha\,n+1}^{trial}, \Theta_{c\,n+1}^{trial}, q_{c\,n+1}^{trial}) \\ &= \|\boldsymbol{t}_{T\,n+1}^{\flat\,trial}\|_{ref} - (\hat{\mu}_0(\Theta_{c\,n+1}^{trial}) - q_{c\,n+1}^{trial})\, t_{N\,n+1} \end{aligned}$$

with $\|\boldsymbol{t}_{T\,n+1}^{\flat\,trial}\|_{ref} = (t_{T\,\alpha\,n+1}^{trial} M_{n+1}^{\alpha\beta} t_{T\,\beta\,n+1}^{trial})^{1/2}$.

IF $\Phi_{c\,n+1}^{trial} \leq 0$ THEN

Set $(\cdot)_{n+1} := (\cdot)_{n+1}^{trial}$ and update database

RETURN

END IF

Step 5. *Isothermal return mapping.* Solve for $\gamma_{c\,n+1}$ and $\Theta_{c\,n+1}$ the implicit nonlinear set of equations:

$$\left.\begin{aligned} \Phi_{c\,n+1} &:= \hat{\Phi}_c(t_{N\,n+1}, t_{T\,\alpha\,n+1}, \Theta_{c\,n+1}, q_{c\,n+1}) = 0, \\ H_{c\,n+1}^e - H_{c\,n}^e &= \frac{\Delta t}{\Theta_{c\,n+1}}(Q_{c\,n+1}^{(1)} + Q_{c\,n+1}^{(2)}) + \frac{\Delta t}{\Theta_{c\,n+1}} \mathcal{D}_{c,mech\,n+1}, \end{aligned}\right\}$$

where

$$\begin{aligned} \Phi_{c\,n+1} &:= \|\boldsymbol{t}_{T\,n+1}^{\flat}\|_{ref} - (\hat{\mu}_0(\Theta_{c\,n+1}) - q_{c\,n+1})\, t_{N\,n+1}, \\ H_{c\,n+1}^e &:= \hat{H}_c^e(g_{N\,n+1}, g_{T\,n+1}^{e\,\alpha}, \Theta_{c\,n+1}, \zeta_{c\,n+1}), \\ H_{c\,n}^e &:= \hat{H}_c^e(g_{N\,n}, g_{T\,n}^{e\,\alpha}, \Theta_{c\,n}, \zeta_{c\,n}), \\ Q_{c\,n+1}^{(1)} &:= \hat{h}_{cond}^{(1)}(t_{N\,n+1}, \Theta_{c\,n+1})(\Theta_{n+1}^{(1)} - \Theta_{c\,n+1}), \\ Q_{c\,n+1}^{(2)} &:= \hat{h}_{cond}^{(2)}(t_{N\,n+1}, \Theta_{c\,n+1})(\Theta_{n+1}^{(2)} - \Theta_{c\,n+1}), \\ \mathcal{D}_{c,mech\,n+1} &:= \gamma_{c\,n+1} \hat{\mu}_0(\Theta_{c\,n+1})\, t_{N\,n+1}/\Delta t, \end{aligned}$$

$$\begin{aligned} t_{T\,\alpha\,n+1} &= t_{T\,\alpha\,n+1}^{trial} - \gamma_{c\,n+1}\, \epsilon_T\, t_{T\,\alpha\,n+1}^{trial} / \|\boldsymbol{t}_{T\,n+1}^{\flat\,trial}\|_{ref}, \\ g_{T\,n+1}^{p\,\alpha} &= g_{T\,n+1}^{p\,\alpha\,trial} + \gamma_{c\,n+1}\, M_{n+1}^{\alpha\beta}\, t_{T\,\beta\,n+1}^{trial} / \|\boldsymbol{t}_{T\,n+1}^{\flat\,trial}\|_{ref}, \\ \zeta_{c\,n+1} &= \zeta_{c\,n+1}^{trial} + \gamma_{c\,n+1}\, t_{N\,n+1}, \\ q_{c\,n+1} &= -\partial_{\zeta_c} \hat{K}_c(\zeta_{c\,n+1}, \Theta_{c\,n+1}), \end{aligned}$$

with $\|\boldsymbol{t}^{\flat}_{T\,n+1}\|_{ref} = (t_{T\alpha\,n+1} M^{\alpha\beta}_{n+1} t_{T\beta\,n+1})^{1/2}$.

Step 6. *Update database.*

$$g^{p\,\alpha}_{T\,n+1} = g^{p\,\alpha\,trial}_{T\,n+1} + \gamma_{c\,n+1}\, M^{\alpha\beta}_{n+1}\, t^{trial}_{T\beta\,n+1} / \|\boldsymbol{t}^{\flat\,trial}_{T\,n+1}\|_{ref},$$
$$\zeta_{c\,n+1} = \zeta^{\,trial}_{c\,n+1} + \gamma_{c\,n+1}\, t_{N\,n+1}.$$

List of Figures

List of Tables